THE UNIVERSITY OF CHICAGO

LOCAL B CELL STATES AND SELECTION MECHANISMS IN HUMAN RENAL ALLOGRAFT REJECTION

A DISSERTATION SUBMITTED TO
THE FACULTY OF THE DIVISION OF THE BIOLOGICAL SCIENCES
AND THE PRITZKER SCHOOL OF MEDICINE
IN CANDIDACY FOR THE DEGREE OF
DOCTOR OF PHILOSOPHY

COMMITTEE ON IMMUNOLOGY

BY

YUTA ASANO

CHICAGO, ILLINOIS

JUNE 2020

Table of Contents

List of Figures iv

List of Tables v

List of Supplementary Tables vi

Acknowledgement vii

Abstract ix

1 Introduction 1

1.1 Germinal centers 1

1.2 Transcriptional regulation in germinal centers 3

1.3 T-independent B cell activation 5

1.4 B cell self-tolerance 10

1.5 Ectopic B cell activation in tertiary lymphoid structures 14

1.6 Antibody-mediated B cell roles in renal allograft rejection 17

1.7 Antibody-independent B cell roles in renal allograft rejection 22

1.8 Aims and significance 23

2 Transcriptional profile of intrarenal B cells in human renal allograft rejection 26

2.1 Introduction 26

2.2 Results 27

2.2.1 Distinct transcriptional states in activated intrarenal and tonsil B cells 27

2.2.2 Intrarenal B cells resemble peritoneal B1 cells 35

2.2.3 Receptor-ligand co-upregulation reveals intrarenal interactions around B cells 42

2.2.4 Serum DSA positivity does not differentiate intrarenal B cell phenotypes 45

2.3 Discussion 49

3 Reactivity and selection of antibodies expressed by intrarenal B cells 54

3.1 Introduction 54

3.2 Results 55

3.2.1 Cloning and recombinant expression of intrarenal antibodies 55

3.2.2 Allo-HLA reactivity does not select intrarenal antibodies 57

3.2.3 Plasma cells dominantly express antinucleolar autoantibodies 61

3.3 Discussion 66

4 Discussion 69

4.1 Overall implications of this work 69

4.2 Current and Future directions 76

5 Materials and Methods 81

6 References 92

List of Figures

Figure 2.1 Gating scheme for cell sorting and QC of scRNA-seq data. 28

Figure 2.2 B cells clustered based on Ig class switch. 30

Figure 2.3 Genes and pathways active in intrarenal B cells represented their unique phenotype. 32

Figure 2.4 AHNAK represents a B1-like transcriptional profile of intrarenal B cells. 37

Figure 2.5 Intrarenal B cells had no association with ABC and HIF signatures. 41

Figure 2.6 Ligand-receptor interactions between intrarenal B cells and rejected allografts. 43

Figure 2.7 QC of the second cohort and data integration. 46

Figure 2.8 B cells from serum DSA-positive and negative patients are similar. 48

Figure 3.1 Antibodies expressed by intrarenal B cells were not selected for allo-HLA reactivity. 56

Figure 3.2 Intrarenal antibodies did not selectively bind to HLAs. 58

Figure 3.3 Clonally expanded plasma cells were selected for antinucleolar reactivity. 62

Figure 3.4 Ki-67 is a specific target of clonally expanded antibodies. 63

Figure 3.5 Changes in Ki-67 reactivity through clonal evolution. 65

List of Tables

Table 2.1 Patient information. 29

Table 2.2 Ig class distribution. 29

List of Supplementary Tables (available online)

Supplementary Table 2.1 Differentially expressed genes

Supplementary Table 2.2 *Ahnak* and *AHNAK*-covariant genes

Supplementary Table 3.1 A summary of expressed antibodies

Supplementary Table 3.2 Single-antigen bead assay results

Acknowledgement

These seven years I spent at the University of Chicago was as rewarding as challenging it was. Without doubt, I could not have gotten where I am today by myself. I would like to thank everyone who helped me along the way.

First I would like to thank my mentor, Marcus Clark. Thank you for giving me this ambitious project. I have learned many things I did not expect when I joined the lab. The fact that I have been contributing to translational science was fulfilling and motivating. In the course of this study, we disagreed over many things. But every discussion with you provided me with a new perspective, which inspired me to try a new analysis or made me realize pitfalls I would have overlooked otherwise. And above all, your help on writing. If this thesis is not a mess, that is thanks to you.

Everyone in Clark lab was also an indispensable part of my experience in this place. Especially, Andrew Kinloch. From when I joined the lab until you left, you had been the only person that I shared this human B cell clan in Clark lab. I was just fortunate that you were there when I started. Thank you for letting me learn a lot from you, not only experimental techniques, but also your attitude toward science. Also our beloved lab manager Margaret Veselits. Thank you for taking care of everything in the lab, or even the whole BSLC 3rd floor. Your courteousness for others and equipment is not something easy to find elsewhere. It was all thanks to you that I and others could do what we had to do every day. You even helped my experiments personally with your excellent techniques. Without that, I would not be writing a thesis right now.

I would like to thank my thesis committees as well. Thank you Patrick Wilson for being a chair of my committee. You were always kind and welcoming when I wanted to ask for your

knowledge on B cells and antibodies. I believe your presence is reassuring to all students here working in this field. Thank you Anita Chong for your input as a professional of transplant immunology. Working on transplant was unexpected when this project started, and our lab had only limited background. But thanks to you and Dharmendra Jain in your lab, we could identify critical questions in the field and convey experiments and analyses to address them. Thank you Aly Khan for your advice on computational analyses. Seven years ago, I was a complete novice who did not even know what Terminal does. Nevertheless, I could write all the codes for analyses done in this study by myself. That would have been impossible without you in the committee. Finally, thank you Bana Jabri for your critical comments. Every committee meeting was tough thanks to you, but that was absolutely necessary for making this study better.

I would also like to thank my family who always support and care about me from Japan, and friends I met in Chicago who helped me enjoy a life here. Finally, I thank my wife Misaki. You have been the reason for which I go to the lab and come back home every day. I could not have survived the last seven years without you. I cannot be grateful enough about that.

Abstract

B cells mount specific antibody responses to protect our body from infection. At the same time, their antibody responses can be directed to local self or alloantigens to drive tissue inflammation. Although similarity is obvious between these two responses, a direct comparison remains to be made. Renal allograft rejection is one of diseases which involve pathogenic antibody responses and tissue-local B cell activation. Serum alloreactivity and intrarenal B cell infiltrates both predict a poor prognosis. However, it is unknown how or whether intrarenal B cells contribute to alloreactive antibody production and allograft rejection. In this study, we performed single cell RNA-sequencing (scRNA-seq) on activated B cells sorted from eight renal allograft rejection biopsies. Their transcriptome was compared with tonsil germinal center (GC) B cells, in order to elucidate a signature specific to intrarenal B cell activation. Our analyses revealed their unique transcriptional state that resembled peritoneal B1 cells including the upregulation of specific innate signaling pathways. Furthermore, comparison to transcriptome of whole rejected renal allografts discovered autocrine and paracrine interactions surrounding intrarenal B cells. Finally, we characterized their antibody reactivity. Although intrarenal B cells expressed highly mutated antibodies, none of them reacted to human leukocyte antigens (HLAs). Autoreactivity was not generally enriched either, leaving their reactivity elusive. However, infiltrating plasma cells showed robust clonal expansion, expressing antibodies that strongly and specifically bound to nucleolar self-antigens including Ki-67. Overall, this study uncovers two unique B cell states in renal allograft rejection: an innate peritoneal B1-like phenotype and plasma cells expressing antibodies to ubiquitous nucleolar self-antigens.

1 Introduction

B cells are the protagonist of humoral immune responses. They produce antibodies to exogenous antigens to protect our body from infection. On the other hand, when their activation is uncontrolled, they drive autoimmune diseases and transplant rejection.

How B cells become activated effectors has been one of the most intensely studied topics in immunology. Today, we know B cells are activated mainly via two pathways: GC responses and T-independent (TI) B cell activation. In this introduction, I will describe what is known about these processes and how they play a role in inflammatory diseases, in particular renal allograft rejection, the main topic of this thesis study.

1.1 Germinal centers

Each B cell expresses unique B cell receptors (BCRs) generated during their development (*1*). When BCRs are made, they tend to have only limited affinity and broad reactivity (*2*). Additionally, only a small fraction of naïve B cells can recognize any given antigen. To confer sufficient humoral protection, B cells need to improve affinity and specificity of their BCRs and expand antigen-reactive clones. Both of them are achieved in GCs.

Upon recognition of cognate antigens, B cells upregulate a chemokine receptor CCR7 and migrate toward T-cell zones (*3*). At the same time, they downregulate S1PR1, a receptor critical for lymphocyte egress from secondary lymphoid organs. Instead of S1PR1, they upregulate another receptor S1PR2 (*4*, *5*). These changes tailor them for dynamic movement and interaction within GCs. At the border of T-B zones, B cells encounter follicular-helper T (Tfh) cells to initiate

a GC response. Within roughly one week after an encounter with antigens, activated B cells and Tfh cells form visible GCs, which also contains follicular dendritic cells (FDCs) (*6*).

GCs have two regions: dark zone (DZ) and light zone (LZ). DZ and LZ are named based on their anatomical features. They are also molecularly marked by expression of CXCR4 and CD83 respectively both in mice and humans (*7*). In DZ, B cells rapidly expand and accumulate somatic hypermutations (SHMs) in the variable region of BCR genes. Proliferation and mutations need to be precisely orchestrated so that they do not happen at the same time. This separation echoes B cell development in bone marrow (*8*). DZ sequesters these processes into two compartments: proliferative DZ (DZp) and differentiating DZ (DZd) (*9*). DZp is where B cells proliferate. DZp cells express both CD83 and CXCR4, which indicates they are a transitional population between LZ and DZ. DZp cells divide only once or twice (*10*). Moreover, they form cell clusters instead of scattering throughout DZ. These observations further indicate that proliferation in DZp is tightly regulated both temporally and spatially. B cells then transition to DZd, where they upregulate *Aicda* encoding a key enzyme, activation-induced cytidine deaminase (AID), to induce SHMs (*11*).

After expansion and mutations, about a half of DZ cells proceed to LZ (*7*, *12*). In LZ, B cells are selected based on affinity and specificity of their mutated BCRs. Antigen-reactive BCRs allow B cells to capture antigens displayed on FDCs (*13*). This BCR engagement induces the first survival signal. B cells then internalize, process and present antigens on major histocompatibility complex (MHC) class II to Tfh cells. Tfh cells in turn provide B cells with the second, more critical survival signal via CD40-CD40L interaction (*14*). B cells in LZ compete for these survival signals based on affinity and specificity of BCRs. This process is called affinity maturation, which completes within just several hours.

Although B cells preferentially migrate from DZ to LZ (*15*), nearly 10 % of LZ cells reenter DZ for further expansion and SHM. This phenomenon, known as cyclic reentry (*7*, *16*), facilitates clonal evolution of BCRs. Each GC starts with a mixture of diverse B cell clones. Those clones compete in the course of GC responses that typically last for around three weeks. In the end, each GC contains much reduced clonal diversity (*17*). However, the extent of the clonal dominance varies highly among GCs. This feature allows multiple clones to affinity-mature in parallel, maintaining diversity of antibody repertoire.

LZ B cells eventually differentiate into antigen-secreting plasma cells or memory cells. Plasma cells can be short-lived or long-lived. The former robustly secretes antibodies during their short lifespan to clear pathogens, whereas the latter homes to bone marrow and supplies antibodies throughout life. Memory B cells enter circulation and contribute to rapid recall responses on occasions of secondary antigen exposure. Plasma cells mainly differentiate from affinity-matured B cells (*18*). On the other hand, B cells with low-affinity BCRs constitute main precursors for memory B cells (*19*). This distinction indicates that affinity-based selection in LZ determines not only survival but also terminal differentiation in GCs.

1.2 Transcriptional regulation in germinal centers

Upon BCR engagement, downstream signaling via NF-κB activates a transcription factor IRF4. IRF4 is critical for the initiation of GC responses, as it upregulates indispensable transcription factors such as BCL6 and OBF1 (*Pou2af1*) (*20*). BCL6 cooperates with another transcription factor, BACH2, to repress genes of various pathways including plasma cell differentiation, apoptosis, interferon (IFN) responses, Toll-like receptor (TLR) signaling (*21*, *22*). This transcriptional repression allows B cells to both initiate and maintain GC responses. On the other

hand, OBF1 and its partner OCT2 (*Pou2f2*) activate a transcriptional program indispensable for GC formation (*23*).

Once GCs are formed, another transcription factor FOXO1 is upregulated in DZd. FOXO1 represses genes related to BCR signaling and plasma cell differentiation (*24*). These pathways are also targeted by BCL6, making a synergistic effect. At the same time, FOXO1 activates genes related to cell cycle, CXCR4 signaling, and DNA damage responses, preparing B cells for proliferation and SHM. SHM is carried out by AID. AID expression is upregulated in DZp by multiple transcription factors such as E2A, PAX5 and IRF8 (*25–27*). FOXO1 also supports SHM by stabilizing AID (*28*).

In addition to SHM, AID mediates another important process called class-switch recombination (CSR). CSR switches constant regions of BCRs, or isotypes, conferring them specific functions. CSR was previously thought to happen in GCs, as AID is highly expressed in GCs. CSR is also impaired in mice lacking transcriptional factors critical for GC responses, such as IRF4 and FOXO1 (*24*, *29*). However, CSR mainly happens at a very early stage of B cell activation, even before GCs are formed (*30*, *31*). Therefore, although AID mediates both SHM and CSR, these two events occur at different timepoints.

In LZ, signaling downstream of BCR engagement sequesters FOXO1 from the nucleus. BCR signaling also downregulates *Foxo1* transcription, turning off the DZ program (*32*). Additionally, strong BCR signaling upregulates *Myc* (c-Myc), which promotes the survival of affinity-selected B cells. c-Myc is also required for cyclic reentry to DZ (*33*). c-Myc expression level remains high in DZp, where it is phosphorylated and activates proliferation (*9*). In this way, c-Myc bridges LZ and DZp.

Survival signals in LZ also drive plasma cell differentiation. Plasma cell differentiation is governed by two transcriptional factors, BLIMP1 (*Prdm1*) and XBP1 (*34*, *35*). Without a cue for differentiation, they are repressed by transcription factors such as BCL6 and PAX5 (*36*, *37*). IRF4 releases this repression, which is induced by strong BCR and CD40 stimulation in LZ (*38*). This role of IRF4 seems in contrast to its function to upregulate *Bcl6* in the initiation of GC responses. These different functions of IRF4 might be explained by distinct dimerization partners in each context (*20*). IRF4 also directly upregulates *Prdm1,* which in turn activates *Xbp1* (*39*). This cascade of transcriptional regulation efficiently directs affinity-matured B cells to plasma cells.

The transcriptional regulation of memory B cell differentiation is not as well defined. In contrast to plasma cells, memory cells emerge mainly from B cells with low-affinity BCRs. In fact, low-affinity BCRs are enriched in GC B cells expressing a memory B cell marker (*18*). Strong CD40 signaling also prevents memory B cell differentiation by repressing *BACH2* (*40*). These findings indicate an inverse association between BCR affinity and memory B cell. However, some memory B cells express high-affinity BCRs. Therefore, multiple mechanisms should govern memory B cell differentiation depending on BCR affinity.

1.3 T-independent B cell activation

Although GCs drive specific and robust humoral responses, B cells can also respond to a class of antigens without GCs and T-cell help. Those antigens are called TI antigens (*41*). TI antigens are divided into TI-1 and TI-2 antigens. TI-1 antigens activate B cells in a BCR-independent manner, via engagement of pattern-recognition receptors (PRRs) inducing innate immune signaling. They include bacterial or viral components such as lipopolysaccharide (LPS) and bacterial DNA. On the other hand, TI-2 antigens only activate mature B cells in BCR-specific manner. They have a

repetitious structure, so that they crosslink multiple BCRs. Without the need of T cell help and GC formation, B cells can respond to these antigens much more rapidly than to conventional antigens. Moreover, B cells secrete antibodies even without antigenic stimuli. Such antibodies, mostly circulating IgM and mucosal IgA, are called natural antibodies (*42*). This rapid or natural antibody production serves the first-line defense against infection. For this specific protection, the immune system has specialized, innate-like B cell subsets called B1 cells and marginal zone (MZ) B cells. This section focuses on B1 cells and delineates their unique phenotype.

B1 cells were originally found as CD5-expressing B cells (*43*). While they account for only a small fraction of B cells in lymphoid organs and circulation, they represent a main B cell subset in body cavities such as peritoneal cavity and pleural cavity. In mice, B1 cells show distinct surface protein expression compared with conventional B (coined as B2) cells, such as higher IgM and lower IgD. Splenic and peritoneal B1 cells also differ (*44*). For instance, most peritoneal B1 cells express CD11b, a component of cell adhesion complex Mac-1, while splenic B1 cells do not. On the other hand, most splenic B1 cells express a cell-surface sialomucin CD43, while some peritoneal B1 cells lack it. In addition to surface markers, peritoneal B1 cells specifically express intracellular molecules as well, such as calcium ions sensors, annexin II and S100a6 (*45*).

These differences could reflect their localization in different tissues. However, CD11b deletion does not alter B1 cell count in peritoneal cavity (*46*). Instead, CD11b promotes B1 cell migration from body cavities to secondary lymphoid organs. Upon influenza infection, type-1 IFN pathways convert CD11b to its high-affinity form, which allows B1 cells to migrate from pleural cavity to mediastinal lymph nodes. Moreover, both annexin II and S100a6 promote proliferation and cell motility, often associated with tumorigenesis (*47*). Therefore, this peritoneal B1-specific gene expression could underlie distinct functions of B1 subsets. Additionally, there is another B1

subset called B1b cells. They share all the surface markers of traditional B1 (or B1a) cells except CD5. Despite their similarity, a reconstitution experiment demonstrated that they have distinct origins (*48*). Their existence further highlights diversity within B1 cells.

B1 cells secrete most natural IgM, and also contribute to the mucosal IgA pool (*49*). IgM production is mediated by a small number of splenic and bone marrow B1 cells, instead of peritoneal B1 cells (*50*). Moreover B1b, but not B1a, cells give rise to IgA plasma cells in the gut (*51*). Importantly, natural antibodies have roles other than protection against infection, such as clearance of apoptotic cells (*52*). Moreover, deletion of secretory IgM markedly reduces immature and mature B cells, and even alters their repertoire (*53*). Therefore, via natural antibody production, B1 cells maintain immune homeostasis.

Their broad roles come from a unique reactivity and repertoire of their antibodies. Each B1 antibody tends to react to multiple, and often self, antigens (*51*, *54*). The most well characterized antigen is a phospholipid phosphatidylcholine (PtC) (*55*). PtC-reactive cells account for nearly 10 % of B1a cells in peritoneal cavity. Their anti-PtC antibodies predominantly utilize V_H11 and V_K9 in C57Bl/6 mice, although other V genes dominate in different strains (*56*). Along with this observation, early studies based on hybridomas or bulk sequencing suggested that B1 cells carry a limited set of V genes and junctional diversity (*57*). Consistently, a large fraction of B1a cells develop in fetuses or neonates, when mice have limited expression of TdT, an enzyme responsible for junctional diversity (*58*). However, more accurate analyses using fluorescence-activated cell sorting (FACS) demonstrated that the disparity between B1 and B2 repertoire is less profound than previously acclaimed (*48*, *59*). Especially, their repertoire is much less skewed in B1a cells generated later in life and B1b cells (*60*).

Nonetheless, some BCR usages are specific for B1 cells, and impact their lineage commitment. For instance, B1 cells dominate in V_H12-transgenic mice (*61*) while only B2 cells develop in V_HB1-8-transgenic mice (*62*). Moreover, Thy-1-specific B1 cells develop only in antigen-sufficient mice (*63*). These results demonstrate that BCRs instruct B1 development via antigen recognition. Additionally, B1a-specific heavy chains allow pro-B cells in fetal liver to expedite light chain rearrangement (*64*). This early IgK rearrangement bypasses a requirement of surrogate light chain and pre-BCR checkpoint, thereby letting autoreactive clones persist. These observations highlight a unique developmental pathway shaping early B1 repertoire. Finally, switching V_HB1-8 to V_H12 in mature B2 cells forces them to acquire a B1 phenotype (*65*). This conversion involves not only surface markers, but also their functions such as peritoneal cavity migration and spontaneous IgM secretion. These results highlight that BCRs are critical for B1 cells to both acquire and maintain their phenotype.

Another unique property of B1 cells is their rapid response to innate stimuli. LPS stimulation robustly induces antibody secretion from B1 cells *in vitro* and *in vivo* (*66*, *67*). This antibody production does not require proliferation, which is distinct from plasma cell differentiation in GCs. In addition to stimulating antibody production, LPS downregulates an adhesion molecule CD9 on B1 cells and promotes egress from peritoneal cavity (*68*). Despite their distinct response to TLR ligands, B1 and B2 cells exhibit similar TLR expression (*69*, *70*). Therefore, rather than receptors, differences in downstream machinery should underlie the phenotype of B1 cells. It remains unclear how they respond to stimuli which activate other innate pathways, such as NOD or inflammasome pathways.

B1 cells have been characterized mostly in mice. In contrast, their human counterpart remains elusive. Although $CD5^+$ B cells exist in humans, their frequency in circulating blood is

much higher than in mice (*71*). In fact, CD5 are broadly expressed in human B cells, including transitional, activated or anergic B cells (*72*). These observations question CD5 as a reliable B1 marker in humans. Instead, it is proposed that another mouse B1 marker CD43 with other markers ($CD20^+$ $CD27^+$ $CD70^-$) defines B1 cells in humans (*73*). However, this definition remains highly controversial (*74*, *75*). Particularly, both CD27 and CD43 are expressed on pre-plasmablasts, another B2 population which spontaneously secrete antibodies (*76*). Collectively, B1 cells are not well defined in humans. Identification of such a population requires more comprehensive profiling of gene/protein expression and functional analyses to demonstrate key B1 properties, such as a response to innate stimuli.

A widely accepted view is that B1 cells produce unmutated low-affinity IgM antibodies. However, B1b cells also class-witch to IgA and produce mucosal antibodies. These IgA antibodies often contain SHMs (*77*). The presence of CSR and SHM indicates B1b cells can express AID in a certain circumstance. Unlike GC responses, mucosal IgA production and their mutations do not totally depend on T-cell help (*78*). It remains to be investigated what induces AID expression in B1 cells. Additionally, B1 cells can also class-switch to IgG. Indirect evidence come from a B1-deficient mouse strain (*79*, *80*). Mice deficient in *Nfkbid* almost completely lack B1 cells, whereas B2 cells develop normally. These mice can mount T-dependent humoral responses at an equivalent level as wildtype mice. In contrast, TI response is severely impaired, including diminished titer of TI antigen-specific IgG. This defect was rescued by transfer of wildtype peritoneal B cells, indicating they contribute to IgG production as well. Moreover, both B1a and B1b cells can express AID and class-switch to IgG upon *in vitro* stimulation (*81*). These *in vitro* stimulated B1 cells even participated in GC responses when transferred into lupus-prone NZB/NZW mice. This system is highly artificial, dependent on multiple signals from CD40 along with cytokines IL4 and BAFF

provided from feeder cells. Nevertheless, this observation demonstrates a potential of B1 cells to acquire a GC-like phenotype.

Although it is unclear whether they mount high-affinity antibody responses, their autoreactive nature implicates them in inflammatory diseases. Indeed, many autoimmune mouse models have an increased number of B1 cells (*82*). Their proinflammatory role has been investigated using hypotonic cell depletion by intraperitoneal H_2O injection (*83*). In this system, B2 cells dominantly refill the depleted B cell pool, allowing investigation of peritoneal B1 cell function. In a mouse model of spinal cord injury, IgM autoantibodies accumulate in lesions and drive tissue destruction (*84*). This tissue damage and IgM deposition is significantly reduced without peritoneal B1 cells. Furthermore, B1 cells infiltrate pancreatic islets of nonobese diabetic mice (*85*). Depletion of peritoneal B1 cells clears B cell infiltrates and ameliorates diabetes. Interestingly, this treatment also reduces anti-DNA IgG titer, although it is not shown whether B1 cells produce these antibodies. These results indicate that B1 cells participate in autoimmune humoral responses.

1.4 B cell self-tolerance

With B1 cells as an exception, self-tolerance mechanisms prevent autoreactive B cells from participating in immune responses. However, stochasticity of BCR rearrangement constantly supplies autoreactive clones. Once these autoreactive B cells become activated, they produce pathogenic antibodies and drive autoimmune or inflammatory diseases.

BCR rearrangement is random. Therefore, it inherently risks developing autoreactive B cells. Nearly 80 % of human early immature B cells express antibodies reactive to human epithelial type-2 (HEp-2) cells, indicating reactivity to ubiquitous self-antigens (*86*). Three mechanisms

tolerize those autoreactive B cells in development: deletion, anergy, and receptor editing (*87–89*). Thanks to these central tolerance mechanisms, frequency of autoreactive B cells drops to 20 % in mature naive B cell repertoire in humans. It is largely unknown why the immune system retains such a substantial number of autoreactive B cells. A large fraction of them are likely to be anergic (*90*). Anergic B cells have a short lifespan in presence of non-autoreactive B cells (*91*). Therefore, it is unclear whether a majority of those autoreactive B cells actually play a role.

In periphery, SHM can also generate *de novo* autoreactive B cells. Peripheral tolerance mechanisms deal with such acquired autoreactivity. Peripheral tolerance has been extensively studied in transgenic mice with hen egg lysozyme (HEL)-reactive BCRs. In mice carrying a HEL transgene and a small population of HEL-reactive B cells, reactive B cells are expelled from B cell follicles (*92*). Additionally, HEL-reactive B cells transferred to HEL-transgenic mice cannot participate in B cell follicles (*93*). Transferred HEL-reactive cells disappear from recipient mice within 60 hours after transfer, suggesting they quickly die. This mechanism is called follicular exclusion. Human B cells expressing autoreactive idiotype 9G4 are also excluded from follicles, suggesting this mechanism is functional in humans as well (*94*). Importantly, follicular exclusion is observed in mice expressing mutated HELs, in which B cells need SHM to become reactive (*95*). Therefore, follicular exclusion also tolerizes *de novo* autoreactive B cells in GCs. Unlike anergy, follicular exclusion requires competition with non-autoreactive B cells. Moreover, excluded, but not anergic, B cells can secrete antibodies with T cell help. Therefore, anergy and follicular exclusion complement each other to ensure peripheral tolerance.

In order to breach these tolerance mechanisms, autoreactive B cells require another cue in addition to BCR engagement. A well-known example is TLR, in particular TLR7 and TLR9 (*96*). TLR7 and TLR9 are intracellular receptors for RNA and DNA respectively. When BCRs

recognize nucleic acids, they are internalized and ligate these TLRs in endosomes. This pathway is critical for development of anti-nucleic acid antibodies, since such reactivity is markedly reduced in autoimmune mice lacking B cell-intrinsic TLR7 or TLR9 (*97*). Antibodies reactive to DNA or RNA are often detected in systemic lupus erythematosus (SLE) patients (*98*). Additionally, single nucleotide polymorphisms (SNPs) in TLR7 and TLR9 loci are associated with SLE (*99*). These observations highlight importance of these TLRs in B cell autoimmunity.

To activate this pathway, B cells do not have to recognize nucleic acids directly. Indeed, various autoimmune diseases manifest antibodies against nuclear components associated with nucleic acids, such as anti-histone antibodies in SLE (*100*) or anti-RNA polymerase antibodies in systemic sclerosis (SSc) (*101*). A striking example is antinucleolar antibodies often detected SSc (*102*). The most extensively studied nucleolar antigen is fibrillarin, a component of protein-RNA complex called small ribonucleoproteins (snoRNPs). snoRNPs facilitate assembly of ribosomal RNAs. This RNA binding allows snoRNPs-reactive antibodies to stimulate TLR7. Indeed, duplication of the *TLR7* locus strongly skews antibody repertoire in lupus mice toward antinucleolar reactivity (*103*, *104*). These results suggest that endosomal TLR stimulation underlies a break in tolerance against broad nuclear and nucleolar antigens.

In addition to the B cell-intrinsic effect, TLR ligation stimulates both type-1 and type-2 IFN production from other immune cells. Type-1 IFNs directly acts on B cells. For instance, both IFN-α and IFN-β enhance survival and proliferation upon BCR engagement (*105*). In vitro incubation with IFN-α robustly upregulates TLR7 in B cells (*106*). On the other hand, B cells deficient for IFN-α receptors respond poorly to TLR7 agonists. In addition to type-1 IFNs, IFN-γ also plays a critical role in autoreactive B cell activation. Mature B cell-specific deletion of an IFN-γ receptor (*Ifngr1*) strongly ameliorates lupus-like symptoms and reduce GC formation (*107*).

In fact, these IFN pathways are the most prominent signature in SLE patients (*108*). These results indicate that TLR and IFN pathways cooperate to break B cell tolerance.

Additionally, both TLR and IFN induces expression of a cytokine BAFF from innate immune cells (*109*). BAFF plays an essential role in B cell activation, survival, and antibody production. BAFF has three receptors (BAFFR, TACI and BCMA), each of which has a distinct expression pattern. Especially TACI is preferentially expressed by B1 cells, while it is downregulated in GC B cells (*110*), suggesting its unique role in these distinct B cell subsets. BAFF is upregulated in many B cell-mediated autoimmune diseases. Efficacy of a BAFF-blocking antibody Belimumab, the only FDA-approved drug for SLE treatment in the last 60 years, underpins importance of BAFF in B cell autoimmunity (*111*). Interestingly, all the pathways mentioned above—TLR, IFN and TACI—are downregulated in GC B cells (*21*, *110*). Their repression might function as a safeguard to prevent aberrant B cell activation in GCs.

Once B cell tolerance is breached, it manifests as circulating autoantibodies. In many cases, autoreactivity detectable in circulation targets ubiquitous self-antigens, such as DNA and histones. However, many autoimmune diseases affect specific organs: kidney in lupus nephritis, joints in rheumatoid arthritis (RA), pancreas in Type-1 diabetes, etc. Tissue lesions often contain antibody deposition, suggesting production of autoantibodies specific to afflicted organs. Those tissue-specific antigens are not readily accessible in secondary lymphoid organs. How do B cells become activated and selected for local antigens? In fact, B cells infiltrate into local tissues and mount *in situ* humoral responses.

1.5 Ectopic B cell activation in tertiary lymphoid structures

Although B cells normally generate specific and high-affinity antibodies in GCs, they can recapitulate the process in non-lymphoid tissues. There, B cells form aggregates called tertiary lymphoid structures (TLS) (*112*). TLS structurally resemble GCs and contain B, T and FDCs. Furthermore, TLS and GCs also share their functions. B cells in TLS often express proliferation markers such as Ki-67, suggesting their expansion (*113*, *114*). Additionally, B cells interact with Tfh cells in TLS (*115*). This interaction accompanies formation of supramolecular activation complex (SMAC), suggesting cognate interaction and T-cell help. Finally, B cells in TLS can express AID, accumulate SHM and class-switch their antibodies (*113*, *116*). These observations suggest TLS function as ectopic GCs.

In fact, affinity selection in TLS can occur in autoimmune diseases. In lupus nephritis, highly mutated antibodies cloned from tissue-infiltrating B cells targeted a self-antigen called vimentin (*117*). Moreover, this reactivity disappeared when mutations were reverted (*118*), suggesting that B cells became affinity-matured and selected for the anti-vimentin reactivity. Importantly, vimentin is highly abundant in inflamed kidneys. In line with this, antibodies expressed in synovia of RA patients frequently target locally abundant antigens such as calreticulin or citrullinated proteins (*119*, *120*). These results suggest that TLS select B cells for reactivity to local antigens.

Supporting the selection for local antigens, antibody repertoire in tissue-infiltrating and circulating B cells are clearly different (*121*, *122*). In the study of anti-vimentin antibodies, we also demonstrated that *in situ* selected antibodies did not react to double-stranded DNA, the most dominant antigen in serum reactivity of SLE patients (*117*). These observations underscore that

we need to study antibody repertoire of tissue-infiltrating B cells in order to fully understand humoral responses at the site of tissue inflammation.

Despite the structural and functional similarities of TLS to GCs, little is known about their transcriptional regulation. One of rare examples is an anti-apoptotic protein BCL2. Although BCL2 is downregulated in GCs, it is highly expressed in B cell infiltrates in lupus nephritis and allograft rejection patients (*123*). Furthermore, Bcl2 inhibition clears tubulointerstitial lymphocytes in lupus mice. These results indicate distinct transcriptional regulation of B cell activation in GCs and local tissues. However, a comprehensive, transcriptomic level comparison has yet to be done.

Furthermore, several local tissue-associated B cell subsets are reported. One is age-associated B cells (ABCs) (*124*). ABCs are originally identified as $CD11c^+$ B cell population enriched in aged mice (*125*, *126*). Their development requires a transcription factor T-bet (*127*). T-bet overexpression is even sufficient to acquire an ABC phenotype. T-bet is strongly induced by TLR7 stimulation. BCR engagement and IFN-γ also enhance the TLR7-mediated T-bet induction. However, BCR and IFN-γ alone have a minimal effect, highlighting importance of innate stimuli for ABCs. In fact, chronic stimulation by a TLR7 agonist greatly increases ABC number in wildtype mice (*125*). This increase is associated with antinuclear autoantibody development, implicating their role in autoimmune diseases. Indeed, ABC-like cells are present in autoimmune patients, especially enriched in afflicted tissues such as the synovium of RA patients (*128*) and the kidney of lupus nephritis patients (*129*, *130*). These results suggest their role in tissue inflammation.

Another interesting feature of ABCs is their similarity to B1 cells. First of all, they robustly secrete antibodies upon TLR7 stimulation (*125*). On the other hand, they are generally inert to

BCR engagement (*126*). They share surface marker expressions as well, such as high CD11b, TACI and low CD21 and CD23 (*125*, *126*). Additionally, despite the high TACI expression, both of them do not depend on BAFF for survival (*126*, *131*). However, they also have clear differences. For instance, ABCs do not express B1 markers CD5 and CD43 (*132*). Furthermore, ABCs express highly diverse, class-switched BCRs with somatic mutations, while B1 cells generally express a restricted set of unmutated IgM (*133*). Therefore, despite the similarities, they are likely to be independent subsets.

Another local inflammation-associated signature is hypoxia. A low oxygen level induces transcription factors which belong to hypoxia-inducible factor (HIF) family. HIF proteins, in particular HIF1a and HIF2a, exert various effects on all immune cell types, from homeostasis of hematopoietic stem cells in bone marrow to effector lymphocyte differentiation in periphery (*134*). Since inflammatory sites are generally hypoxic, local inflammation highly activates the HIF pathway in infiltrating cells. In fact, HIF1a^{+} CD4 and CD8 T cells infiltrate the kidney of lupus mice and patients (*135*). Pharmacological and genetic Inhibition of HIF1a ameliorates renal injury, suggesting a fundamental role of HIF1a in lupus nephritis.

These pathways are activated in local inflammation and seemingly drive pathogenesis. However, it is unknown whether they are characteristic to tissue-infiltrating cells or pathogenic immune responses. For instance, an ABC-like phenotype is acquired in protective B cell responses as well. T-bet expression by B cells is required to control chronic viral infection in mice (*136*). Albeit transiently, ABC-like cells appear in flu-vaccinated individuals as well (*137*). These observations indicate that the ABC-like phenotype is a mode of B cell activation involved in humoral responses in general. Additionally, GC B cells highly activate the HIF pathway (*9*, *138*). Hypoxia slows down antibody production and attenuates AID expression, indicating that the HIF

pathway regulates GC responses. Moreover, HIF1a can be induced by BCR engagement or LPS stimulation even at a normal oxygen concentration. Taken together, it is unclear whether these phenotypes represent tissue-local B cell activation. In order to define a phenotype specific to *in situ* B cell activation, we need to directly compare B cell activation signatures in GCs and local tissues.

For this purpose, I propose to investigate *in situ* B cell activation in renal allograft rejection patients. Although kidney biopsy is invasive, high prevalence of kidney transplant and location of allografts in front abdomen makes it easier to access than other diseases. Additionally, a phenotype of graft-infiltrating B cells is unknown. In particular, it is a long-standing question whether graft-infiltrating B cells become locally selected to donor HLAs. In the following sections, I describe how B cells participate in renal allograft rejection, what remains unknown, and how this study addresses it.

1.6 Antibody-mediated B cell roles in renal allograft rejection

Kidney transplant is by far the most common type of solid organ transplant. In the United States, more than 23,000 people received a kidney transplant in 2019 (Organ Procurement and Transplantation Network). This number has surged by nearly 40% within the last 10 years, due to increased prevalence of causal diseases such as diabetes and hypertension. Despite drastic improvement of immunosuppressive regimens, at least 10 % of recipients experience rejection one year after transplant. Furthermore, rejection rate is as high as 25% considering the first five years after transplant (*139*). Therefore, it is urgent to understand mechanisms of renal allograft rejection.

Humoral immune responses against allografts is a critical pathway driving rejection. The most frequently targeted antigens are HLAs. HLA loci are the most polymorphic regions in the

human genome: more than 26,000 alleles have been reported to date (*140*). Therefore, it is very common that a donor and a recipient have HLA mismatches. Mismatched HLAs elicit humoral responses in recipients, which develops donor HLA-specific antibodies (DSAs). Serum DSAs strongly indicate a worse transplant outcome (*141–143*). For this reason, serum DSA is one of the key criteria for diagnosis of allograft rejection.

DSAs are clinically tested using Luminex-based solid phase assays (*144*). HLA-binding assays are divided into two types: mixed-antigen and single-antigen bead (SAB) assay. Mix-antigen assay is a screening test, in which each Luminex bead is coated with a mixture of class-I or class-II HLAs. On the other hand, each bead in SAB assay is coated with a single allotype of HLA. SAB is preferentially used in clinics, since it can reveal specific allotypes targeted by antibodies. However, SAB assay is subject to false positive. Since SABs are coated without beta-2 microglobulins (β2m), epitopes masked with β2m *in vivo* are exposed. Purification and coating of HLAs also induces denaturation, creating non-native epitopes (*145*). Additionally, variation among lots and manufacturers is evident (*146*, *147*). Therefore, one needs to account for such false positives in order to draw a reliable conclusion.

Eplets help clinicians identify true HLA reactivity (*148*). Eplets are polymorphic amino acid residues in HLAs. Structural proximity defines them so that each eplet represents a domain which antibodies can recognize. Given HLAs share a distinct set of eplets. Therefore, serum reactivity is suggested to be true if it targets multiple HLA allotypes sharing eplets which are specifically expressed by a donor.

In addition to DSAs, antibodies against several non-HLA antigens have been detected in recipients' serum (*149*). Vascular endothelial cells in particular are speculated as a source of non-HLA antigens. In fact, serum reactivity to endothelial cells can develop in rejection patients (*150*).

Several antigens expressed by endothelial cells have been identified as targets, such as Angiotensin type 1 receptor (AT1R) and perlecan, a component of vascular walls (*151*, *152*). Development of such non-HLA reactivity suggests a break in tolerance.

However, such non-HLA antibodies are not necessarily a manifestation of autoimmunity. A study of genome-wide non-synonymous SNPs demonstrated that non-HLA mismatches between a recipient and a donor are associated with graft loss, independently of HLA mismatches (*153*). Furthermore, allograft recipients developed antibodies against epitopes predicted from the non-HLA mismatches. This finding suggests that non-HLA reactivity could also arise from allotypic differences.

A representative example of such non-HLA alloantigens is minor histocompatibility antigens. It has been long known that minor histocompatibility antigens underlie rejection in HLA-matched transplant (*154*). Most well-studied antigens are those encoded on Y chromosome, so-called HY antigens. Although X and Y chromosomes are highly homologous, proteins encoded in distinct regions on Y chromosome become immunogenic when transplanted into females. In kidney transplant, male-to-female transplant has the highest risk of rejection (*155*). Antibodies directed to HY antigens indicate that HY antigens drive B cell selection in renal allograft rejection (*156*). Additionally, autosomal minor antigens were also characterized (*157*). MHC class I polypeptide-related sequence A (MICA) is one of them. As MICA is encoded in an HLA locus, it is highly polymorphic. In fact, MICA antibodies are associated with renal allograft rejection (*158*). Although most other autosomal minor antigens are restricted to class-I HLA, class-II restricted antigens have been also reported. Therefore, those antigens could also elicit humoral responses.

Produced graft-reactive antibodies damage tissues via Fc receptor-mediated cytotoxicity (*159*) or complement activation (*160*). In particular C4d, a product of complement activation, is

often deposited in rejected renal allografts. C4d deposition indicates activation of the complement pathway that directly damages tissues. In fact, C4d deposition predicts early graft loss (*161*). These observations highlight a direct role of antibodies in allograft rejection.

One of the central questions is how B cells are selected for antigens in allograft, especially HLAs. Although GCs in secondary lymphoid organs would plausibly be where DSAs and other anti-graft antibodies develop, they could possibly be produced by *in situ* B cell activation as well. B cell aggregates in allografts were associated with poor prognosis in several studies (*162–164*). Although a few studies failed to reproduce this association (*165–167*), the discrepancy could be due to the vague definition of "B cell clusters," limited sample sizes or inter-patient variation. These graft-infiltrating B cells showed clonal expansion and SHMs (*168*, *169*). Additionally, $CD138^+$ or $CD38^+$, but not $CD20^+$, clusters are associated with serum DSAs (*163*, *170*, *171*). Albeit in explants, organized TLS have also been reported (*172*). Taken together, an *in situ* origin of DSAs is an interesting hypothesis to test. However, studies have been hampered by difficulty in accessing patient tissues.

To circumvent this problem, various animal models have been created. Some of them involve B cell infiltration in allografts (*173–176*). However, renal allografts tend to become rejected within a few weeks in animal models (*177*), which contrasts with human cases where rejection can take years to proceed. Therefore, animal models do not well represent kinetics of B cell selection in human renal allograft rejection. Most importantly, mouse transplant models often rely on a complete MHC mismatch. Therefore, B cell responses in mouse models are heavily skewed toward allo-MHCs. On the other hand, as discussed above, humoral responses in transplant patients target a broad range of non-HLA antigens as well. In one study, more than 40 % of patients who were positive for tissue C4d deposition did not have detectable serum DSA (*178*). These

observations suggest that developmental mechanisms of anti-graft antibodies are much more complex in humans.

There is one mouse model which develops non-HLA antibodies. This model utilizes a mismatch of only three amino acids in MHC-II I-A between C57BL/6 and bm12 strains (*179*). In this model, recipient mice develop antinuclear autoantibodies. Interestingly, this autoantibody production depends on donor $CD4^+$ T cells, at least in the context of cardiac allografts (*180*). These findings indicate that so-called "passenger" cells present in allografts play an active role in shaping B cell reactivity in allograft rejection (*181*, *182*). However, as this model fails to mount anti-MHC humoral responses, it has not been considered to model typical cases of allograft rejection. Taken together, these mouse models are not ideal for studying how B cell reactivity is locally selected in patients. In order to understand how B cell reactivity is shaped in renal allografts, we need to directly study it in humans.

One study tackled this challenge, by producing monoclonal antibodies from graft-infiltrating B cells in one patient (*183*). In this study, they found only two HLA-reactive clones out of more than 100 clones tested, despite serum DSA positivity of the subject. This result indicates that graft-infiltrating B cells do not produce DSAs. Their antibodies were not selected for ubiquitous self-antigens either. As an alternative mechanism selecting B cell reactivity, they proposed polyreactivity. Polyreactive antibodies can bind to structurally distinct antigens, which is usually measured by an enzyme-linked immunosorbent assay (ELISA) with plates coated with double-stranded DNA, LPS and insulin (*86*). However, frequency of polyreactive antibodies they found were no higher than that in naïve B cell repertoire (*86*). Therefore, it is unknown for what reactivity intrarenal B cells are selected.

This lack of apparent affinity selections echoes another mouse study, in which antigen non-specific T cells can also infiltrate allografts (*184*). However, even such specificity-independent migration requires other antigen-specific T cells. Furthermore, B cells need to encounter local antigens to reside in tissues (*185*). These mouse studies indicate that graft-infiltrating B cells should recognize, and be possibly selected for, local antigens.

Importantly, this previous human study had several caveats. First of all, they studied only one subject, which makes it impossible to generalize their findings. Moreover, their observation does not necessarily reflect what is happening in the course of rejection, since they investigated an explant, a "dead" kidney allograft at the end stage of rejection. Finally, they collected B cells using a pan-B cell marker CD20 alone, which missed plasma cells. Therefore, another study with more subjects, especially focused on activated B cells in an early stage of rejection, is desired.

1.7 Antibody-independent B cell roles in renal allograft rejection

Although antibodies definitely play a critical role in rejection, B cells modulate immune responses via cytokines as well (*186*). B cells express a wide array of cytokines upon *in vitro* stimulation. Interestingly, B cells co-stimulated with Th1 cells express type-1 cytokines such as IFN-γ, while coculture with Th2 cells upregulates type-2 cytokines such as IL-6 (*187*). Those polarized B cells in turn dictate differentiation of naïve T cells. These results suggest that a complex interplay in a local immune environment controls cytokine production by B cells.

B cell-derived cytokines have profound effects in inflammation. One such example is IL-15. IL-15 is a potent proinflammatory cytokine upregulated in many inflammatory diseases. Although a majority of IL-15 is believed to be produced by monocytes or epithelial cells (*188*), B cells also express IL-15 (*189*). In multiple sclerosis patients, B cell-derived IL-15 enhances

cytotoxicity of CD8 T cells. Although IL-15 overexpression is associated with renal allograft rejection as well (*190*), it is entirely unknown whether B cells express IL-15 in this context.

Regarding allograft rejection, however, the most notable is a phenotype called regulatory B (Breg) cells (*191*). Breg cells express an immunosuppressive cytokine IL-10 and induce graft tolerance. Murine Breg cells often express B1 marker CD5, suggesting their B1 origin. However, paralleling the elusiveness of human B1 cells, studies failed to associate human Breg cells with a specific B cell subset (*192*). A suppressive function of mouse Breg cells were demonstrated both *in vitro* and *in vivo* (*176*, *193*). The presence of suppressive B cells has been indirectly suggested in humans as well. In healthy individuals, a small fraction of circulating B cells produce IL-10 upon *ex vivo* stimulation and suppress T-cell activation (*194*, *195*). In the context of transplant, tolerant recipients had increased circulating B cells (*196*, *197*). Moreover, pan-B cell depletion by rituximab induced acute allograft rejection in five out of six (83 %) patients (*198*). This incidence was much higher than a control group treated with an anti-CD25 antibody (14 %) or even compared with patients without an induction therapy (35 %) (*199*). Although these accumulating evidence highlight a regulatory role of B cells, it is unknown whether graft-infiltrating B cells have this phenotype. The lack of knowledge on *in situ* B cell phenotype further underpins the need for their detailed characterization.

1.8 Aims and significance

Despite our growing understanding of the mechanisms of GC responses and accumulating observations of TLS and B cell infiltrates in various diseases, differences in regulatory mechanisms of B cell activation at different sites still remain a fundamental question in the field of B cell biology. Given their presence at the very site of inflammation, elucidation of phenotypes

of TLS-forming B cells should provide important insights into how B cells drive tissue-local inflammation.

Although sample limitation has been the biggest barrier to studying human TLS, recent advances of next-generation sequencing (NGS) have enabled us to obtain a tremendous amount of data from small biopsies. Especially, scRNA-seq provides transcriptomic analyses with an incredible depth of information. At the same time, its single cell-level resolution allows BCR repertoire analyses and production of recombinant antibodies to identify their targets. Collectively, it is an ideal approach to study *in situ* B cell biology in human diseases (*200*, *201*).

Here, I present a study to unveil transcriptional characteristics of local B cell activation in rejecting kidneys of transplant patients. I set out to accomplish two specific aims:

Aim 1:

To identify an *in situ* B cell phenotype in human renal allograft rejection. For this aim, I perform scRNA-seq on activated B cells collected from biopsies of renal allograft rejection patients and compare them to those in tonsil GCs. I hypothesize that local B cell activation in rejecting allografts has a transcriptional profile distinct from that in tonsil GC responses. Furthermore, I postulate that these differences will reflect both unique proinflammatory functions and mechanisms of intrarenal B cell activation.

Aim 2:

To characterize reactivity and selection of *in situ* antibody repertoire in human renal allograft rejection. I hypothesize that there is *in situ* selection for anti-HLA reactivity. Therefore, I will identify HLA-reactive antibodies using a clinically approved Luminex-

based assay. I will also screen for autoreactivity with HEp-2 cell staining. When selection for self-antigens is obvious, specific targets will be identified with mass spectrometry. These analyses will identify antigens and potential mechanisms driving *in situ* B cell selection.

This study reveals that intrarenal B cells have a unique innate phenotype reminiscent of peritoneal B1 cells. Additionally, comparison with gene expression in whole renal allografts demonstrate complex local interactions around B cells. Surprisingly, their antibodies did not react to allo-HLAs. Instead, plasma cells expressed antibodies clonally selected to nucleolar self-antigens including Ki-67. These findings highlight the importance of investigating what is happening *in situ* of afflicted organs in order to understand mechanisms of tissue inflammation.

2 Transcriptional profile of intrarenal B cells in human renal allograft rejection

2.1 Introduction

GCs orchestrate clonal expansion, SHM and affinity selection to produce high-affinity antibodies and immunological memory (*6*). However, the same process also drives pathogenic humoral responses in many inflammatory and autoimmune diseases. Self-destructive B cell activation often accompanies formation of GC-like structures in afflicted organs, called TLS (*112*). TLS exhibit hallmarks of B cell selection including clonal expansion and SHM. However, despite the functional similarity between GCs and TLS, little is known about transcriptional regulation of TLS. To comprehensively understand mechanisms underlying tissue-local B cell responses, a direct transcriptomic comparison of B cell activation between a local tissue and a secondary lymphoid organ is necessary.

For this purpose, human renal allograft rejection serves as an interesting subject. B cells infiltrate rejecting renal allografts and form TLS. Intrarenal B cell clusters predict poor graft survival (*162–164*). However, their role in rejection is unknown. They could be promoting tissue destruction by producing allograft-reactive antibodies. Additionally, they could be modulating a local immune environment by cytokines. Elucidating a phenotype and mechanisms of antigen selection of intrarenal B cells would provide insights into how they contribute to allograft rejection.

Here, I present a direct transcriptomic comparison of activated B cells in rejecting renal allografts and tonsil GCs, utilizing scRNA-seq. Analyses revealed that intrarenal B cells have a unique transcriptional state that resembles innate-like peritoneal B1 cells. Furthermore, intrarenal B cells displayed complex autocrine and paracrine interactions within allografts. These data highlight a site-specific B cell phenotype and potential mechanisms driving local inflammation.

2.2 Results

2.2.1 Distinct transcriptional states in activated intrarenal and tonsil B cells

To better understand *in situ* B cell responses in renal allograft rejection, $CD45^+$ $DAPI^-$ $Calcein^+$ $CD19^+$ $CD38^+$ activated B cells were sorted from five renal allograft biopsies and four tonsillectomy samples (Figure 2.1A). B cell infiltration was confirmed in a paired biopsy from each allograft patients by immunohistochemistry (Figure 2.1B). Those biopsies were reviewed by a blinded renal pathologist for diagnosis. C4d deposition and serum DSA were also clinically tested. Results and clinical characteristics for each patient are summarized in Table 2.1.

Sorted B cells were then subjected to scRNA-seq following the Smart-Seq2 protocol (*202*). To ensure a high-quality dataset, we excluded cells which had less than 3,000 or more than 15,000 expressed genes (Figure 2.1C). We also removed potential non-B cells which had low expression of immunoglobulin (Ig) constant region genes. After this quality control (QC), 655 renal and 129 tonsil B cells were used for subsequent analyses. Batch effects from separate sequencing runs were normalized using an External RNA Control Consortium (ERCC) spike-in control and RUVSeq R package (*203*) (Figure 2.1D and E).

To assess cell population heterogeneity, sequenced cells were mapped onto a t-distributed stochastic neighbor embedding (t-SNE) space. As demonstrated in Figure 2.2A, renal B cells formed one diffuse cluster while tonsil B cells formed two distinct clusters, one of which overlapped with the kidney cluster and the other that was distinct. This clustering was not due to batch-associated differences, suggesting that B cells in renal allograft and tonsil had distinct transcriptional profiles. Moreover, B cells from all five renal biopsies were distributed similarly in the t-SNE space. Therefore, intrarenal B cells had a similar transcriptional profile across patients

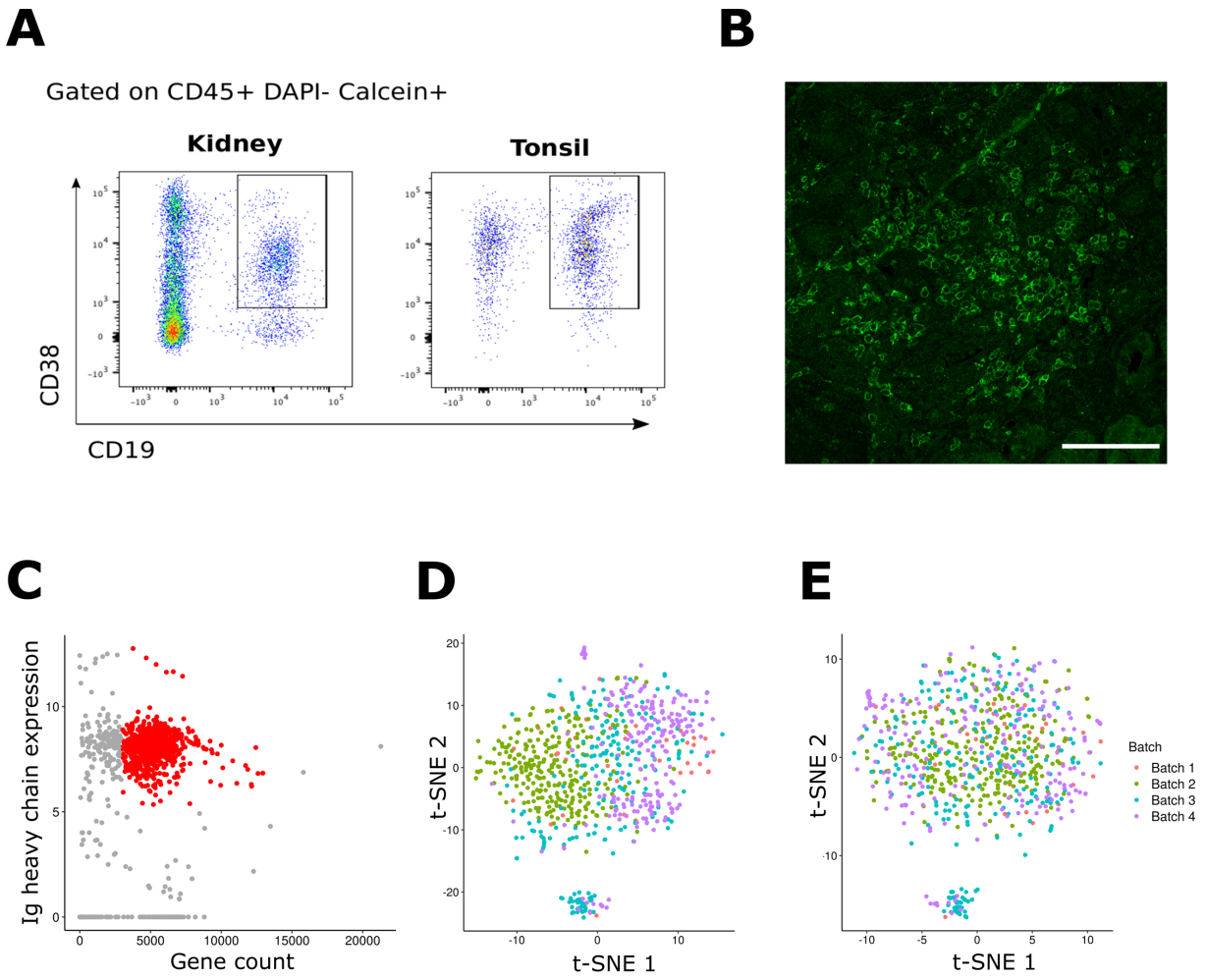

Figure 2.1 Gating scheme for cell sorting and QC of scRNA-seq data.

(A) Gating scheme for single-cell sorting of $CD19^{+}$ $CD38^{+}$ activated B cells in renal allograft and tonsil samples. (B) A representative image of a $CD19^{+}$ cell cluster observed in patient biopsies. A scale bar indicates 50 μm. (C) A scatter plot showing detected gene count and Ig heavy chain gene expression on the x and y axis respectively. Cells which passed QC are colored in red. (D and E) t-SNE plots colored by experimental batches before (D) and after (E) batch normalization with ERCC spike-in and RUVSeq.

Table 2.1 Patient information.

Cohort	First									Second					
Patient	Kidney 1	Kidney 2	Kidney 3	Kidney 4	Kidney 5	Tonsil 1	Tonsil 2	Tonsil 3	Tonsil 4	Kidney 6	Kidney 7	Kidney 8	Tonsil 5	Tonsil 6	Tonsil 7
Gender	4 Females and 1 Male					NA				3 males			NA		
Age	Mean = 50, s.d. = 15.6									Mean = 55, s.d. = 9.5					
Kidney survival (yr)	Mean = 11.3, s.d = 8.6									Mean = 9.2, s.d.= 11.1					
Disease*	HT	IgAN	HT	RN	MCKD					T2D, HT	HT	T1D			
C4d deposition	No	No	No	Yes	No					Yes	Yes	Yes			
Serum DSA	No	No	No	Yes	No					Yes	Yes	No			
Sorted cells	96	336	96	192	192	48	48	96	96	192	96	96	96	96	96
Cells after QC	71	262	69	77	176	43	41	21	24	137	51	77	87	81	84

* HT: Hypertension, IgAN: IgA nephropathy, RN: Reflux nephropathy, MCKD: Medullary cystic kidney disease, T1D/T2D: Type-1/2 diabetes

Table 2.2 Ig class distribution.

Cohort	First									Second						
Ig class	Kidney 1	Kidney 2	Kidney 3	Kidney 4	Kidney 5	Tonsil 1	Tonsil 2	Tonsil 3	Tonsil 4	Kidney 6	Kidney 7	Kidney 8	Tonsil 5	Tonsil 6	Tonsil 7	Total
IGHM	27	165	31	68	111	33	20	15	10	13	19	33	37	21	43	646
IGHD	0	10	0	0	0	0	0	1	0	10	2	1	8	14	26	72
IGHA1	10	13	9	2	18	1	1	3	0	10	7	11	8	11	3	107
IGHA2	1	3	1	0	2	0	0	0	0	0	1	4	1	0	1	14
IGHG1	23	52	19	2	30	6	15	1	11	88	16	11	16	23	4	317
IGHG2	4	13	2	3	11	0	1	0	0	4	2	8	6	4	5	63
IGHG3	6	6	7	2	3	3	4	1	3	12	2	9	11	8	2	79
IGHG4	0	0	0	0	0	0	0	0	0	0	1	0	0	0	0	1
IGHE	0	0	0	0	1	0	0	0	0	0	1	0	0	0	0	2
Total	71	262	69	77	176	43	41	21	24	137	51	77	87	81	84	1301

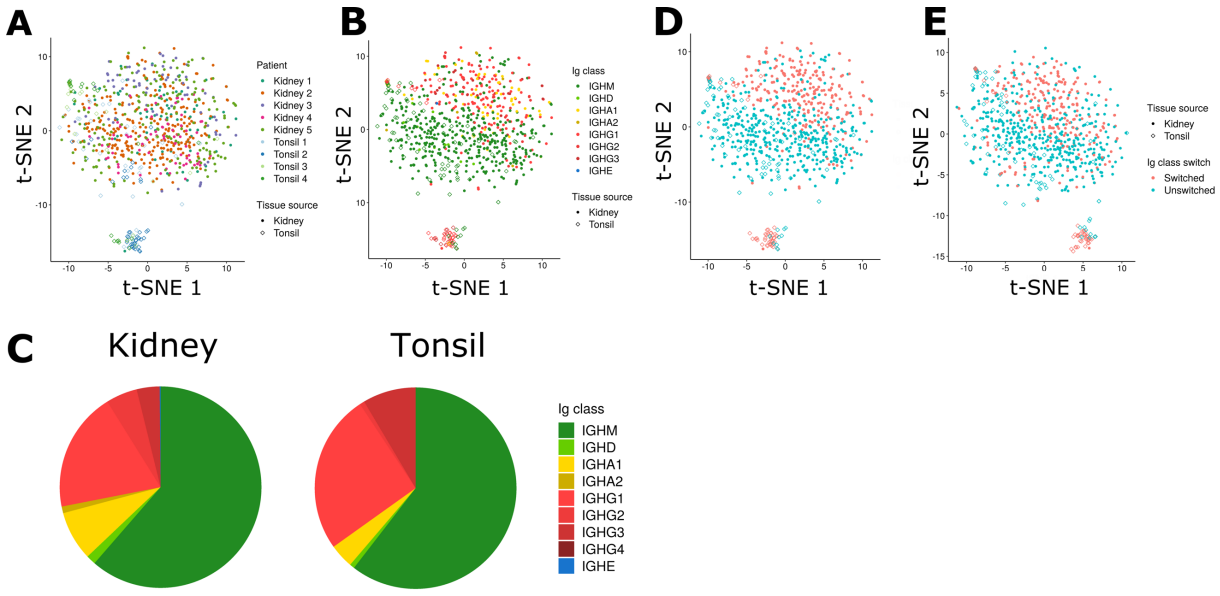

Figure 2.2 B cells clustered based on Ig class switch.

(A and B) t-SNE plots showing B cell distribution in scRNA-seq data. Shape indicates tissue sources from which cells were derived. Color indicates patients (A) or expressed Ig classes (B). (C) Pie charts showing distribution of expressed Ig classes. (D and E) t-SNE plots showing clustering dependent on Ig class switch with (D) or without (E) Ig heavy chain constant region genes. Ig-unswitched (IgM or IgD expressing) cells are colored in blue, and switched (otherwise) cells are colored in red.

regardless of clinical features.

Although intrarenal B cells formed a single diffuse cluster on t-SNE, this population split based on Ig class-switching states (Figure 2.2B). About 70 % of both renal and tonsil B cells expressed IgM, and the remaining cells mostly expressed IgG or IgA (Figure 2.2C). Each patient had different proportions of Ig-class switched cells (Table 2.2). However, across patients, unswitched and class-switched cells were similarly distributed in the t-SNE space. Ig class also distinguished the two tonsil B cell clusters. Unswitched tonsil and renal B cells largely overlapped while each switched population formed distinct clusters. Importantly, this separation remained when genes encoding Ig heavy chain constant regions were removed from analysis (Figure 2.2D and E). These data suggest that B cells in rejected renal allografts and tonsil are similar prior to CSR but diverge thereafter.

Differential gene expression was then assessed across tissue sources and Ig class-switch states. These comparisons identified 2855 differentially expressed genes (DEGs) in total (Supplementary Table 2.1). Hierarchical clustering divided them into five clusters (Figure 2.3A). Cluster 1 contained genes specifically downregulated in switched tonsil cells. Clusters 2 and 3 were genes preferentially expressed in intrarenal cells. On the other hand, cluster 4 represented genes repressed in intrarenal cells. Finally, cluster 5 contained genes specifically upregulated in switched tonsil cells.

Pathway enrichment analysis based on Gene Ontology (GO) and Kyoto Encyclopedia of Genes and Genomes (KEGG) databases revealed specific biological pathways enriched in each cluster (Figure 2.3B). Cluster 1 was highly enriched for IFN-related pathways. IFN-γ signaling-related genes in clusters 1 and 2 included *STAT1*, *IRF1* and *NLRC5* (Figure 2.3C). IFN-γ activates STAT1, which induces *IRF1* and *NLRC5* (*204*). NLRC5 activates genes encoding HLA class I and

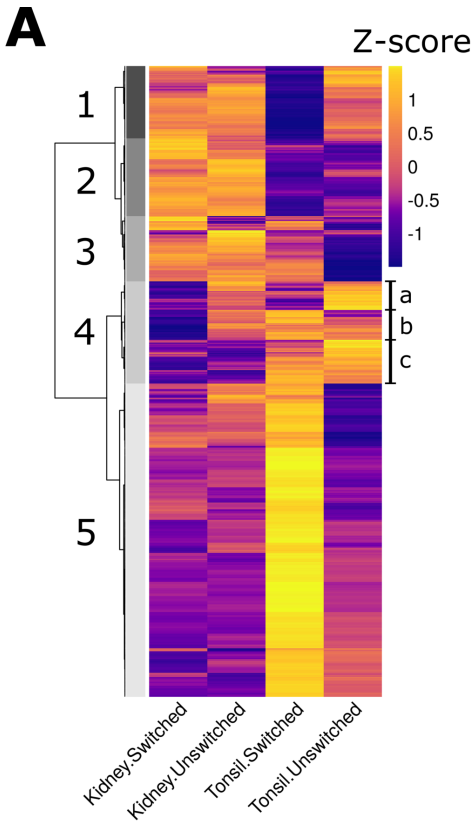

Figure 2.3 Genes and pathways active in intrarenal B cells represented their unique phenotype. (A) A heatmap showing hierarchical clustering of the 2855 DEGs. Row Z-scores were calculated from mean expression values of each gene in the four populations based on their tissue sources and Ig class switch states. (B) Enrichment of GO terms and KEGG pathways in the five gene clusters. At most 10 most significantly enriched pathways were shown per cluster.
(Continued on the next page) (C-F) Violin plots showing expression levels of representative genes in indicated pathways. Cells are grouped by tissue sources and Ig class-switch states.

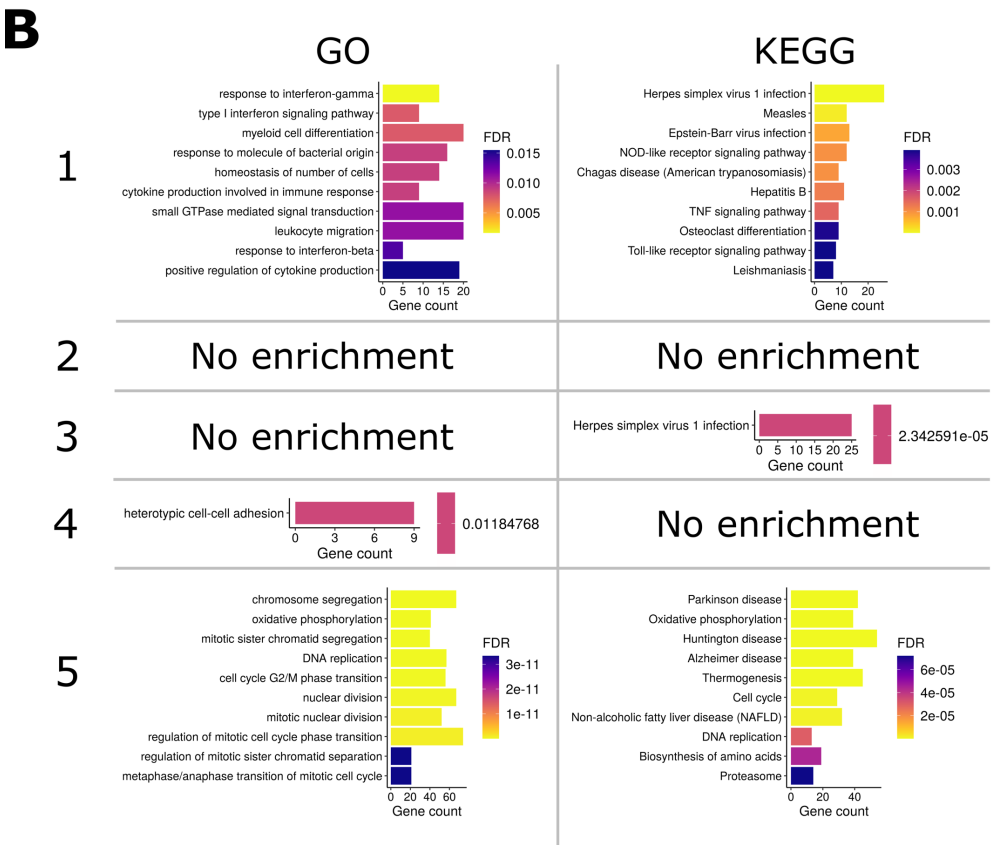

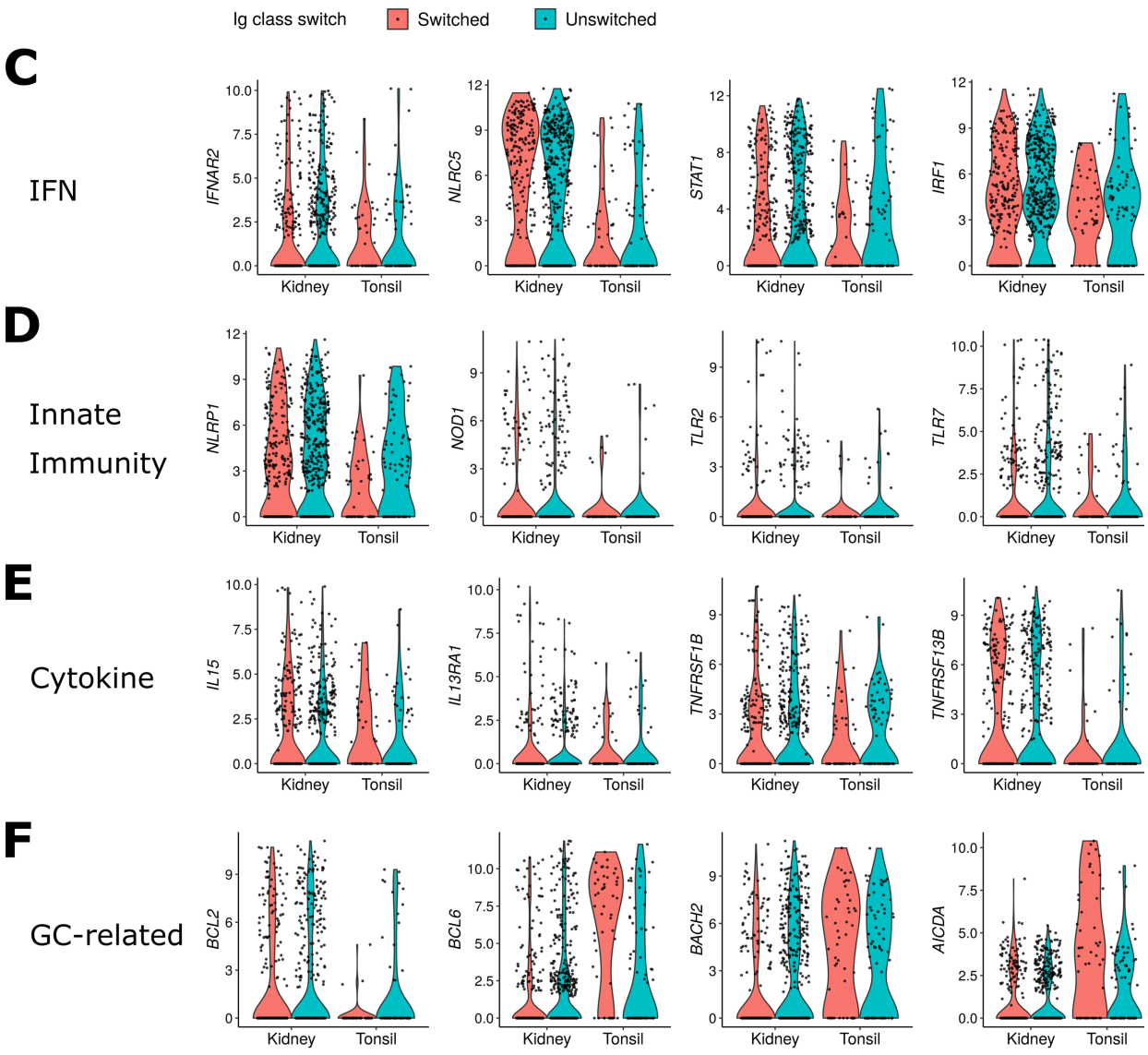

Figure 2.3 (Continued)

their machinery. Clusters 1 and 2 contained *HLA-C*, *B2M*, *TAPBP*. *STAT1* and *IRF1* are shared with type-1 IFN signaling downstream of *IFNAR2*, which was also present in cluster 2. These results suggest that IFN pathways are globally activated in intrarenal B cells.

IFN stimulation enhances sensitivity of B cells to innate stimuli (*106*). Indeed, both GO and KEGG pathways pointed out enrichment of innate immune signaling pathways in cluster 1. Intrarenal B cells highly expressed specific pattern recognition receptors (PRRs) in clusters 1 and 2, including *NLRP1*, *NOD1*, *TLR2 and TLR7* (Figure 2.3D). In addition to these PRRs, clusters 1 and 2 contained their downstream signaling components as well, such as *TRAF3*, *TRAF6*, *RIPK1* and *MAPK13*. Therefore, intrarenal B cells highly express genes of innate immune sensing and signaling pathways.

Many of these innate immune genes were also associated with cytokine production-related pathways, which were enriched in cluster 1. In line with this, cluster 2 and 3 had several cytokine ligands and receptors preferentially expressed by intrarenal B cells: *IFNAR2, IL15*, *TNFRSF1B*, and *TNFRSF13B* (Figure 2.3E). Among them, *TNFRSF13B* had the most significant difference between intrarenal and tonsil B cells. *TNFRSF13B* encodes TACI, a receptor for B cell-activating cytokine BAFF. BAFF is abundant in rejecting renal allografts (*205*). Therefore, the high expression of *TNFRSF13B* could be important for intrarenal B cells activation by BAFF.

Anti-apoptotic factor *BCL2* was also found in cluster 1 (Figure 2.3F). This is consistent with our previous report that intrarenal B cells highly express BCL2 in human renal allograft rejection and lupus nephritis (*123*). Along with *BCL2*, many of the pathways enriched in cluster 1, such as IFN, TLR, or cytokine production-related pathways are direct targets of BCL6, a transcriptional repressor in GC responses (*21*). Indeed, expression of *BCL6* was lower in renal B cells as well as another transcriptional repressor *BACH2*, which shares targets with BCL6 (*22*).

These results suggest that some of the intrarenal B cell phenotype might be due to a lack of *BCL6* and *BACH2* expression.

BCL6 and *BACH2* belonged to cluster 5. This cluster was enriched for several pathways that have been ascribed to GC B cells, including proliferation and SHM. Notably, *AICDA* was expressed in class-switched tonsil B cells but not significantly in other B cell populations. We did not find differential expression of other genes encoding GC-related transcription factors, such as *POU2AF1*, *POU2F2*, *IRF4*, *FOXO1*, and *MYC*. Collectively, these results indicate that intrarenal class-switched B cells lack the essential transcriptional features of GC B cells, which could be mainly attributed to repressed *BCL6* and *BACH2*.

Along with cluster 5, cluster 4 contained genes suppressed in intrarenal B cells. Although cluster 4 had only one enriched pathway, this cluster also contained several genes implicated in B cell functions. Cluster 4 splits into three subclusters (a, b, c). Cluster 4a contained genes commonly downregulated in class-switched cells, such as *IGHD* and *IGHM*. On the other hand, cluster 4b and 4c respectively contained genes suppressed in class-switched, or both switched and unswitched, intrarenal B cells. Cluster 4b contained regulators of BCR signaling, *CD79B* and *FCRL3* (*206*), whereas cluster 4c contained several HLA class-II genes. This differential expression might underlie distinct modes of activation between intrarenal and tonsil B cells.

2.2.2 Intrarenal B cells resemble peritoneal B1 cells

Clusters 2 and 3 represented genes highly expressed by intrarenal B cells. However, neither of them demonstrated enrichment of specific GO terms. Instead, examination of individual DEGs revealed potentially important differences. Most notable was *AHNAK* (Figure 2.4A). *AHNAK* mRNA levels were far higher in intrarenal B cells compared with tonsil B cells regardless of Ig

class switch (Figure 2.4B). Expression of the AHNAK protein in intrarenal B cells was confirmed by confocal microscopy (Figure 2.4C).

Although AHNAK is important for regulation of calcium signaling in activated T cells in mice (*207*), its role in B cell biology is unknown. Interestingly, within mouse B cell subsets, *Ahnak* is preferentially expressed in peritoneal cavity B1 cells (ImmGen (*208*), Figure 2.4D). Furthermore, cluster 2 had other genes specifically expressed in peritoneal B1 cells, such as *ITGAM* (CD11b) and *S100A6* (Figure 2.4E and F). These observations motivated us to examine whether cluster 2 was enriched for genes having this peritoneal B1-specific expression pattern.

333 mouse genes had an expression pattern similar to *Ahnak* in peripheral B cell subsets (ImmGen, correlation coefficient $\geq$ 0.8) (Figure 2.4G and Supplementary Table 2.2). The *Ahnak*-covariant mouse genes corresponded to 293 human homologs. These "*AHNAK*-covariant" human genes had enrichment of pathways related to cell adhesion, lymphocyte activation and LPS responses, reflecting a unique phenotype of peritoneal B1 cells (Figure 2.4H and I). *AHNAK*-covariant genes were highly enriched in cluster 2 and to a lesser degree in clusters 1 and 3 (Figure2.4J). These results suggest that *AHNAK*-covariant genes represent *in situ* B cell activation in renal allograft rejection.

Although *AHNAK*-covariant genes were enriched in cluster 2, they represented only 5% of the cluster. Therefore, we next tested if cluster 2 genes were generally enriched in peritoneal B1 cells. Using ImmGen microarray data, B cell subsets were scored for expression of genes in each DEG cluster. This analysis demonstrated that peritoneal B1 cells had a higher score for cluster 2 than the other populations (Figure 2.4K). This trend was weaker, but still present, when scores were calculated without *Ahnak*-covariant genes (Figure 2.4L). This result suggests that intrarenal B cells highly express genes associated with peritoneal B1 cells.

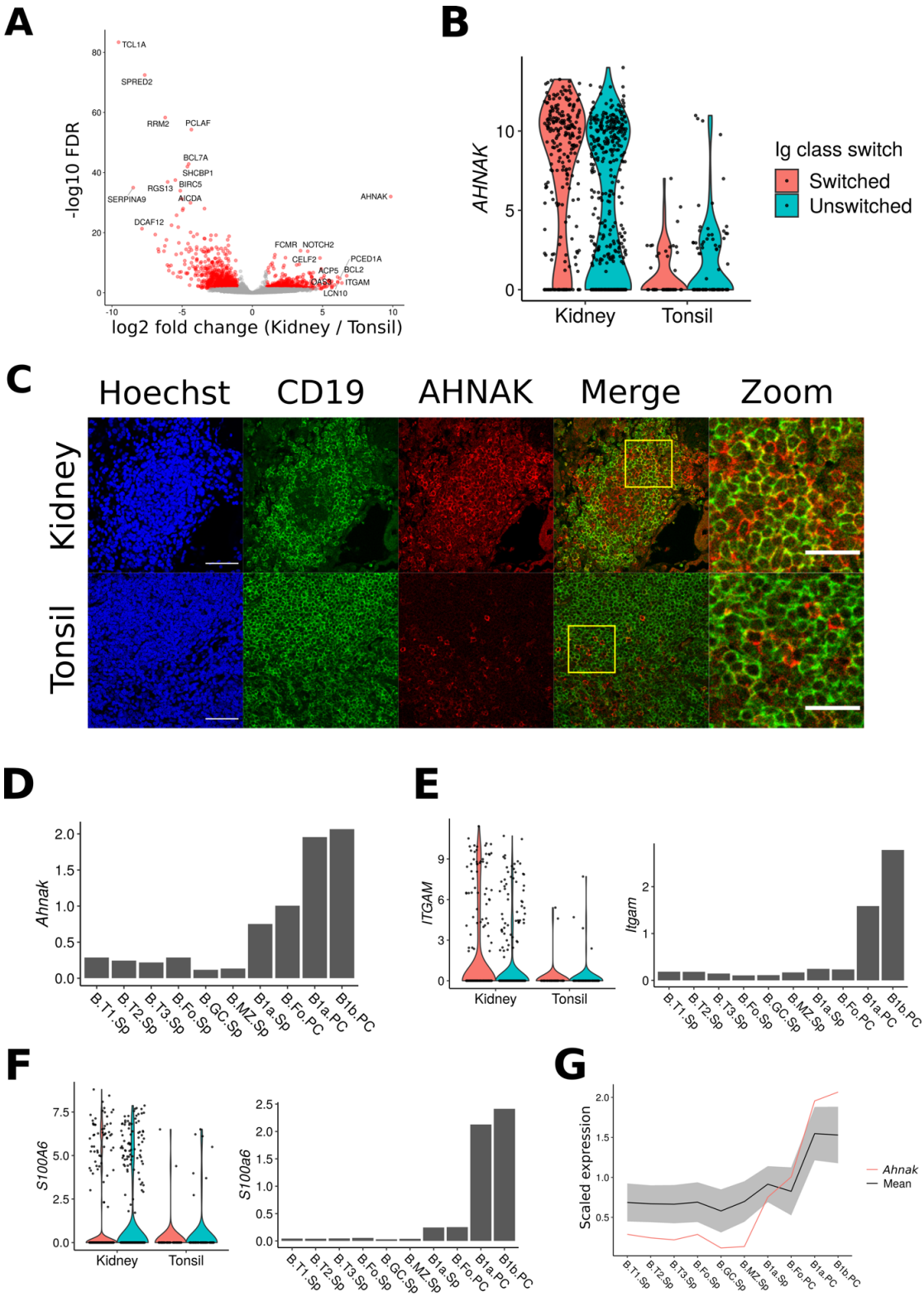

Figure 2.4 AHNAK represents a B1-like transcriptional profile of intrarenal B cells.

(Continued from the previous page) (A) A volcano plot showing DEGs between Ig class-switched intrarenal and tonsil B cells. Genes expressed higher in intrarenal B cells are shown on the right side of the plot. Genes with a significant difference are colored in red. (B) A violin plot demonstrating mRNA expression of *AHNAK*. (C) Staining images of AHNAK with nuclei (Hoechst) and a B-cell marker CD19 in rejected renal allograft and tonsil. The high-magnification panel corresponds to the yellow square on the merged panel. Scale bars indicate 50 μm or 25 μm (high-magnification panel). (D) *Ahnak* expression pattern in peripheral mouse B cell subsets. T: transitional, Fo: follicular, GC: germinal center, MZ: marginal zone, Sp: spleen, and PC: peritoneal cavity. (E and F) Violin plots and expression patterns of a murine homolog of *ITGAM* (E) and *S100A6* (F). (G) Expression of 333 mouse genes that correlate with *Ahnak*. The mean value of the 333 *Ahnak*-covariant genes (including *Ahnak* itself) is shown as a black line with a grey shade indicating standard deviation. The red line indicates *Ahnak* expression.

(Continued on the next page) (H and I) Enrichment of GO terms and KEGG pathways in the 293 *AHNAK*-covariant genes. At most 10 most significantly enriched pathways are shown. (J) Enrichment of the *AHNAK*-covariant genes in each gene cluster from Figure 2.3A. (K and L) (K and L) Heatmaps showing DGE cluster scores of each murine B cell subset, calculated with (K) or without (L) *Ahnak*-covariant genes. Rows and columns respectively represent gene clusters and murine B cell subsets. DEG scores were scaled by row to obtain Z-scores. Rows and columns respectively represent gene clusters and murine B cell subpopulations. DEG scores were scaled to obtain row Z-scores. (M) Gene expression scores for *AHNAK*-covariant genes tagged to “innate immune response” GO term. * $p = 0.016$

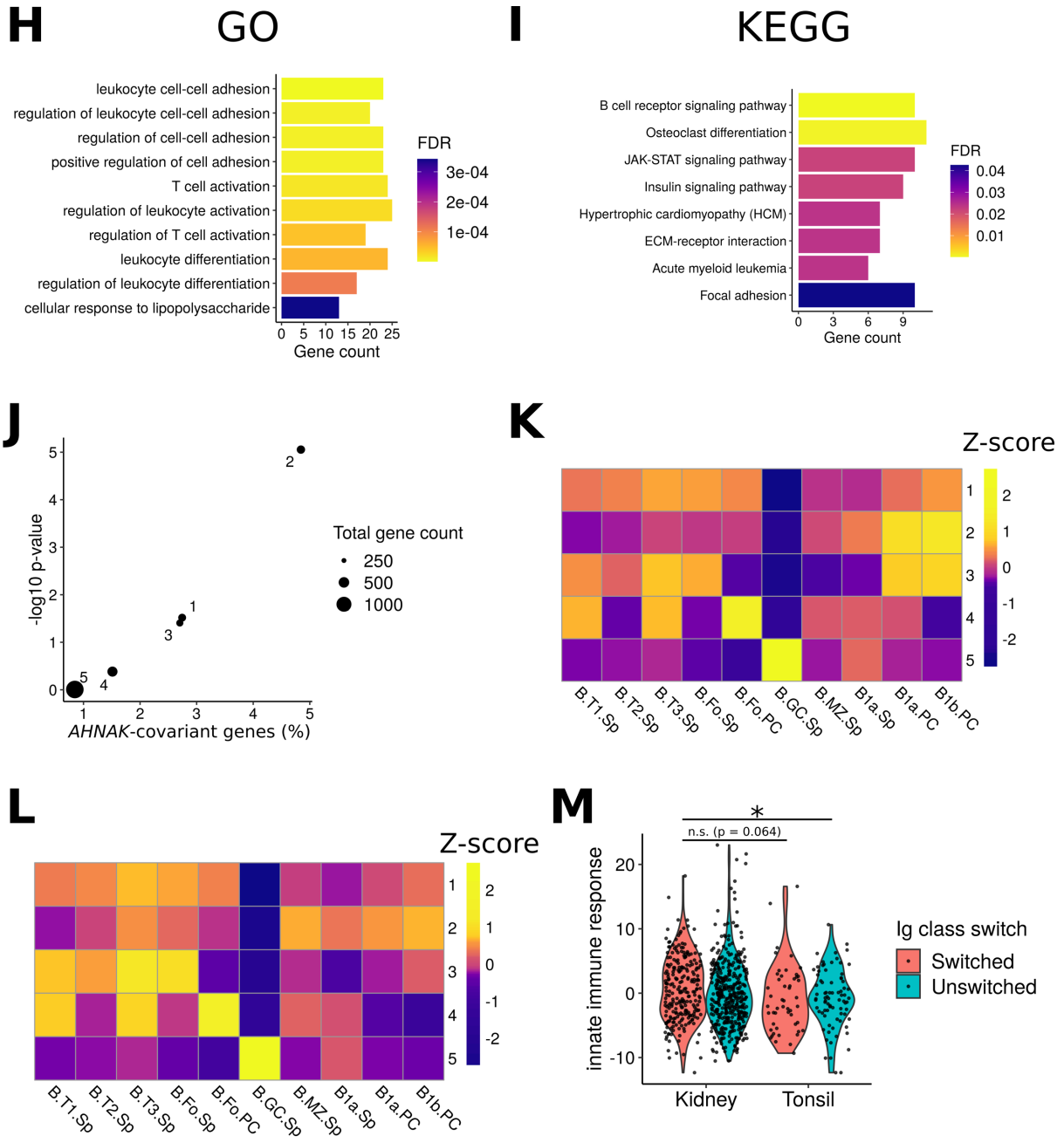

Figure 2.4 (Continued)

B1 cells are known as innate-like B cell subsets. Intrarenal B cells also highly expressed genes encoding PRRs and their signaling components. Therefore, we next investigated whether intrarenal B cells and mouse peritoneal B1 cells expressed a similar set of innate immune genes. As a reference of innate immune genes characteristic to peritoneal B1 cells, we identified *AHNAK*-covariant genes which were tagged to "innate immune response" GO term (Supplementary Table 2.2). When scores were calculated for expression of those genes, Ig-switched intrarenal B cells had a significantly higher score than Ig-unswitched tonsil B cells (Figure 2.4M). Albeit insignificant ($p = 0.064$), this trend was present between Ig-switched intrarenal and tonsil B cells. Collectively, these results indicate that intrarenal B cells resemble peritoneal B1 cells in terms of innate gene expression as well.

We also investigated if intrarenal B cells expressed gene programs previously ascribed to *in situ* B cell phenotypes associated with other inflammatory renal diseases. One such phenotype is the age-associated B cell (ABCs). In human lupus nephritis, ABC-like gene expression was associated with activation of tissue-infiltrating B cells (*130*). A hallmark of an ABC phenotype is expression of T-bet (*Tbx21*). T-bet induction in B cells depends on stimuli from TLR7 and IFN-γ (*127*), pathways upregulated in intrarenal B cells. However, most intrarenal and tonsil B cells did not express *TBX21* at a detectable level. Indeed, they had no difference in overall expression of 26 genes associated with ABCs (Figure 2.5A). Therefore, despite some similarities, intrarenal B cells are distinct from ABCs.

HIF-1 pathway is another gene signature upregulated by tissue-infiltrating B and T cells in lupus nephritis patients (*135*, *209*). However, none of HIF-family genes were upregulated in intrarenal B cells compared with tonsil B cells (Figure 2.5B-F). These data indicate that the hypoxia-induced pathway is not characteristic for intrarenal B cells in allograft rejection.

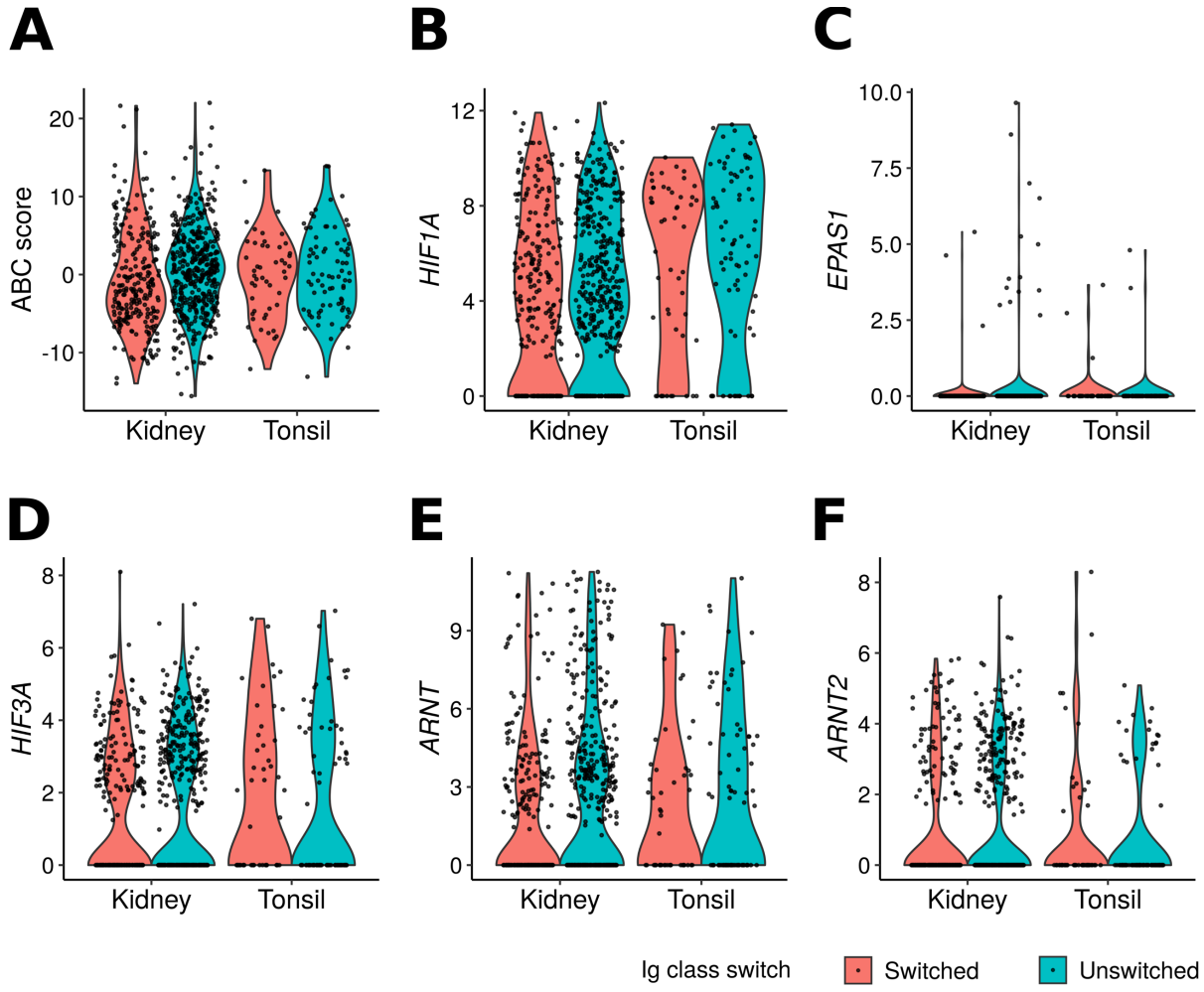

Figure 2.5 Intrarenal B cells had no association with ABC and HIF signatures.
(A-F) Violin plots showing the gene expression of ABC-associated genes (A), *HIF1A* (B), *HIF2A* (C), *HIF3A* (D), *HIF1B* (E), or *HIF2B* (F). Cells were grouped by their tissue source and Ig class-switch state.

ABC and HIF-1 gene signatures are activated in normal B cell activation (*137*, *138*). Therefore, finding no difference compared with tonsil B cells does not necessarily mean these pathways are not important for intrarenal B cell activation. Nevertheless, these data demonstrate that class-switched intrarenal B cells in allograft rejection have a unique transcriptional profile reminiscent of innate peritoneal B1 cells.

2.2.3 Receptor-ligand co-upregulation reveals intrarenal interactions around B cells

We next examined the relationships between intrarenal B cells and other cell populations in rejecting renal allografts. For this purpose, we first identified genes known or postulated to encode a ligand or a receptor (*210*) that were preferentially expressed in Ig class-switched renal versus tonsil B cells. We then queried whole tissue microarray data for ligands and receptors upregulated in rejected renal allografts (*162*). With these genesets, we tested whether intrarenal B cells and rejected tissues co-upregulated any ligand-receptor pairs.

This analysis identified 10 ligand-receptor pairs co-upregulated (Figure 2.6A). One of them was *IL15-IL15RA*, encoding a proinflammatory cytokine IL-15 and a component of its receptor complex. Tissue staining showed no detectable IL-15 expression in tonsil (Figure 2.6B). In contrast, infiltrating B and other immune cells highly expressed IL-15 in rejected renal allografts. IL-15RA was moderately expressed in both tonsil and renal allograft tissue. However, it was most abundant in renal tubular cells. IL-15RA trans-presents IL-15 to immune cells expressing another receptor dimer IL2RB/IL2RG (*211*). This staining pattern indicates that IL-15 secreted by B cells might be captured by tubular cells for presentation to surrounding immune cells. These data suggest an interplay between intrarenal B cells, tubular cells and other cellular components in allograft rejection.

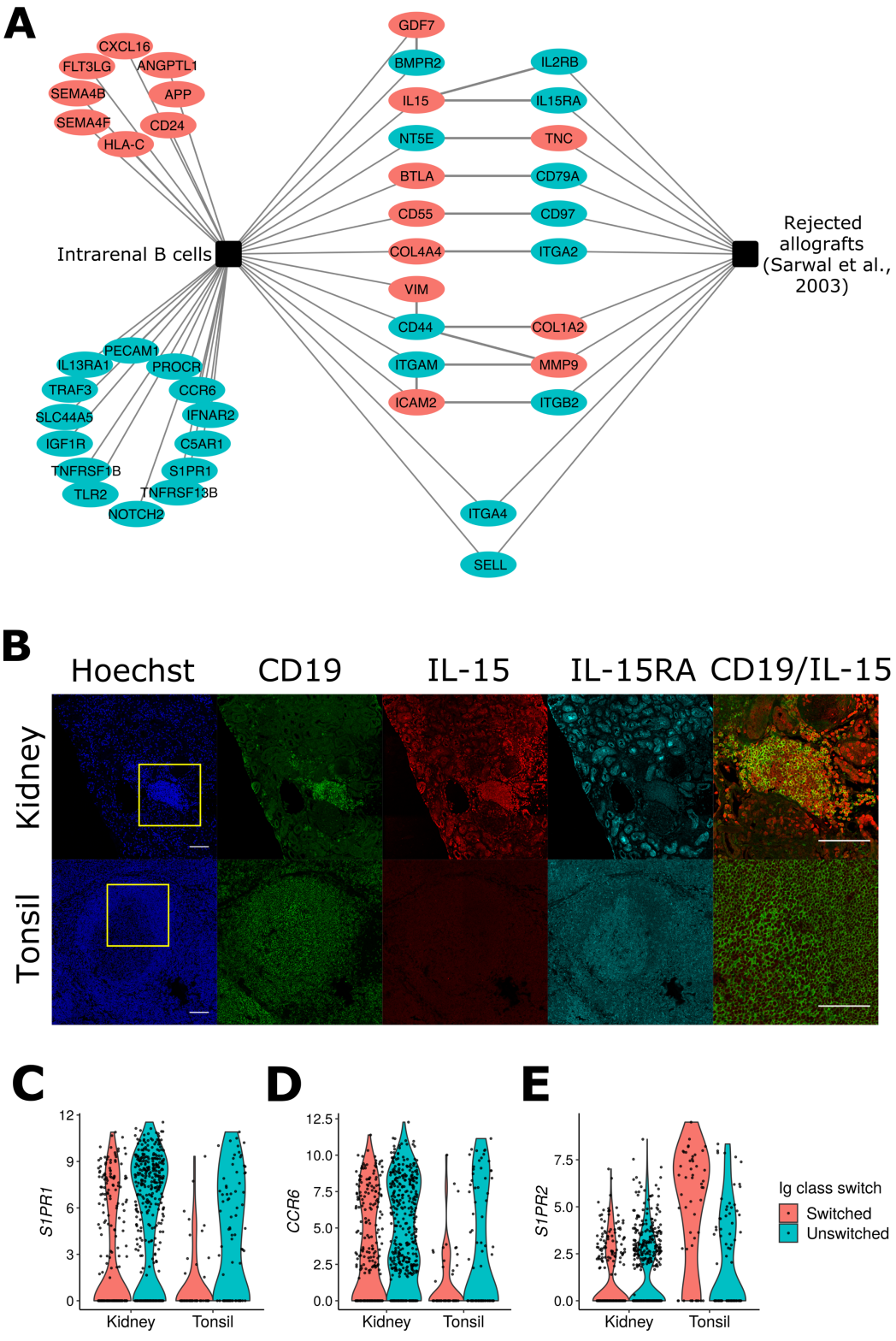

Figure 2.6 Ligand-receptor interactions between intrarenal B cells and rejected allografts.

(Continued from the previous page) (A) Ligand or receptor-encoding genes upregulated in Ig class-switched renal B cells (vs. switched tonsil B cells) and rejected renal allografts (vs. normal allografts). Gene names were connected to each other when both their ligand and receptor were present. Color (red and blue) indicates ligands and receptors respectively. (B) Staining images of nuclei (Hoechst), CD19, IL-15, and IL-15RA in rejected renal allograft and tonsil tissues. The merged CD19/IL-15 panels were a magnification of the yellow box in merge panels. Scale bars indicate 100 μm. (C-E) Gene expression level of *S1PR1* (C), *CCR6* (D), or *S1PR2* (E).

The other co-expressed pairs contained several cell migration-related axes, such as *NT5E-TNC*, *CD55-CD97*, *COL4A4-ITGA2*, *CD44-COL1A2*, *ICAM2-ITGB2*. Although not paired with their ligands, both B cells and renal tissue also expressed *ITGA4* and *SELL*. These receptor-ligand pairs could explain potential mechanisms for migration and retention of B cells within rejecting renal allografts.

Another co-upregulated pair was *BTLA* and *CD79A*. B cells ubiquitously express CD79A, as it encodes a signaling chain of BCR, Igα. Additionally, BTLA binds to Igα on the same cell surface to attenuate BCR signaling (*212*). Therefore, the *BTLA-CD79A* axis represents autocrine interaction in B cells, rather than communication with other cells. Intrarenal B cells expressed both a ligand and a receptor for several other axes, thereby indicating autocrine or inter-B cell interaction: *GDF7-BMPR2*, *VIM-CD44* and *ITGAM-ICAM2*. A role of GDF7-BMPR2 in B cell activation is unknown. However, other receptors and ligands of their family attenuates CD40 signaling (*213*). On the other hand, CD44 and CD11b (*ITGAM*) both mediate cell adhesion (*214*, *215*). Therefore, these pathways could autonomously regulate B cell activation and interaction in rejecting renal allografts.

Although not paired with tissue-upregulated genes, intrarenal B cells expressed other migration-related genes: *APP, CD24, CXCL16, CCR6, PECAM1* and *S1PR1*. S1PR1 is critical for

B cell egress from lymphoid organs (*4*). Therefore, B cells need to downregulate it to participate in GC responses. Indeed, *S1PR1* expression was significantly repressed in tonsil B cells upon class switch, while it was largely retained in intrarenal B cells (Figure 2.6C). This expression pattern of *S1PR1* mirrors that of another gene encoding an important chemokine receptor *CCR6*. Consistent with the fact that GC B cells do not express CCR6 (*19*), its expression was repressed in class-switched tonsil B cells, whereas intrarenal B cells expressed it at a high level (Figure 2.6D). In contrast with these two receptors, S1PR2 is highly expressed in GC B cells and coordinates their migration (*5*). Indeed, *S1PR2* was upregulated in class-switched tonsil B cells, while it remains low in intrarenal B cells. (Figure 2.6E). These results demonstrate that intrarenal B cells lack an expression pattern of migratory molecules characteristic to GC B cells, further highlighting their distinct phenotypes.

2.2.4 Serum DSA positivity does not differentiate intrarenal B cell phenotypes

In renal allograft rejection, serum DSAs predict a worse clinical outcome (*141–143*). However, it is unknown where B cells produce DSAs or whether DSA-producing B cells have a unique phenotype. To begin to address these questions, we tested whether serum DSA positivity was associated with differences in transcriptional programs of intrarenal B cells. Since our initial cohort had only one DSA-positive patient, we obtained three additional renal biopsies (two from DSA-positive patients and one from a DSA-negative patient) as well as three tonsillectomy samples. From these samples, activated B cells were sorted and subjected to scRNA-seq (Table 2.1).

After filtering for both gene coverage and Ig expression, we had 513 cells to integrate with the first cohort (Figure 2.7A). The second cohort had a lower sequence coverage compared to the first cohort (Figure 2.7B). Since normalizing scRNA-seq data with different sequencing depth by

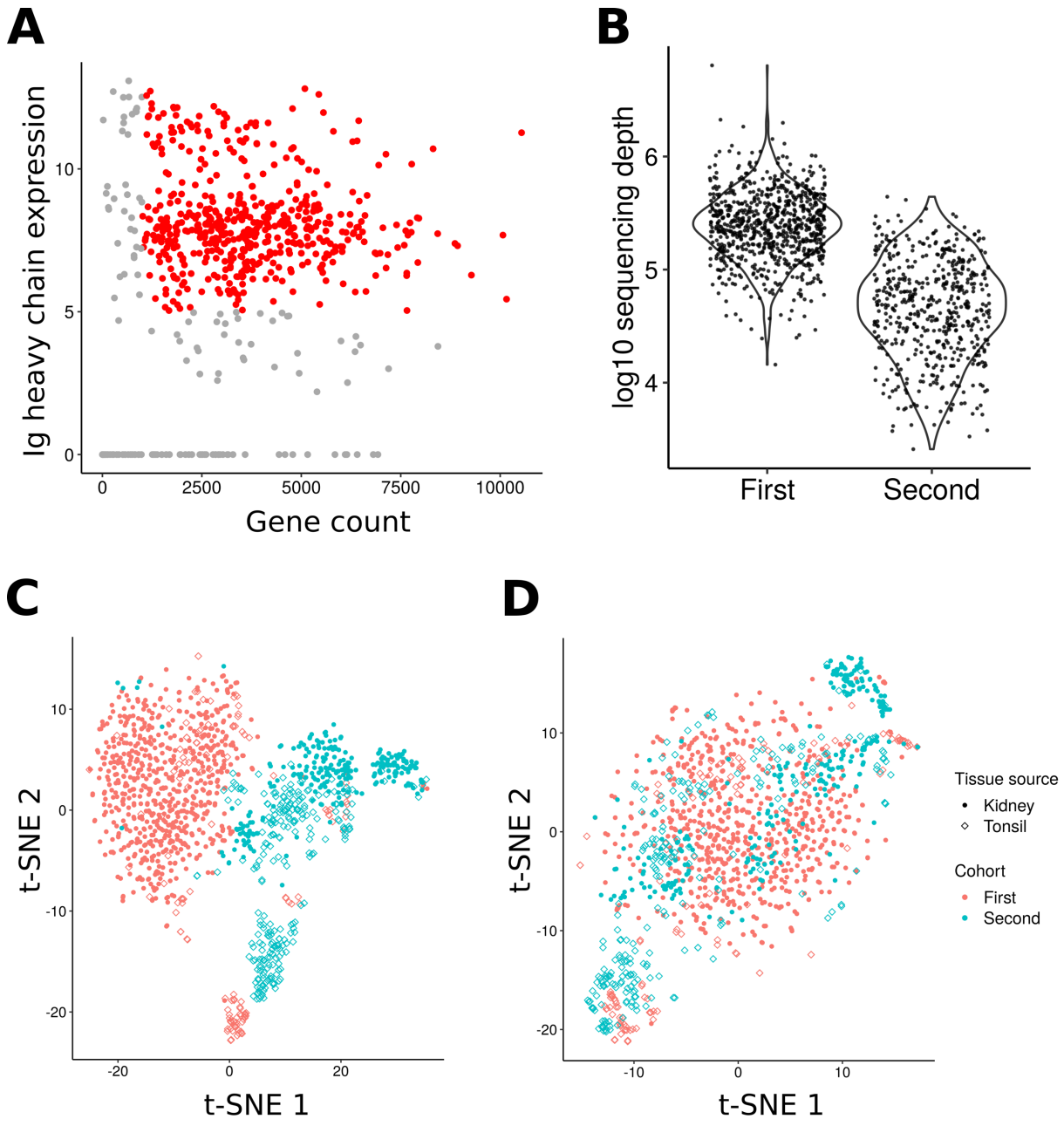

Figure 2.7 QC of the second cohort and data integration. (A) A scatter plot showing detected gene count and Ig Heavy chain gene expression on the x and y axis respectively. Cells which passed QC are colored in red. (B) A violin plot showing sequencing depth of cells which passed QC in each cohort. (C and D) t-SNE plots made from the data normalized by log2 count per million (cpm) without data integration (C) or the data normalized by SCTransform and integrated by ComBat (D). Color and shape respectively indicate cohorts and tissue sources.

a single scaling factor (e.g. total mapped reads) introduces bias (*216*, *217*), we first normalized our data by SCTransform implemented in Seurat (*217*, *218*). The data were then integrated by ComBat (*219*) to cancel batch effects between cohorts (Figure 2.7C and D).

The resulting integrated data had a similar t-SNE projection to that of the first cohort reproducing the distinct renal and tonsil B cell clusters (Figure 2.8A). As in the previous analysis, class switched B cells were separate whereas unswitched cells clustered together (Figure 2.8B). In addition, there was a plasma cell cluster which highly expressed *PRDM1* (Figure 2.8C and D). This population was mostly derived from a newly recruited rejection patient 6 with a few cells coming from another DSA-positive and three DSA-negative patients.

Except for plasma cells, B cells did not cluster depending on patients' serum DSA positivity (Figure 2.8E). Comparing gene expression of the non-plasma cells from the DSA-positive and negative patients, we could identify only three genes differentially expressed (Figure 2.8F). In contrast, we detected nearly 500 differentially expressed genes between class-switched renal and tonsil non-plasma cells (Figure 2.8G). These results suggest that a transcriptional profile of intrerenal B cells does not reflect a difference in serum DSA positivity.

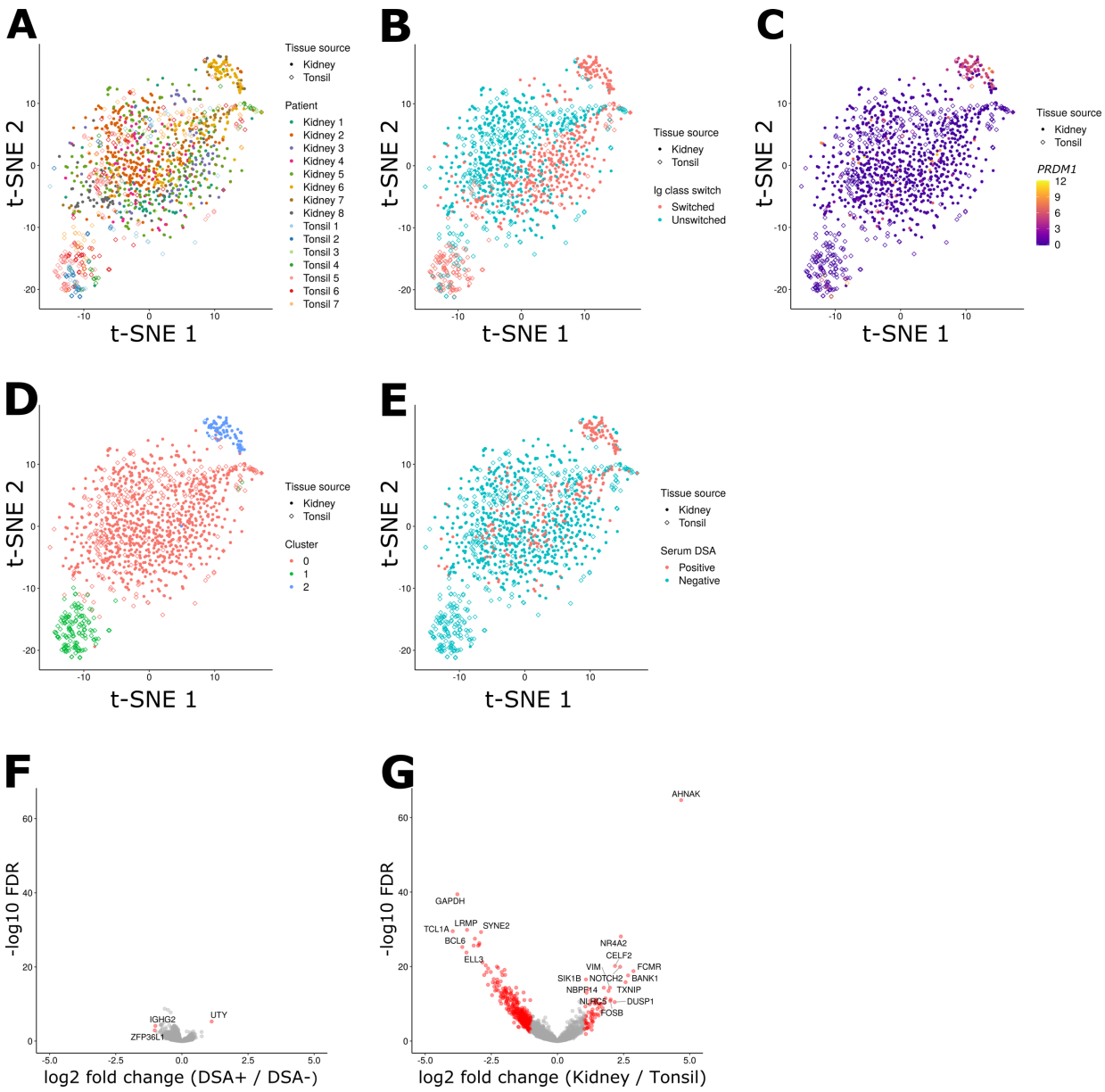

Figure 2.8 B cells from serum DSA-positive and negative patients are similar.
(A-E) t-SNE plots of the integrated data of the two cohorts. Shape indicates tissue source, and color indicates patients (A), Ig class-switch state (B), *PRDM1* expression (C), clusters assigned by Seurat (D), and serum DSA positivity (E). (F and G) Volcano plots showing differential gene expression in non-plasma B cells, comparing DSA-positive and negative patients (F), or Ig class-switched renal and tonsil cells (G). Shown on the right side of the plots are genes upregulated in B cells from DSA-positive patients (F) or intrarenal B cells (G). Genes above the significance threshold were colored in red, and names of top-hit genes were labeled.

2.3 Discussion

Here, I demonstrate that intrarenal B cells have a phenotype distinct from tonsil GC B cells. They highly expressed multiple pathways which activate B cells, such as IFN and innate immune pathways. In particular, innate-like phenotype paralleled with their peritoneal B1-like gene expression. Overall, this study revealed a unique *in situ* B cell phenotype in human renal allograft rejection.

Our data indicate that intrarenal B cells lack a GC-associated transcriptional program. They expressed much lower *AICDA* and genes associated with an active cell cycle compared with tonsil B cells. This lack of GC programs is also highlighted by their expression pattern of chemokine receptors. Intrarenal B cells had high *S1PR1* and *CCR6*, and low *S1PR2* expression. This pattern is an opposite of GC B cells, which rather resembles memory B cells. Finally, intrarenal B cells lack critical transcription factors *BCL6* and *BACH2*. This differential expression underscores that intrarenal B cell activation is distinct from GC responses.

Consistent with a lack of BCL6-mediated repression, intrarenal B cells highly expressed genes of IFN and TLR signaling pathways (*21*). IFN pathways are implicated in renal allograft rejection. IFN-α treatment alone can induce rejection of renal allografts (*220*). IFN-γ pathway is also upregulated in rejecting renal allografts (*221*). Both type-1 and type-2 IFNs also activate B cells, by enhancing an effect of BCR engagement (*105*). The upregulation of IFN pathways in intrarenal B cells indicate that IFNs might promote allograft rejection partly via B cell activation.

IFN pathways crosstalk with TLR pathways. In particular, IFN-α is sufficient to upregulate *TLR7*, one of identified DEGs, in B cells. TLR7 is also highly expressed by infiltrating immune cells in rejected renal allografts, even compared with nephritic kidneys of SLE patients (*222*).

Given TLR stimulation has profound effects on B cell activation and selection (*223*), this pathway might be important in intrarenal B cell activation as well.

However, we did not find an evidence of TLR7 activation in our data. In mice, TLR7 stimulation is sufficient for *Tbx21* upregulation in B cells, as shown for ABCs (*125*). Most of our intrarenal B cells did not express *TBX21* at a detectable level. This lack of detection cannot be explained by insufficient sequencing depth, since scRNA-seq with lower depth could detect *TBX21* expression (*130*). This lack of *TBX21* expression could indicate that intrarenal B cells were not, at least recently, activated via TLR7.

Among PRRs upregulated in intrarenal B cells, the most differentially expressed one in our data was *NLRP1*. NLRP1 is a key component of inflammasome pathways (*224*). Importance of this pathway has been extensively characterized in macrophages and monocytes (*225*). However, it is unknown if the NLRP1 inflammasome is functional in B cells. In fact, expression of mouse homologs *Nlrp1a* and *Nlrp1b* are negligible in B cells (ImmGen). However, *NLRP1* is more broadly expressed in humans, including B cells. Although roles of NLRP1 or inflammasome in general are largely unknown in the context of allograft rejection, our data indicate that NLRP1 could play a role in intrarenal B cell activation.

In addition to enriched pathways, *AHNAK* provided another clue to understand an intrarenal B cell phenotype. *AHNAK* was one of the most significantly upregulated genes in intrarenal B cells. *AHNAK* expression was much higher in intrarenal than tonsil B cells regardless of Ig class switch suggesting that AHNAK is a general feature of intrarenal B cells. A B cell-related role of AHNAK is largely unknown. However, AHNAK regulates calcium flux upon T cell receptor (TCR) stimulation, which is indispensable for T cell activation (*207*). Given a

similarity between BCR and TCR signaling (*226*), AHNAK could be important for B cell activation as well.

A mouse homolog of *AHNAK* is specifically expressed in peritoneal B1 cells. Genes with this expression pattern were significantly enriched in cluster 2, indicating that intrarenal B cells resemble peritoneal B1 cells. As B1 cells are known as innate-like B cells, *AHNAK*-covariant genes were also enriched for genes involved in innate immune responses. These innate immune genes include migration related genes such as *ITGAM* and *CD44*, as well as signaling components *RIPK1* and *JAK3*. Some of those genes were also upregulated by intrarenal B cells compared with tonsil B cells. Indeed, overall expression of those *AHNAK*-covariant innate genes was higher in intrarenal B cells. This result indicates that this innate, peritoneal B1-like gene signature is a general feature of intrarenal B cells in allograft rejection.

To identify this B cell subset-specific gene signature, we used mouse transcriptomic data, instead of those of humans. This is because mouse data covers a broader list of B cell subsets including those in the peritoneal cavity, while currently available human data are limited to a few B cell subsets in circulating blood. This comprehensiveness of the mouse data allowed us to identify the unique expression pattern of *Ahnak.* Although a global expression pattern of orthologs are largely conserved in humans and mice (*227*), individual genes could be expressed differently in these two species. Therefore, it is possible that a true peritoneal B1 signature in humans is different from what we found in this study.

Moreover, definition of human B1 cells is elusive. Although several markers have been proposed, they are highly controversial (*73–75*). In our data, none of previously reported B1 markers (CD5, CD27, CD43 and CD70) were differentially expressed between intrarenal and tonsil B cells. Another B1 phenotype is high IgM and low IgD expression. Again, these Ig genes

were not differentially expressed between intrarenal and tonsil B cells. Moreover, activated B2 cells also upregulate B1 markers such as CD5 and CD27. Therefore, these markers are not very useful to identify a B1-like population in activated B cells like those in our data.

Although *AHNAK*-covariant genes were strongly enriched in cluster 2, they accounted for only 5 % of the cluster. Therefore, the peritoneal B1-like signature is only a portion of unique features of intrarenal B cell activation. This peritoneal B1-like feature might reflect their higher sensitivity to innate stimuli, or more likely, their presence in a local non-lymphoid organ.

In fact, our analyses revealed potential interactions around B cells in rejecting allografts, many of which were related to cell adhesion and migration. Those genes included *ITGAM,* one of *AHNAK*-covariant genes. *ITGAM* encoding a peritoneal B1 marker CD11b. CD11b composes a protein complex Mac-1, which binds to ICAM1 and ICAM2 (*215*). ICAM1 is highly expressed by over 90 % of proximal tubular cells (*228*). Our data also suggest ICAM2 is expressed by intrarenal B cells. Taken together, CD11b also likely to play an important role for B cells to localize and interact in renal allografts. Once functional importance of CD11b and other adhesion pathways is proven, they could be therapeutic targets to abrogate graft infiltration of B cells. In fact, CD11b-blocking antibody effectively inhibit migration of myeloid cells into an inflamed site (*229*). It is interesting to test its effect on B cell infiltration into allografts.

An important question is how intrarenal B cells affect rejection. B1 cells are postulated to be a main producer of IL-10. IL-10-producing Breg cells have been also implicated in transplant tolerance in mice and humans. However, our data found no upregulation of their markers, such as *IL10* and *FOXP3*. Instead, intrarenal B cells expressed the proinflammatory cytokine IL-15. IL-15-producing B cells have been reported in multiple sclerosis patients (*189*). B cell-derived IL-15 promotes cytotoxic activity of T cells. Therefore, intrarenal B cells could promote allograft

rejection via IL-15 in the same mechanism. In line with this hypothesis, high IL-15 expression is associated with renal allograft rejection (*190*). In mice, antagonizing IL-15 protects from cardiac allograft rejection (*230*). On the other hand, in non-human primates, IL-15 blockade failed to show efficacy (*231*). However, the result is arguable because only two subjects were in each treatment group. Therefore, a role of IL-15 in a context of renal allograft rejection, especially B cell-intrinsic one, remains to be elucidated.

IL-15 expression in B cells can be induced *ex vivo* by CD40, but not LPS or CpG, stimulation (*189*). If the same mechanism underlies IL-15 expression in our data, that would indicate T-dependent activation of intrarenal B cells. T-cell help is a critical component that drives B cell affinity selection and antibody production, which is the most obvious proinflammatory role of B cells. Pathogenic antibodies drive inflammation in many inflammatory diseases. Renal allograft rejection is no exception. In the next chapter, I will explore reactivity of antibodies expressed by intrarenal B cells.

3 Reactivity and selection of antibodies expressed by intrarenal B cells

3.1 Introduction

DSAs are a critical driver of antibody-mediated rejection. A central question is where and how they develop. Graft-infiltrating B cells are potential producers of DSAs given they can clonally expand and somatically mutate their antibodies (*168*, *169*). However, association between DSAs and $CD20^+$ infiltrates is unclear. Furthermore, one study suggested that graft-infiltrating B cells rarely express DSAs (*183*). Nevertheless, as mentioned in chapter 1.6, this study had several caveats. Therefore, the question still remains open.

scRNA-seq applied in the previous chapter allows us to clone matched Ig heavy and light chain genes. This advantage provides us with an opportunity to investigate their reactivity and affinity selection, in multiple patients with ongoing rejection. Another interesting feature of our cohort is the presence of IgG-expressing plasma cells, which makes this study the first to demonstrate clonality and reactivity in plasma cells in renal allografts.

Here I demonstrate complete absence of HLA reactivity in intrarenal antibodies. Non-plasma cells were not selected for autoreactivity either. In contrast, plasma cells were clonally related, and strongly selected for self, particularly nucleolar, antigens. These results clearly demonstrate that DSAs do not emerge from *in situ* B cell responses. Rather, our data suggest that local immune responses can breach B cell tolerance in renal allograft rejection.

3.2 Results

3.2.1 Cloning and recombinant expression of intrarenal antibodies

In order to characterize antibody selection in intrarenal B cells, we set out to create recombinant antibodies. Pre-amplified cDNA of scRNA-seq'ed B cells were recovered for seven renal biopsies and two tonsil samples. From the cDNA, Variable regions of Ig genes were further amplified using nested polymerase chain reaction (PCR) as previously described (*232*). Obtained sequences were aligned to IMGT reference using IMGT/HighV-QUEST (*233*, *234*) and analyzed for somatic mutations. In total, we identified full-length Ig heavy chain variable regions from 457 B cells in seven rejection patients and 77 in two tonsillectomy patients (Figure 3.1A).

Somatic mutation burden was similar between rejection and tonsillectomy samples (Figure 3.1B). In general, unswitched B cells had less mutations than switched cells. A small fraction of both switched and unswitched intrarenal B cells had exceptionally high frequencies of mutations. Since subcloning was not performed before Sanger sequencing, PCR and/or sequencing errors must have inflated the mutation burden shown here.

Next, clonal relationships were investigated among the sequenced antibodies. Antibodies were determined to be clonally related, when they shared the same variable (V), diversity (D), joining (J) segments and complementarity-determining region (CDR) 3 length. Despite high mutation rates, only a limited number of shared clonal families existed in most patients (Figure 3.1C). In contrast, many of the plasma cells were clonally related. This population contained 15 clonal families in patient 6, and two clonal families in patient 7. This result suggests that plasma cell populations were clonally expanded, and likely selected *in situ* for specific antigens.

In order to characterize their reactivity, we next expressed recombinant antibodies. Paired

A

Patient	Kidney 1	Kidney 2	Kidney 3	Kidney 4	Kidney 5	Kidney 6	Kidney 7	Tonsil 1	Tonsil 2	Total
Switched	11	42	31	7	28	92	17	7	20	255
Unswitched	5	90	23	51	41	11	8	32	18	279
Total	16	132	54	58	69	103	25	39	38	534
Expanded clonal families	0	1	2	1	0	15	2	0	0	21

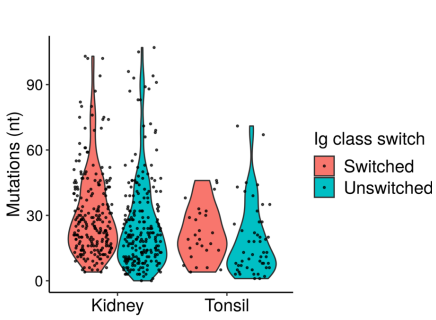

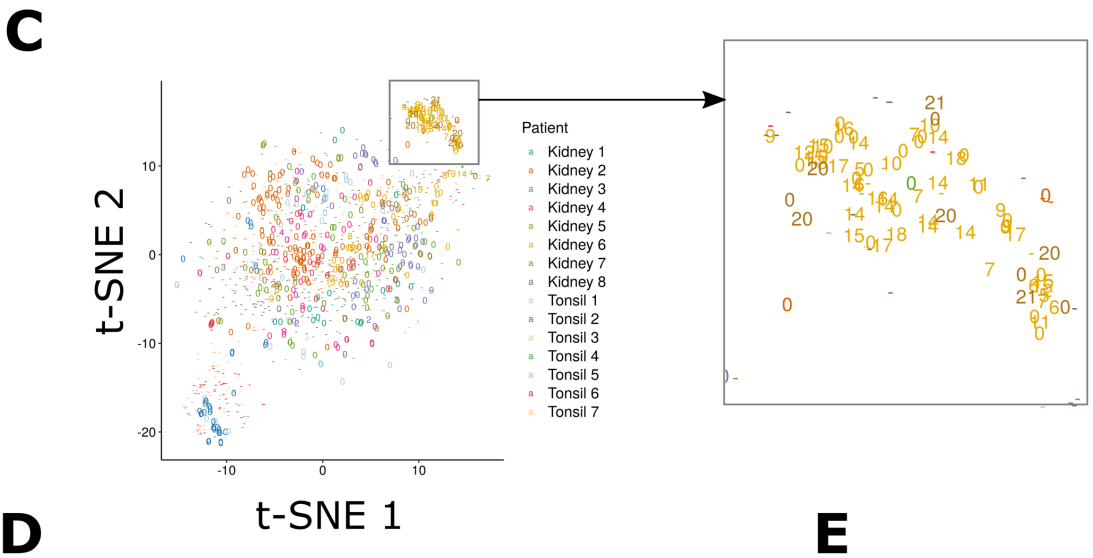

D

Patient	Kidney 1	Kidney 2	Kidney 3	Kidney 4	Kidney 5	Kidney 6	Kidney 7	Tonsil 1	Tonsil 2	Total
IgG	5	13	10	4	3	21	4	2	7	69
IgA	2	2	5	2	2	0	1	0	0	14
IgM	1	6	6	8	3	0	7	5	5	41
Total	8	21	21	14	8	21	12	7	12	124

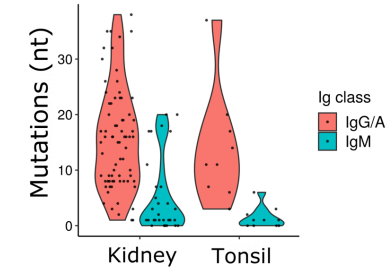

Figure 3.1 Antibodies expressed by intrarenal B cells were not selected for allo-HLA reactivity. (A) A table showing distribution of number and Ig classes of the sequenced antibody heavy chains as well as number of expanded clonal families across patients (B) A violin plot showing distribution of mutations in the variable region of Ig heavy chains, grouped by tissue source and the Ig class-switch state. (C) t-SNE plots as in Figure 2.8, with data points labeled with their clonal family. "-": antibody genes were not sequenced; "0": the cells did not share their clonotype with others; 1-21: cells shared a clonotype with other B cells with the same number. (D) A table showing distribution of number and Ig class of the recombinantly produced antibodies across patients. (E) A violin plot showing distribution of mutations in recombinantly expressed antibodies.

heavy and light Ig variable regions were cloned into human IgG expression vectors. The C-terminal of the heavy-chain construct was modified with a FLAG tag, so that we could stain tissues circumventing IgG-expressing cells or IgG deposition *(53)*. Antibodies were expressed in human embryonic kidney (HEK) 293A cells and purified with protein A beads. In total, 105 antibodies (74 IgG/A and 31 IgM) were expressed from intrarenal B cells in seven allograft patients (Figure 3.1D and Supplementary Table 3.1), covering 11 out of the 21 expanded clones. For patient 6, antibodies were exclusively cloned from IgG-expressing plasma cells. Additional 19 antibodies (9 IgG and 10 IgM) were also expressed from two tonsillectomy patients. As expected, the mutation rate was higher in IgG/IgA antibodies than IgM (Figure 3.1E).

3.2.2 Allo-HLA reactivity does not select intrarenal antibodies

To characterize HLA reactivity, expressed antibodies were subjected to a screening assay. In this assay, a mixture of HLA class-I or class-II antigens coat Luminex beads. Antibody binding was evaluated by normalized background (NBG) ratio which is fold-increase binding over negative control serum after binding to naked beads is subtracted. Binding was positive when NGB ratio was equal to or higher than 2.2. When tested in phosphate-buffered saline (PBS), 17 % (18 / 105) of intrarenal antibodies were positive (Figure 3.2A). We observed 19 % positive (9 / 47) in serum DSA-positive patients, while 16 % (9 / 58) in negative patients. Therefore, this HLA binding was not associated with serum DSA positivity ($p = 0.82$, chi-squared test). Additionally, we observed 21 % (4 /19) positivity in tonsil antibodies. Although this latter sample was small, it suggested that this HLA binding was not a specific feature of intrarenal B cells. Furthermore, all the class II-binding antibodies also bound to class I antigens, suggesting that at least some of the observed

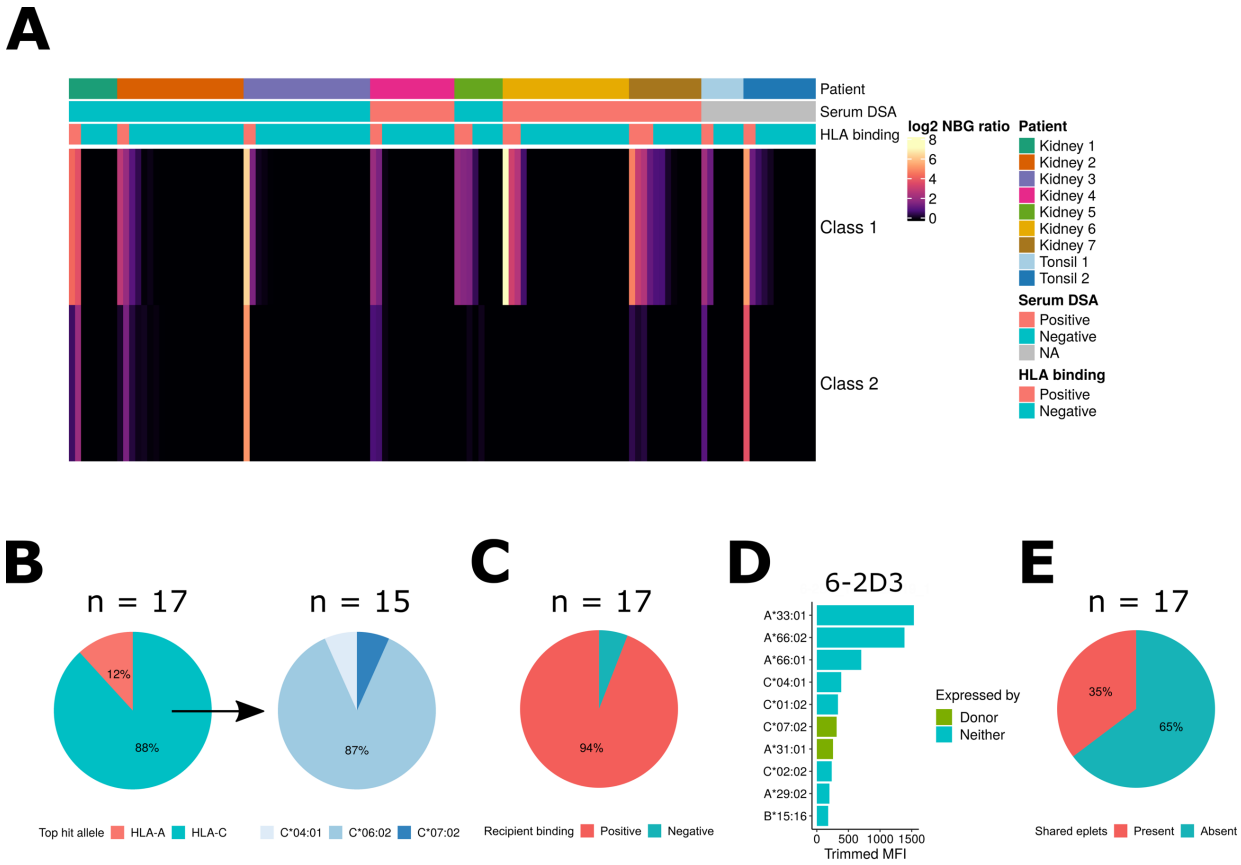

Figure 3.2 Intrarenal antibodies did not selectively bind to HLAs. (A) A heatmap showing screening HLA-binding assay results. Columns correspond to antibodies, and maximum NBG ratio within class-1 or class-2 beads are shown. The header label indicates patients, serum DSA positivity, and whether observed reactivity was above the positivity threshold. (B) Pie charts showing top-hit alleles in the SAB assay. 17

(Continued from the previous page) antibodies with trimmed MFI ≥ 1,000 were analyzed. (C) A ratio of antibodies that had a recipient-expressed antigen among top-10 hits. (D) Trimmed MFI of 6-2D3. Donor-expressed antigens are colored in green. (E) A ratio of antibodies whose top-10 hits shared eplets. (F) Trimmed MFI of a representative antibody 3-1E12 with a shared eplet. A recipient-expressed antigen is colored in red. (F) Eplets (columns) present in antigens (rows) detected in (G). Eplets shared among more than five antigens are shown. Eplets shared among all the top-10 hits are highlighted in red. (H) Change in HLA binding in the Screening assay tested in negative control human serum.

HLA binding is not even epitope-specific.

To further delineate the HLA binding, screening-positive renal antibodies were tested on a single-antigen bead (SAB) assay, in which only a single type of HLA antigens is present on each bead. Out of 18 tested antibodies, 17 antibodies showed trimmed mean fluorescent intensity (MFI) higher than 1,000. 15 of the 17 antibodies detected HLA-C, specifically HLA-Cw*06:02 as the top hit (Figure 3.2B and Supplementary Table 3.2). These HLA-C antigens were also present in top 10 hits of HLA-A-bound antibodies. These antigens were detected regardless of whether a donor expressed them or not. In fact, except one antibody, 6-2D3, all these antibodies had a recipient-expressed antigen in their top-10 hits (Figure 3.2C). These results indicate that most of the observed HLA binding is not specific to donor antigens.

Eplets represent polymorphic epitopes in HLAs, which can be useful to investigate specificity of HLA binding. However, even 6-2D3 showed a broad reactivity to HLA-A and C antigens (Figure 3.2D), which did not share eplets. Including 6-2D3, a majority of antibodies (11 out of 17) did not had an eplet shared among all their top-10 hits (Figure 3.2E). Therefore, their binding could not be explained by eplets either. All the 6 antibodies whose top-10 hits shared an eplet bound to HLA-C antigens (Figure 3.2F and G). Again, their binding patterns were not donor-specific.

These HLA-C antigens could be problematic, because HLA-C binding detected by solid phase assays tend to be false positive caused by denatured antigens (*235–237*). Moreover, our antibodies were tested without blocking, which could have allowed them to manifest polyreactivity. Therefore, the observed binding could be non-specific, even for the antibodies with shared eplets.

Only six out of 17 antibodies had an eplet shared among all their top 10 hits, suggesting that a majority of observed binding are not epitope-specific (Figure 3.2D and Supplementary Table 3.2). All the antibodies with a shared eplet bound to HLA-C antigens. However, HLA-C antigens can be problematic, because HLA-C binding detected by solid phase assays tend to be false positive caused by denatured antigens (*235–237*). Moreover, our antibodies were tested without blocking, which could have allowed them to manifest polyreactivity. Therefore, the observed binding could be non-specific, even for the antibodies with shared eplets.

If the observed HLA binding comes from non-specific binding, adding a blocking reagent could absorb it (*238*). Therefore, we next retested antibodies on the screening assay in presence of negative control human serum. Strikingly, all the previously positive antibodies lost their binding (Figure 3.2E). Of note, as far as we tested, the ELISA used to determine polyreactivity could not distinguish binding to coated antigens from that to uncoated plate surface (data not shown). Therefore, we could not demonstrate that intrarenal antibodies bind to multiple antigens with ELISA. Nevertheless, the loss of binding with blocking indicate that the observed HLA binding is polyrectivity, instead of specific reactivity to alloantigens.

Polyreactivity is often associated with increased autoreactivity (*86*). Therefore, we investigated whether the observed promiscuous binging was a manifestation of autoreactivity. For this purpose, intrarenal antibodies were tested for their reactivity to HEp-2 cells by immunofluorescence microscopy. For antibodies cloned from allograft patients except patient 6,

frequency of HEp-2-reactive clones was 18 % (15 / 84) (Figure 2.3A). This frequency is similar to that reported for naive or tonsil GC repertoires (*86*, *239*). HEp-2 reactivity was slightly more common in HLA-polyreactive antibodies (27%, 4 / 15 vs. 16%, 11 / 69). However, this difference was not statistically significant ($p = 0.54$, chi-squared test). These results suggest that neither are these antibodies selected for autoreactivity, nor does the promiscuous HLA binding reflect autoreactivity.

3.2.3 Plasma cells dominantly express antinucleolar autoantibodies

In contrast, within the clonally expanded plasma cells, 76 % of (16 / 21) antibodies reacted to HEp-2 cells (Figure 3.3A). Reactive clones spread across 8 different clonal families. These antibodies had a high prevalence of antinucleolar antibodies (Figure 3.3B). The similar staining patterns among multiple clones suggest that these plasma cells were selected for the same or closely associated antigens.

To identify potential antigens, we selected three antinuclear antibodies (6-2A4, 6-2B9 and 6-1B5) from different clonal families. We selected 6-A4 as it represents the most expanded clonal family. 6-2B9 showed the strongest signal in HEp-2 staining, and 6-1B5 showed the most specific staining pattern to nucleoli. Using these antibodies, we performed western blot on a nuclear fraction of HEp-2 cell lysates. Out of the three antibodies tested, 6-2A4 and 6-2B9 showed similar broad immunoreactivity above a relative molecular weight higher than 50 kDa, while 6-1B5 did not show detectable bands (Figure 3.4A).

Next, immunoprecipitations (IP) was performed with the three antibodies from the lysates of HEp-2 nuclear fractions. IP was also performed with two negative control antibodies: 7A5 and 7E3 which bound to neither HLA nor HEp-2 cells. Precipitates were washed and resolved by

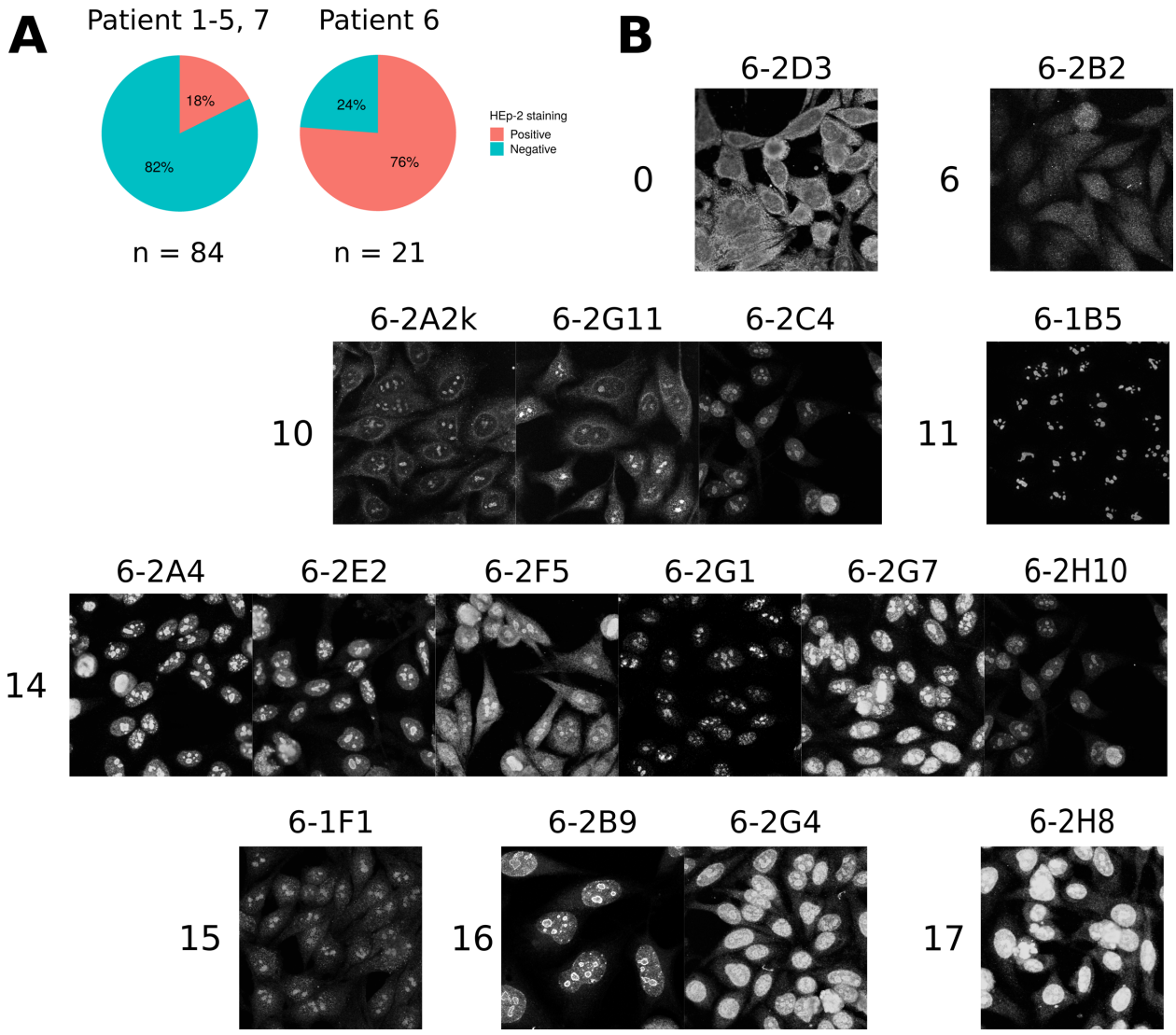

Figure 3.3 Clonally expanded plasma cells were selected for antinucleolar reactivity. (A) Frequency of HEp-2-reactive antibodies in indicated patients. (A) HEp-2 staining images of the 16 positive antibodies cloned from patient 6 plasma cells. Antibodies of the same clonal family are grouped together. Numbers on the left side of images indicate their clonal family number as in Figure 3.1C.

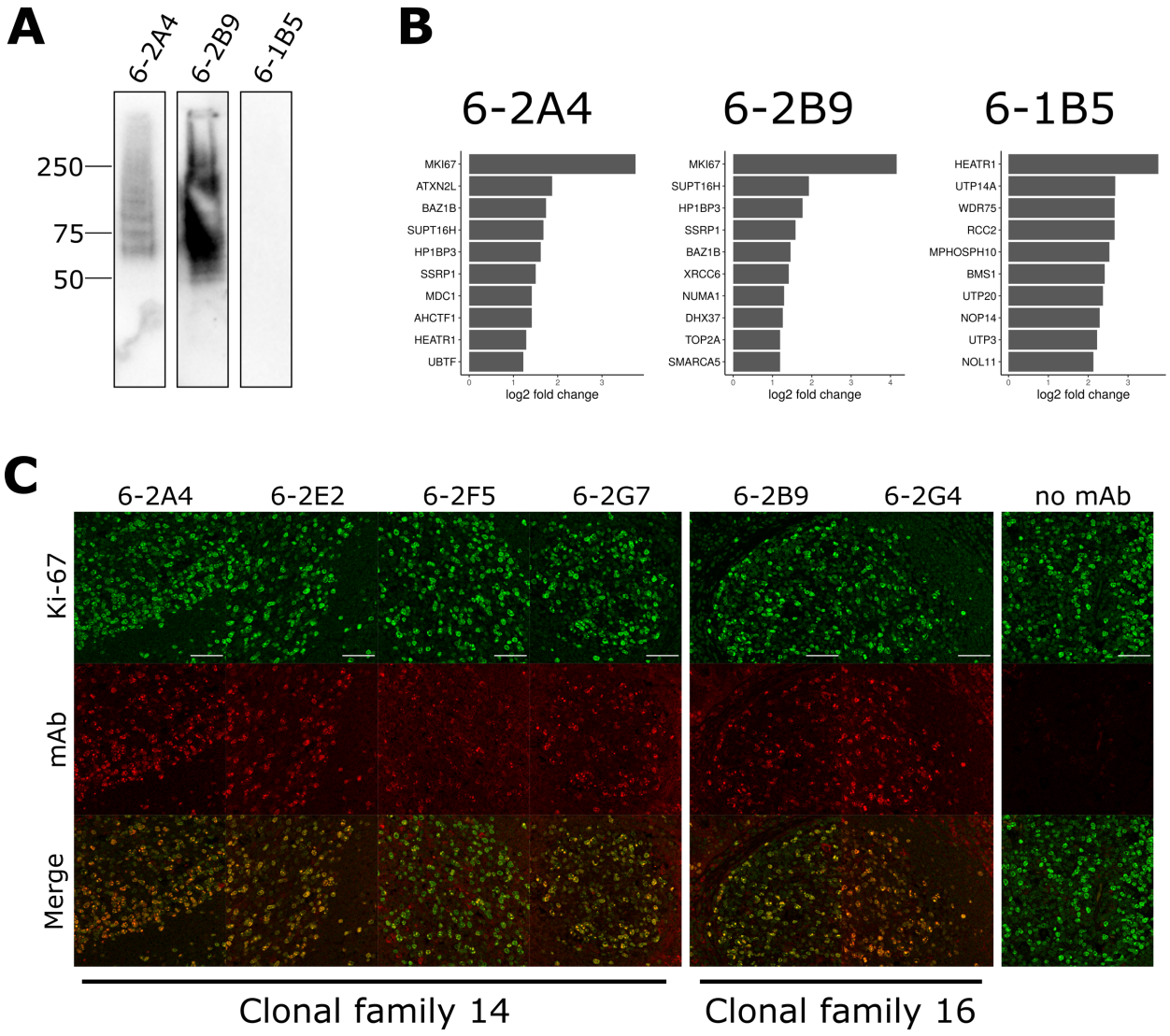

Figure 3.4 Ki-67 is a specific target of clonally expanded antibodies. (A) Western blot on HEp-2 nuclear lysates using the three antibodies, 6-2A4, 6-2B9 and 6-1B5. (B) Top-10 preferentially bound antigens detected in the IP/mass spectrometry analysis. Log2 fold changes of signal intensity over the mean of the two negative control antibodies are shown. (C) Staining images showing signal co-localization between antinucleolar intrarenal antibodies and a commercial anti-Ki-67 antibody on human tonsil tissue. Scale bars indicate 50 µm.

sodium dodecyl sulfate–polyacrylamide gel electrophoresis (SDS-PAGE). The gels were Coomassie-stained and lane regions above IgG heavy chain (> 50 kDa) were excised and subjected to tandem mass spectrometry. Detected peptides were mapped to the human proteome according to UniProt database. Signal intensity was normalized to median, and fold changes were calculated for the three antinucleolar antibodies over the mean intensity of the two negative control antibodies.

This experiment revealed that two of the three antinucleolar antibodies (6-2A4 and 6-2B9) detected a nucleolar antigen Ki-67 as the top hit (Figure 3.4B). The other positive antibody, 6-1B5, had another nucleolar antigen HEATR1 as the top hit. HEATR1 was also found in the top 10 hits of 6-2B9. Therefore, it is possible that these antibodies bind to the same or associated protein complex. Next, other plasma cell antibodies were tested for anti-Ki-67 reactivity by tissue staining. Since Ki-67 is highly expressed in proliferating cells, tonsil tissues were stained to test co-localization of signals from the antinucleolar antibodies and a commercial anti-Ki-67 antibody. A total of six antibodies showed co-localization with Ki-67, including 6-2A4 and 6-2B9 (Figure 3.4C). The additional four antibodies belonged to the same clonal family as either 6-2A4 or 6-2B9. These results indicate Ki-67 reactivity drives *in situ* clonal selection.

Within the clonal family of 6-2A4, two antibodies did not show detectable signal on tonsil staining. Therefore, we investigated their phylogenetic tree to see whether Ki-67 reactivity was gained or lost during clonal evolution. An analysis of heavy chains showed that costaining-positive 6-2G7 and negative 6-2G1 shared the same amino acid sequence (Figure 3.5A). On the other hand, these two antibodies had different light chain sequences (Figure 3.5B). Therefore, their different staining results came from mutations in light chains. For both heavy and light chains, 6-2A4 had the sequences most similar to germline antibody. The other antibodies in this clonal family shared

the amino acid mutations present in 6-2A4. These observations suggest that Ki-67 costaining capability was lost by mutations, while antinucleolar reactivity persisted through a series of mutations. Although development of Ki-67 is unclear at this point, these results collectively demonstrate that intrarenal plasma cells breach tolerance and become strongly selected for self nucleolar antigens in renal allograft rejection.

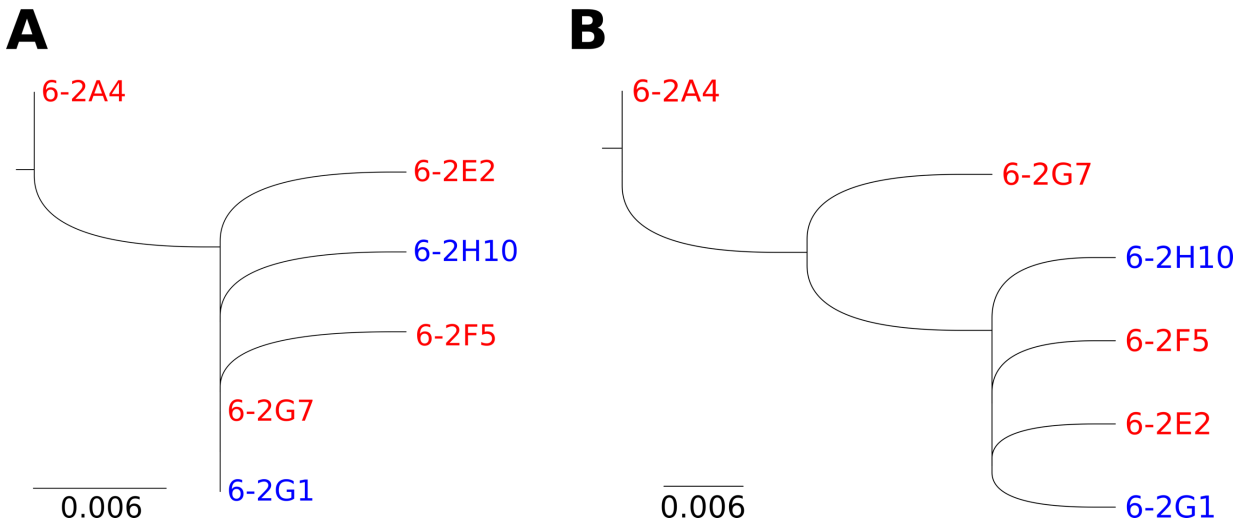

Figure 3.5 Changes in Ki-67 reactivity through clonal evolution.
(A and B) Phylogenetic trees showing amino acid changes in heavy (A) and light (B) chains of antibodies in clonal family 14 that 6-2A4 belongs to. Color indicates Ki-67 costaining results (red: positive, blue: negative).

3.3 Discussion

Here we demonstrate that intrarenal B cells are not selected for HLA reactivity. Instead, ubiquitous self-antigens strongly drive selection in plasma cells. This study is the first to demonstrate that a break in self-tolerance happens in *in situ* B cell repertoire in renal allograft rejection.

Intrarenal B cells expressed much less *AICDA* than tonsil B cells. Therefore, it was surprising to find a comparable amount of SHMs in their antibody genes. Despite this high mutation burden, we found few clonally expanded B cells. Therefore, they could be activated and mutated in secondary lymphoid organs and recruited into the graft afterword, instead of being activated and selected locally.

Alternative hypothesis is that the low *AICDA* expression in intrarenal B cells might be sufficient to induce SHMs. In fact, a fraction of naive B cells express a very low level of *AICDA* (*240*). These $AICDA^{low}$ B cells contain less, but a substantial number of SHMs compared to GC B cells. B cell activation in rejecting allografts is not necessarily as acute as GC responses. Therefore, the observed mutations might have accumulated slowly with low *AICDA*.

A majority of B cells were selected for neither HLA nor self-antigens. This observation is consistent with the previous study (*183*). However, our study overcame their caveats. Firstly, we demonstrated lack of HLA reactivity in multiple patients. Secondly, we tested reactivity in activated B cells, including clonally expanded plasma cells. Lastly, we isolated B cells from diagnostic biopsies, instead of an explant. Collectively, our results generalized the notion that DSAs are not produced *in situ*.

When tested without serum blocking, nearly 20 % of antibodies bound to HLA-coated beads. However, SAB analysis demonstrated that this binding can explained by neither selection to donor antigens nor shared eplets. Most importantly, it completely disappeared in presence of

serum blocking. Therefore, none of the observed HLA binding was a result of antigen-specific selection, including the seemingly donor-specific antibody 6-2D3 or antibodies which bound to antigens with shared eplets. Taken together, this HLA binding is manifestation of polyreactivity, which does not likely to happen in patients. These results also highlight importance of proper blocking for studying specificity of monoclonal antibodies.

In addition to HLA reactivity, we did not find enrichment of autoreactivity in most patients. This lack of obvious selection could indicate that intrarenal B cells generally express a low-affinity antibody repertoire. In fact, we rarely found clonally expanded populations. A mouse model of cardiac allograft rejection has shown that antigen non-specific T cells can be recruited in local tissues (*184*). Therefore, it is possible that intrarenal B cells observed here is a result of such non-specific recruitment.

The same study also showed that even such non-specific recruitment needs to accompany other antigen-specific T cells. This requirement of cognate antigens has been shown for tissue resident memory B cells as well (*185*). In our study, about 20 % of B cells expressed antibodies reactive to HEp-2 cells. It is possible that these self-reactive clones opened a door to other non-reactive B cells for graft infiltration.

The other possibility is that a majority of intrarenal B cells are reactive to kidney-specific antigens which were not tested in this study. In line with this possibility, serum from rejection patients often reacts to kidney-specific antigens expressed by renal vascular endothelial cells (*150*, *159*). Considering the absence of clonal expansion in our cohort, it is unlikely that those intrarenal B cells are going through *in situ* affinity maturation. Nevertheless, a more comprehensive set of antigens need to be tested to define true reactivity of intrarenal antibodies.

On the other hand, plasma cells showed robust clonal expansion. Despite serum DSA positivity of the patient they were derived from, they did not bind to HLAs. Instead, they showed strong selection for nucleolar self-antigens. Those plasma cells were mostly derived from one patient. Several studies associated DSA with $CD38^{high}$ or $CD138^{+}$ plasma cell infiltrates (*163*, *170*, *171*). Therefore, it is possible that plasma cells could be selected for allo-HLA reactivity in other cases. Nevertheless, our results clearly demonstrate that plasma cells can breach tolerance and selected for non-HLA, nucleolar self-antigens.

It is interesting how such reactivity develops in renal allograft rejection. Even in the patient with plasma cells, clonal expansion was not observed in non-plasma cells. Additionally, most of non-plasma cells were not clonally related to plasma cells. *AICDA* was also mostly lacked in plasma cells. These results indicate that plasma cell differentiation and selection did not happen *in situ*. Instead, they are more likely recruited to the graft after being selected in secondary lymphoid organs.

Finally, mass spectrometry analysis identified two potential nucleolar antigens, Ki-67 and HEATR1. Albeit rare, anti-Ki-67 antibodies are reported in murine and human SLE (*241*, *242*). It is interesting to test whether such reactivity can be detected in serum of transplant patients as well. Additionally, HEATR1 is reported as a minor histocompatibility antigen (*243*). However, the reported HEATR1 epitope is restricted to class-I HLA, HLA-B8. Therefore, the reported epitope is unlikely to select BCR specificity. Additionally, neither patient 6 and his donor carried HLA-B8, making it unclear whether HEATR1 behaves as a histocompatibility antigen in that patient.

4 Discussion

4.1 Overall implications of this work

Here I demonstrated that infiltrating B cells in allograft rejection have a unique transcriptional profile. They expressed high innate immune genes as well as a series of genes characteristic to peritoneal B1 cells. On the other hand, they expressed a much lower level of GC-signature genes, such as *AICDA* and *BCL6*. These results highlight distinct phenotypes of activated B cells in GCs and rejecting allografts.

While intrarenal B cells expressed heavily mutated antibodies, we found little evidence of clonal expansion. In line with these observations, they were neither antigenically selected by allotypic differences nor ubiquitous self-antigens. Therefore, they are not likely to be going through *in situ* affinity maturation and selection, although their reactivity to kidney-specific antigens remains to be tested. Importantly, this gene expression and lack of selection was shared across patients regardless of their clinical features, indicating that the phenotype found in this study commonly applies to graft-infiltrating B cells in renal allograft rejection.

In contrast, plasma cells exhibited a high degree of clonal expansion and SHM. Surprisingly, none of those plasma cell-derived antibodies reacted to HLAs. Rather, multiple clones from expanded clonal families recognized nucleolar self-antigens. These results suggest that renal allograft rejection can breach tolerance in plasma cells, selecting their reactivity to nucleolar self-antigens, instead of mismatched HLAs. Since we had only one patient with this phenomenon, it needs to be investigated how common such reactivity is.

In this study, we did not focus on TLS. All the studied patients had histological evidence of antibody-mediated rejection with B cell infiltrates. Those B cell infiltrates formed diffused

aggregates as shown in Figure 2.1B which often contained $CD4^+$ cells as well. However, we did not delineate whether those aggregates had a TLS signature, such as presence of Tfh cells and FDCs. The lack of a GC signature such as *BCL6* and *AICDA* indicates that intrarenal B cells studied in this study were not derived from TLS.

Albeit infrequently, $BCL6^+$ AID^+ B cell clusters have been observed in explants (*172*). Since we studied an earlier stage of rejection using diagnostic biopsies, it is possible that *in situ* B cell selection in TLS could happen at a later stage of rejection. Importantly, even in explants with GC-like B cell clusters, antibodies produced in the graft did not reflect allo-HLA reactivity detected in serum. Therefore, intrarenal B cells do not contribute to serum DSAs, whether they form TLS or not.

In line with this and other previous studies (*168*, *169*), our results suggest that intrarenal B cells have a unique antibody repertoire compared with circulating antibody repertoire. Especially, even in serum DSA-positive patients, intrarenal B cells did not produce anti-HLA antibodies. These findings indicate that an *in situ* B cell repertoire is selected in a mechanism distinct from allo-reactivity development in secondary lymphoid organs.

Firstly, intrarenal B cells could be reactive to antigens specifically expressed by kidney-specific antigens which were not tested in this study. In mice, tissue recruitment of lymphocytes require cognate antigens (*184*, *185*). Antibody production to kidney endothelial cells has been also reported in allograft rejection patients (*149*). Therefore, it is important to investigate reactivity of *in situ* produced antibodies to kidney endothelial cells, as well as a more comprehensive set of antigens using a protein array.

If these antibodies are not reactive to kidney-specific antigens either, it is possible that a majority of intrarenal B cells are recruited in a BCR-non-specific manner. Antigen-non-specific

cells can infiltrate tissues as a bystander, in presence of other antigen-specific cells (*184*). We observed HEp-2 reactivity in about 20 % of non-plasma cells. It is possible that this reactivity was sufficient to allow other non-reactive B cells to be recruited.

As an alternative possibility, low-affinity B cells could be preferentially recruited to the graft. Compared with tonsil B cells, intrarenal B cells highly expressed *CCR6.* CCR6 expression in activated B cells is a marker of memory cells. Memory cells in general express lower-affinity antibodies compared with plasma cells. $CCR6^+$ GC B cells also represent memory B cell precursors expressing low-affinity antibodies (*19*). In addition to *CCR6*, intrarenal B cells exhibited a similar gene expression pattern to this population, such as high *S1PR1*, *CD44*, *TNFRSF13B,* and low *S1PR2* and cell cycle genes. These results suggest that a majority of intrarenal cells could be low-affinity memory B cells instead of high-affinity plasma cells.

Plasma cells from one patient were clonally selected for reactivity to nucleolar self-antigens. They showed robust clonal expansion, and a few plasma cells shared a clonotype with non-plasma cells as well. These observations indicate that plasma cells could be clonally selected, and even differentiate *in situ* in rejecting allografts. Since we have not tested reactivity of non-plasma cells in the patient 6, we do not know whether B cells broke self-tolerance *in situ*. Given that more than 80 % of infiltrating B cells expressed class-switched antibodies, it is likely that they were pre-activated before being recruited to the graft. It is interesting to test reactivity of non-plasma cells in this patient and their germline antibodies, so as to understand the development of the antinucleolar reactivity.

Importantly, the plasma cell-positive patient did not have a history of autoimmune diseases. Therefore, inflammation in allograft rejection was sufficient for B cells to break self-tolerance. Such broken tolerance with antinuclear autoantibodies has been reported in the C57BL/6-bm12

mouse model of renal allograft rejection (*179*). This model has only a three amino-acid mismatch in MHC class II, driving humoral responses to autoreactivity instead of alloreactivity. This mouse model would provide an important insight into how B cells break tolerance in the context of allograft rejection.

The combination of C57BL/6 and bm12 strains is better known in the context of lupus nephritis. Transfer of bm12 splenocytes into a C57BL/6 mouse, or *vice versa*, induces a graft-versus-host disease (GVHD) with lupus-like symptoms, including antinuclear antibody production (*244*). In this setting, recipient class-II MHCs present self-antigens to donor $CD4^+$ T cells, which is recognized as non-self due to the MHC mismatch. This activation of $CD4^+$ T cells is essential for autoantibody production in this lupus model. It would be possible that antigen presentation by mismatched MHCs/HLAs drive production of antinuclear antibodies in the C57BL/6-bm12 transplant model and our human case. Indeed, a cardiac allograft model of C57BL/6-bm12 requires donor $CD4^+$ T cells for rejection (*180*). This persistence of donor "passenger" cells in allografts and their potential participation in immune responses is known as microchimerism, which has been observed in both mice and humans (*181*, *182*).

However, microchimerism is much less frequent and persistent in kidney transplant compared with other solid organ transplant: donor-derived cells are completely cleared from circulation within 150 days after transplant (*181*). Therefore, it is not likely that donor immune cells contribute to rejection happening several years after kidney transplant.

Rather than donor immune cells, antigen presentation could be mediated by non-immune cells, such as fibroblast and epithelial cells. In fact, MHC class II expression by intestinal epithelial cells is required for GVHD in the gut (*245*). In the kidney, kidney-intrinsic MHC class II expression is critical for development of glomerulonephritis (*246*). It would be interesting to

investigate an expression pattern of class-II HLAs in rejected allografts, as well as which cell types present class-II antigens in the C57BL/6-bm12 renal allograft model.

Although T cell help is fundamental for B cell affinity selection, B cell intrinsic mechanisms also promote the development of antinucleolar antibodies. TLR7 is one of such key factors. TLR7 has been associated with antinucleolar antibodies both in mice and humans (*247*). Intrarenal B cells in our data highly expressed *TLR7*. Identified potential antigens, Ki-67 and HEATR1, also interact with RNA. Ki-67 binds to RNA via an accessory protein NIFK (*248*). HEATR1 is one of snoRNPs that assembles ribosomal RNAs (*249*). Therefore, it is possible that antibodies recognizing Ki-67 or HEATR1 activate TLR7. Taken together, the upregulation of innate immune pathways might contribute to the selection of antinucleolar reactivity observed in this study.

Although intrarenal B cells upregulated *TLR7* along with its downstream signaling components such as *TRAF3* and *TRAF6*, they did not express *TBX21*, a gene directly upregulated by TLR7 stimulation. This lack of TBX21 expression was true for plasma cells as well. TLR7 stimulation is critical for the development of antinucleolar antibodies in mouse models (*97*, *104*). Nevertheless, we do not have an evidence of TLR7 activation in these cells at this point.

In addition to innate signaling pathways like *TLR7,* intrarenal B cells highly expressed genes of other B cell-activating pathways, such as type-1 and type-2 IFN pathways. Since both type-1 and type-2 IFNs are abundant in rejecting renal allografts (*221*, *250*), it is likely that intrarenal B cells receive an activation signal from them. IFN-α upregulates *TLR7,* which could explain how intrarenal B cells highly express it.

Another important B cell-activation pathway implicated in this study is BAFF. Intrarenal B cells highly expressed *TNFRSF13B* encoding a BAFF receptor TACI. Pathological role of BAFF

has been extensively characterized in autoimmune diseases such as SLE (*109*). In renal allograft rejection, serum BAFF level is correlated with onset of antibody-mediated rejection (*251*). BAFF is also expressed in rejected allografts (*252*). These results indicate that BAFF could play an important role in B cell activation in renal allografts.

Not only receiving signals from these inflammatory mediators, B cells also secrete cytokines. Studies of circulating B cells in mice and humans have implicated immunosupressive Breg cells producing IL-10. However, we instead found that intrarenal B cells produce a proinflammatory cytokine IL-15. IL-15-expressing B cells were previously reported in multiple sclerosis patients (*189*). In that study, B cell-derived IL-15 enhanced cytotoxic activity of $CD8^+$ T cells. IL-15 also acts on more abundant $CD4^+$ T cells, rendering them resistant to suppression by Tregs or upregulating their NK receptor expression (*253*). In renal allograft rejection, IL-15 transcripts are abundant in rejected allografts (*190*). Our result also showed that many infiltrating immune cells expressed IL-15. These observations collectively indicate that B cells could contribute to allograft rejection via IL-15 production.

In addition to these well characterized pathways discussed above, a unique signature was identified by an analysis of *AHNAK*. Although a role of AHNAK in B cell biology is unknown, it is specifically expressed in peritoneal B1 cells. Interestingly, our analysis revealed that other genes with a similar expression pattern were enriched in a geneset upregulated in intrarenal B cells. Along with the lack of a GC transcriptional signature, this peritoneal B1-like gene expression highlights the uniqueness of the intrarenal B cell phenotype.

Nevertheless, those *AHNAK*-covariant genes accounted for only a small fraction of genes upregulated in intrarenal B cells. Therefore, intrarenal B cells do not completely recapitulate peritoneal B1 cells. *ANHAK*-covariant genes, including those related to innate immune responses,

contained several genes involved in cell migration and adhesion, such as *ITGAM* and *CD44*. Taken together with the fact that intrarenal B cells were not enriched for autoreactivity, they are presumably B2 cells which acquired a phenotype adapted to a local non-lymphoid tissue.

Many of migration-related genes upregulated by intrarenal B cells were also paired with those upregulated at the tissue level. Upregulation of several identified genes, such as *ITGAM*, *ITGA4* and *SELL*, is associated with lymphocyte infiltration in in tumor tissues (*254*). Therefore, these migration-related genes could be commonly important for lymphocyte infiltration in a local tissue. These identified axes could also be therapeutic targets to block immune cell infiltration in allografts.

Interestingly, activated B cells in lupus nephritis tissues express *AHNAK*-covariant genes such as *AHNAK* and *ITGAM* at a higher frequency and expression level compared with naïve B cells (*130*). On the other hand, liver carcinoma-infiltrating B cells express equivalent level of *AHNAK* compared to circulating B cells (*255*). These results indicate that upregulation of *AHNAK*-covariant genes should depend not only on a presence in non-lymphoid tissues, but also on a local inflammatory environment. In lupus nephritis, IFN-stimulated B cells do not highly express *AHNAK*. Also in our data, IFN signature did not correlate with *AHNAK* expression (data not shown). These data indicate that IFN is not likely a driver of *AHNAK*-covariant gene expression in inflamed kidneys. Focusing on other pathways commonly upregulated in renal allograft rejection and lupus nephritis could provide insights into how intrarenal B cells upregulate this gene signature.

Activated B cells in lupus nephritis tissues have an ABC-like phenotype. However, our intrarenal B cells did not show this signature. In particular, intrarenal B cells in allografts lacked *TBX21* expression. Although it is possible that the RNA-seq setting we employed could not

reliably capture *TBX21* transcripts, our results indicate that intrarenal B cells in rejecting allografts have a phenotype distinct from ABCs in lupus nephritis. Interestingly, in mice, T-bet expression in B cells is stable (which lasts at least 40 days), and T-bet$^+$ and T-bet$^-$ antigen-specific memory B cells are derived from different clonal populations (*256*). It is unknown whether receptor affinity or specificity affects *TBX21* expression in B cells. Intrarenal B cells in lupus nephritis are selected to ubiquitous self-antigens such as vimentin (*117*), while those in rejecting allografts are not. It is interesting whether the deference in their antibody reactivity underlies the differential expression of *TBX21*.

Overall, this study demonstrates a unique transcriptional phenotype and antibody reactivity of B cells infiltrating rejecting renal allografts. These insights shown here could have never been obtained from only studying circulating B cells or mouse models. Our findings underscore that we need to focus on what is happening *in situ* to truly understand mechanisms driving tissue inflammation.

4.2 Current and Future directions

Additional experiments are ongoing to more precisely characterize antibody reactivity of intrarenal B cells. In our data, non-plasma cells were not selected for allo or self-reactivity. However, it is possible that they are selected for antigens specific to inflamed kidney tissues. We have stained rejected renal allografts using a few highly mutated antibodies, which turned out negative (data not shown). However, immunofluorescent tissue staining is not very sensitive. Moreover, tissue staining is laborious, which makes it challenging to test more than 100 expressed antibodies. To circumvent these drawbacks, we are planning to test their reactivity on kidney endothelial cells, which are recognized as a source of non-HLA antigens in renal allografts. Endothelial staining

allows us to test antibody reactivity in a higher-throughput manner. Additionally, we can also test whether immunological activation of endothelial cells affects antibody binding. These experiments will provide us with more detailed understanding on their reactivity and selection.

Plasma cells were clearly selected for nucleolar self-antigens. Mass spectrometry and tissue staining identified Ki-67 as a potential target in nucleoli. However, these experiments do not necessarily indicate direct binding. To demonstrate direct binding, we are currently cloning recombinant Ki-67. Ki-67 weighs more than 300 kDa, which is too huge to clone as a whole. Therefore, we fragmented it and cloned into a histidine-tagged pET-24b (+) vector. This expression system is what we previously employed to make recombinant vimentin (*117*). Once antigens are expressed and purified, they will be coated on plates for ELISA. If direct binding is proven, it would be interesting to investigate whether anti-Ki-67 antibodies can be detected in serum of transplant recipients, and whether they can predict clinical outcomes.

The clonal expansion and affinity selection in plasma cells suggest T-dependent B cell activation. Therefore, graft-infiltrating T cells could have a corresponding specificity. TLS in renal allografts almost always contain $CD4^+$ T cells along with B cells. Additionally, we previously demonstrated functional interaction between B cells and Tfh cells in allografts (*115*). Characterization of intrarenal T cell repertoire is indispensable to completely understand how *in situ* B cell repertoire is shaped in allograft rejection.

Compared with $CD4^+$ T cells, $CD8^+$ T cells are less abundant in renal allografts. Without a clear implication of their role in B cell activation, interaction between B cells and $CD8^+$ T cells has not been extensively studied. However, B cells can present antigens to $CD8^+$ T cells (*257*). Moreover, $CD8^+$ T cells can also express CD40L (*258*). Although not widely accepted, $CD8^+$ T cells with a Tfh-like phenotype have been also reported (*259*). Therefore, it is possible that $CD8^+$

T cells activate B cells. In fact, our data showed an upregulation of class-I MHC in intrarenal B cells. These observations make it interesting to investigate possible interaction between B cells and $CD8^+$ T cells. For this purpose, cell-distance mapping developed in our laboratory will be a very powerful tool (*115*, *260*). We are currently accumulating tissue staining data, so that we can measure distance B cells and $CD4^+$ or $CD8^+$ T cells in an unbiased and high-throughput manner. Testing association between cell distance and clinical features will provide functional implication of their interaction.

In terms of interaction between B cells and others, our data demonstrated potential axes present in rejected renal allografts. We compared our B cell data with whole tissue data. Therefore, we could not visualize which cell types are actually interacting with B cells. Throughput of scRNA-seq is becoming higher and higher, allowing analysis of 10,000 cells altogether. Therefore, it will be feasible to analyze all cell types present in rejecting allografts, In fact, such studies have been carried out for other diseases (*130*, *261*). Such a comprehensive analysis of intrarenal cells will definitely provide a higher-resolution picture of how they are interacting *in situ*.

To examine phenotypes of such tissue-local immune cells, having a control population from secondary lymphoid organs, such as tonsil B cells in this study, would be very informative. However, in our study, tonsil donors were deidentified. Causes of tonsillectomy are mainly two types: tonsillitis due to recurrent infection, or sleep apnea caused by airway obstruction without apparent inflammation (*262*). Our study design did not allow us to tell which was the case. Moreover, we cannot tell medical background of those tonsil donors, such as history of autoimmune diseases and organ transplant. Because of this limitation, we cannot call those tonsil B cells or their antibodies a “healthy” control. We believe they represent GC B cells, since they expressed a clear GC gene signature and tonsil B cells from all the seven donors showed the same

clustering on a t-SNE space. Nevertheless, we should make sure that we have access to their medical information in future studies.

Moreover, we had an unexpected discrepancy in scRNA-seq data quality between cohorts. As shown in Figure 2.7B, the second cohorts had much lower sequencing depth. As a result, the resolution of the second-cohort data was limited compared with the first cohort. The normalization scheme we employed effectively integrated the two cohorts. However, as well as technical variation, true biological information was surely lost by this normalization. In fact, several DEGs found in the first cohort, such as *TLR7* and *IL15*, did not reproduce in the integrated data. For this reason, we could not analyze the integrated data as thoroughly as we did on the first cohort data. In future studies, every omics study must be carefully designed so as to minimize batch effects.

Another caveat of our study is that we lack functional data. The biggest barrier for functional studies is accessibility of patient samples. Therefore, we need animal models which recapitulate B-cell infiltration in rejecting allografts. Fortunately, our collaborator developed a mouse model of renal allograft rejection which involves B-cell infiltration (*176*). This mouse model will allow us to mechanistically study intrarenal B1 cells. For example, we would be able to study a role of B1 cells by combining this model with a genetic background which lack B1 cells (*79*) or peritoneal B1 cell depletion (*83*). Utilizing genetics, we could also investigate a B cell-intrinsic role of specific genes such as TLRs and *Ahnak*.

Regarding mouse models, the C57BL/6-bm12 transplant model is interesting to study (*179*). This model develops antinuclear autoantibodies, which makes it a unique model for studying how B cell break self-tolerance to nuclear antigens in the context of transplant rejection. For example, blocking of BAFF and APRIL with TACI-Ig diminishes this reactivity in this model. Such global blockade of BAFF/APRIL should profoundly affect B cells outside allografts as well. Nevertheless,

intrarenal B cells highly express *TNFRSF13B* encoding a BAFF receptor TACI. Given high BAFF expression reported in rejecting allografts (*251*, *252*), BAFF could be important for activating intrarenal B cells and shaping their antibody reactivity. Including BAFF, this mouse model could help us investigate whether factors found in this study, such as TLR7 and IFNs, play a role in development of antinucleolar antibodies in allografts.

The study revealed a previously unknown phenotype of intrarenal B cells in allograft rejection patients. Our findings underscore the importance of studying immune responses at the very site of inflammation. At the same time, our finding provides new questions which need to be addressed in future studies. I would be excited to see how these questions will be answered, eventually leading to development of new therapeutics.

5 Materials and Methods

Clinical sample collection

Kidney biopsies were collected as an additional biopsy core from consented patients. Presence of antibody-mediated rejection was clinically confirmed for all the sequenced transplant patients. Tonsil samples were deidentified and collected from tonsillectomy cases. All the clinical samples were collected on the day of biopsy at the University of Chicago Hospital. Sample collection was approved by the Internal Review Board at the University of Chicago.

Cell sorting

Within 5 hours after collection, tissues were minced and digested with Liberase TL (Sigma-Aldrich) for 15 minutes at 37 °C. Cells were washed and stained for 30 minutes at 4 °C with Calcein AM (eBioscience) and antibodies: PE-CD19 (eBioscience, SJ25C1), APC-CD38 (BD, HIT2), PE-Cy7-CD45 (eBioscience, HI30). Stained cells were washed, and DAPI (Thermo Fisher Scientific) was added to the single-cell suspension immediately before the samples were subjected to BD FACSAria Fusion for sorting. Doublets were excluded by FSC-A/FSC-H gating, and CD45+ Calcein+ DAPI- CD19+ CD38+ activated B cells were single-cell sorted into 96-well plates with catching buffer (RLT lysis buffer (Qiagen) with 1% 2-mercaptoethanol (Sigma-Aldrich)). Sorted cells were immediately spun down and stored at -80 °C until being processed for scRNA-seq.

scRNA-seq

scRNA-seq was performed following Smart-seq 2 protocol (*202*). mRNA was purified from sorted

cell lysates using SPRI beads (Beckman Coulter), and reverse transcribed to cDNA with ERCC spike-in controls (Thermo Fisher Scientific). cDNA was amplified for 20 cycles using KAPA HiFi HotStart ReadyMix PCR Kit (Kapa Biosystems). Aliquots of the amplified cDNA were also used for antibody cloning later. cDNA library was generated using Nextera XT DNA Library Preparation Kit (Illumina), pooled and sequenced with Illumina sequencer.

Read alignment, quality control and data integration

For mapping sequencing reads, a human transcriptome (GRCh38) was obtained from Ensembl database. Low-complexity regions were masked from the transcriptome using RepeatMasker 4.1.0 (*263*) with "-noint -norna -qq" options. The masked transcriptome was used for pseudoalignment by kallisto 0.46.1 (*264*). For the first cohort, poor-quality cells were excluded from the analyses if they were expressing less than 3,000 genes or more than 15,000 genes. Furthermore, to exclude cells which could be non-B cells, cells were filtered out if a sum of log2-cpm of Ig heavy chain constant region genes was below 5. Batch effects were corrected by normalizing counts to ERCC using the RUVSeq 1.16.1 (*203*) with "k = 2" option. For the second cohort, read alignment and QC was done in the same manner except that 1,000 genes were used for gene count cut off. In order to normalize the difference in sequencing depths between the first and second cohorts, SCTransform in Seurat R package 3.1.1 (*217*, *218*) was applied. The normalized data were further processed by ComBat in sva package R package 3.32.1 (*219*) to remove batch effects between the two cohorts.

t-SNE projection and cell cluster assignment for the differential gene expression analysis

Gene expression similarity among single cells were visualized by t-SNE plots, whose coordinates

were calculated by Rtsne package 0.15. Expressed Ig isotypes were determined from the scRNA-seq data by assigning the most highly expressed Ig constant region gene. Cells were categorized as "unswitched" if their isotype was IgM or IgD, and categorized as "switched" otherwise. For the first cohort, the ERCC-normalized data was scaled by log2 cpm before making t-SNE plots. For the integrated data, clusters were assigned by Seurat, and the plasma cell cluster was identified by *PRDM1* expression. Plasma cells were removed from differential expression analyses.

Differential gene expression analysis

Differential expression was tested on genes expressed by at least 10% of each category to be compared. For the first cohort, raw pseudocounts were rounded and subjected to edgeR 3.26.8 (*265*) with unwanted variables calculated by RUVSeq in the design matrix. For the integrated data, independent t-tests were applied to expression values after ComBat. For both analyses, false discovery rate (FDR) was calculated by adjusting p values for multiple testing by the Benjamin-Hochberg method. Genes with FDR $\leq$ 0.05 and log2 fold change $\geq$ 1 were categorized as differentially expressed.

Hierarchical clustering of 2855 DEG

For the first cohort, differential expression was tested in four comparisons (class-switched renal vs. tonsil, unswitched renal vs. tonsil, renal class-switched vs. unswitched, and tonsil class-switched vs. unswitched). Mean expression values of identified 2855 DEG were calculated in four populations (renal switched, renal unswitched, tonsil switched, tonsil unswitched). Then hierarchical clustering was performed based on their expression pattern across the four population

means, identifying 5 gene clusters. A heatmap was produced using pheatmap R package 1.0.12 based on the clustering and row Z-scores calculated from the mean values.

Pathway enrichment analysis

GO and KEGG enrichment was tested using clusterProfiler 3.12.0 (*266*) and org.Hs.eg.db annotation database 3.8.2. FDR 0.05 was used for a significance cutoff. When there were more than 10 significantly enriched GO terms, redundant terms were removed using "simplify" function in clusterProfiler library with its default setting.

Enrichment analysis of AHNAK-covariant genes

Gene expression in mouse B cell subsets in the spleen or peritoneal cavity were fetched from ImmGen (*208*). Genes were identified as *Ahnak*-covariant genes, when their expression pattern within the peripheral B cell subsets had a correlation coefficient $\geq$ 0.8 with *Ahnak*. The *Ahnak*-covariant genes were converted to their human orthologs as *AHNAK*-covariant genes using Ensembl database. Then enrichment of the *AHNAK*-covariant genes in DEG clusters was tested by a hypergeometric test. For the background frequency, we used the frequency of the *Ahnak*-covariant genes within all the mouse genes detected in ImmGen microarray data.

Calculation of gene expression scores

Geneset-based scores were calculated as a sum of scaled expression values of genes present in each geneset. For DEG cluster scores in mouse B-cell subsets, DEG in each gene cluster were converted to mouse orthologs in the same manner described above. Then, scores for the mouse genes were calculated for each replicate in ImmGen data. A mean score was calculated for each

B-cell subset, scaled to Z-scores and visualized as a heatmap. For innate immune genes, genes tagged to "innate immune response" GO term were identified in *AHNAK*-covariant genes. Within the identified genes, those expressed by at least 10 % of cells were used to calculate a score. For ABC-associated genes, 17 ABC-upregulated genes and 9 ABC-downregulated genes were defined according to a previous study (*130*). Then a difference between a scaled sum of expression of ABC-upregulated and downregulated genes were used as the score.

Ligand-receptor co-expression analysis

For a geneset expressed by intrarenal B cells, we used DEG which were highly expressed in intrarenal B cells in the "class-switched renal vs. tonsil" comparison. To obtain a geneset expressed in rejected renal allografts, we referred to publicly available microarray data *(5)*. Since the data had three categories of rejection (acute, chronic, and drug or infection-induced), they were grouped together as "rejection." Then gene expression was compared between the rejection and normal allografts using t-test, in order to identify genes upregulated in rejected renal allografts. Within the identified DEG, genes encoding a receptor or a ligand were identified by crossmatching them with Functional Annotation of the Mammalian Genome (FANTOM) 5 database (*210*). Connections of identified ligands and receptors were visualized using Cytoscape 3.7.2 (*267*).

Tissue staining

Paraffin-embedded formalin-fixed tissue blocks were sectioned by 3 μm thickness. Tissue sections were deparaffinized with xylene and ethanol, and subjected to antigen retrieval with 10 mM citrate buffer pH 6.0 (ThermoFisher Scientific). Tissue sections were blocked with Tris-buffered saline (TBS) containing 10 % normal donkey serum (Jackson ImmunoResearch Laboratories), and

incubated with a combination of primary antibodies: rat or rabbit anti-CD19 (Invitrogen, 6OMP31 or abcam, EPR5906 respectively), rabbit anti-AHNAK (Proteintech, 16637-1-AP), mouse anti-IL15 (abcam, ab55276), and rabbit anti-Ki-67 (abcam, EPR3610). Antibody binding was detected by fluorophore-conjugated highly cross-adsorbed secondary antibodies (ThermoFisher Scientific), and nuclei were stained with Hoechst 33342 (ThermoFisher Scientific). For staining of FLAG-tagged recombinant antibodies cloned from rejection patients, rat anti-DYKDDDDK (BioLegend, L5) was used as the secondary antibody, which was then detected with fluorophore-conjugated anti-rat IgG antibodies. Stained sections were mounted in ProLong™ Gold Antifade Mountant (ThermoFisher Scientific) and analyzed on SP8 confocal microscopy (Leica).

Sequencing of antibody genes and clonality analysis

Variable regions of antibody heavy and light chain genes were amplified from cDNA using nested PCR (*232*). PCR products were Sanger-sequenced, and mapped to IMGT reference (*233*). Antibodies were determined to belong to the same clonal family when they shared the same VDJ segments and CDR3 length. Phylogenetic trees were constructed using Clustal Omega (*268*) and FigTree 1.4.4 (*269*).

Antibody cloning and recombinant expression

Heavy and light chain variable regions were cloned into AbVec IgG expression vectors. The vector had a FLAG tag at the C terminus of IgG constant region to enable tissue staining in the presence of IgG-expressing cells or IgG deposition (*118*). A pair of cloned heavy and light chain vectors were transfected to HEK293A cells. After five days of culture, secreted IgG was purified using

Protein A agarose beads (Pierce), eluted in 0.1 M glycine-HCl pH 2.8, neutralized with 1M Tris buffer pH 9.0 and stored in PBS with 0.05% sodium azide.

HLA-binding assay

Antibodies were diluted at 150 μg/mL in PBS and tested on LAB Screen™ Mixed or Single Antigen (OneLambda) according to the manufacturer's protocol. To test the binding in the presence of blocking, positive antibodies from intrarenal B cells were prepared in PBS, then diluted 1:1 in PBS or negative control serum included in the kit, and subjected to the assay. NBG ratio was calculated as the experimental readout according to the manufacturer's protocol:

$$NBGratio_i = \frac{S_i - S_0}{N_i - N_0}$$

S_i and S_0 are sample signals from the i th antigen-coated beads and negative beads, and N_i and N_0 are negative serum signals from the i th antigen-coated beads and negative beads. NBG ratio ≥ 2.2 was used as the positivity threshold. For SAB assay, differences in trimmed MFI between antibodies and negative control serum were used as a readout. Eplets information was fetched from HLA Epitope Registry (*270*).

HEp-2 cell staining

Antibodies were diluted at 50 μg/mL in PBS, and tested on NOVA Lite® HEp-2 ANA kit (Inova Diagnostics) according to the manufacturer's protocol. Antibody binding was detected on SP8 confocal microscopy by fluorescent signal from fluorescein isothiocyanate (FITC)-conjugated polyclonal anti-human IgG secondary antibody included in the kit.

Western blot

HEp-2 cells (ATCC® CCL-23TM) were cultured and harvested. A nuclear fraction was prepared using Nuclear Extraction Kit (Abcam) following the manufacturer's protocol. Before the final centrifugation step, lysates were sonicated with three times of a 10-second pulse on ice. Lysates were boiled in Laemmli buffer at 95 °C for 5 minutes, and resolved by SDS-PAGE. Proteins on the gel were transferred to a polyvinylidene fluoride membrane, blocked by 5 % bovine serum albumin-containing TBS, and incubated with 10 μg/mL antibody diluted in the blocking buffer at 4 °C overnight. The membrane was washed and incubated with a horseradish peroxidase-conjugated anti-human IgG antibody, and binding was detected with Pierce™ ECL Western Blotting Substrate (ThermoFisher Scientific).

IP from a nuclear fraction of HEp-2 cell lysates

HEp-2 nuclear lysates were precleared with Protein A Agarose beads, and incubated with 5 μg of antibodies at 4 °C overnight. The beads were washed with Tween20-containing PBS, and captured antibody-antigen complexes were eluted and resolved by SDS-PAGE. Gels were stained with InstantBlue® Protein Stain (Expedeon) at 4 °C overnight. Stained gels were destained in deionized water, excised leaving molecular weight higher than IgG heavy chain, and used for mass spectrometry.

Sample preparation for mass spectrometry

Gel Samples were excised and chopped into ~1 mm^3 pieces. Each section was washed in distilled water and destained using 100 mM NH_4HCO_3 pH7.5 in 50 % acetonitrile. A reduction step was performed by addition of 100 μL 50 mM NH_4HCO_3 pH 7.5 and 10 μL of 200 mM tris (2-

carboxyethyl) phosphine HCl at 37 °C for 30 minutes. The proteins were alkylated by addition of 100 µL of 50 mM iodoacetamide in 50 mM NH_4HCO_3 pH 7.5 buffer, and allowed to react in the dark at 20 °C for 30 minutes. Gel sections were washed in water and acetonitrile, and vacuum dried. Trypsin digestion was carried out overnight at 37 °C with 1:50 - 1:100 enzyme-protein ratio of sequencing grade-modified trypsin (Promega) in 50 mM NH_4HCO_3 pH 7.5, and 20 mM $CaCl_2$. Peptides were extracted first with 5 % formic acid, then with 75 % ACN:5 % formic acid, combined and vacuum dried. Digested peptides were cleaned up on a C18 column (Pierce), speed vacuumed and sent for liquid chromatography–tandem mass spectrometry (LC-MS/MS).

High-performance liquid chromatography (HPLC) for mass spectrometry

All samples were resuspended in Burdick & Jackson HPLC-grade water containing 0.2 % formic acid (Fluka), 0.1% TFA (Pierce), and 0.002% Zwittergent 3-16 (Calbiochem), a sulfobetaine detergent that contributes the following distinct peaks at the end of chromatograms: MH^+ at 392, and in-source dimer [2M + H^+] at 783, and some minor impurities of Zwittergent 3-12 seen as MH^+ at 336. The peptide samples were loaded to a 0.25 µL C8 OptiPak trapping cartridge custom-packed with Michrom Magic (Optimize Technologies) C8, washed, then switched in-line with a 20 cm by 75 µm C18 packed spray tip nano column packed with Michrom Magic C18AQ, for a 2-step gradient. Mobile phase A was water/acetonitrile/formic acid (98/2/0.2) and mobile phase B was acetonitrile/isopropanol/water/formic acid (80/10/10/0.2). Using a flow rate of 350 nL/min, a 90-minute 2-step LC gradient was run from 5 % B to 50 % B in 60 minutes, followed by 50 % - 95 % B over the next 10 minutes, held 10 minutes at 95 % B, back to starting conditions and re-equilibrated.

LC-MS/MS data acquisition and analysis

The samples were analyzed via data-dependent electrospray tandem mass spectrometry (LC-MS/MS) on a Thermo Q-Exactive Orbitrap mass spectrometer, using a 70,000 RP survey scan in profile mode, m/z 360-2000 Da, with lockmasses, followed by 20 HCD fragmentation scans at 17,500 resolution on doubly and triply charged precursors. Single charged ions were excluded, and ions selected for MS/MS were placed on an exclusion list for 60 seconds.

All LC-MS/MS *.raw Data files were analyzed with MaxQuant version 1.5.2.8, searching against the UniProt Human database (Download 9/16/2019 with isoforms, 192928 entries) *.fasta sequence, using the following criteria: LFQ was selected for Quantitation with a minimum of 1 high confidence peptide to assign LFQ Intensities. Trypsin was selected as the protease with maximum missing cleavage set to 2. Carbamidomethyl (C) was selected as a fixed modification. Variable modifications were set to Oxidization (M), Formylation (N-term), Deamidation (NQ). Orbitrap mass spectrometer was selected using an MS error of 20 ppm and a MS/MS error of 0.5 Da. 1% FDR cutoff was selected for peptide, protein, and site identifications. Ratios were reported based on the LFQ Intensities of protein peak areas determined by MaxQuant (version 1.5.2.8) and reported in the proteinGroups.txt. The proteingroups.txt file was processed in Perseus (version 1.6.7). Proteins were removed from this results file if they were flagged by MaxQuant as “Contaminants”, “Reverse” or “Only identified by site”. Three biological replicates were performed. Samples were filtered to require hits to have been seen in at least two replicates per condition. Intensities were normalized by median intensity within each sample. Median intensity of the two negative control antibodies were calculated for detected proteins. Then, log2 fold changes over the means of negative controls were obtained for the three antinucleolar antibodies.

Statistical Analyses

To adjust p-values for multiple testing, the Benjamin-Hochberg method was used throughout this study. Geneset enrichment was tested by a hypergeometric test (Figure 2.3B and 2.4J). For Figure 2.3B, p-values were adjusted for multiple. A t-test was used to assess differences in innate immune gene scores (Figure 2.4M). Differential gene expression in integrated RNA-seq data was also tested by t-test, and p-values were adjusted for multiple testing (Figure 2.8F and G).

6 References

1. S. Tonegawa, Somatic generation of antibody diversity. *Nature*. **302**, 575–581 (1983).

2. H. N. Eisen, G. W. Siskind, VARIATIONS IN AFFINITIES OF ANTIBODIES DURING THE IMMUNE RESPONSE. *Biochemistry*. **3**, 996–1008 (1964).

3. T. Okada, M. J. Miller, I. Parker, M. F. Krummel, M. Neighbors, S. B. Hartley, A. O'Garra, M. D. Cahalan, J. G. Cyster, Antigen-engaged B cells undergo chemotaxis toward the T zone and form motile conjugates with helper T cells. *PLoS Biol.* **3**, e150 (2005).

4. J. G. Cyster, S. R. Schwab, Sphingosine-1-phosphate and lymphocyte egress from lymphoid organs. *Annu. Rev. Immunol.* **30**, 69–94 (2012).

5. J. A. Green, J. G. Cyster, S1PR2 links germinal center confinement and growth regulation. *Immunol. Rev.* **247**, 36–51 (2012).

6. G. D. Victora, M. C. Nussenzweig, Germinal centers. *Annu Rev Immunol*. **30**, 429–457 (2012).

7. G. D. Victora, T. A. Schwickert, D. R. Fooksman, A. O. Kamphorst, M. Meyer-Hermann, M. L. Dustin, M. C. Nussenzweig, Germinal center dynamics revealed by multiphoton microscopy with a photoactivatable fluorescent reporter. *Cell*. **143**, 592–605 (2010).

8. M. R. Clark, M. Mandal, K. Ochiai, H. Singh, Orchestrating B cell lymphopoiesis through interplay of IL-7 receptor and pre-B cell receptor signalling. *Nat. Rev. Immunol.* **14**, 69–80 (2014).

9. D. Kennedy, M. Okoreeh, M. Maienschein-Cline, J. Ai, M. Veselits, K. McLean, Y. Dhugana, H. Wang, J. Peng, H. Chi, M. Mandal, M. Clark, Novel specialized cell state and spatial compartments within the germinal center.

10. A. D. Gitlin, Z. Shulman, M. C. Nussenzweig, Clonal selection in the germinal centre by regulated proliferation and hypermutation. *Nature*. **509**, 637–640 (2014).

11. M. Muramatsu, K. Kinoshita, S. Fagarasan, S. Yamada, Y. Shinkai, T. Honjo, Class switch recombination and hypermutation require activation-induced cytidine deaminase (AID), a potential RNA editing enzyme. *Cell*. **102**, 553–563 (2000).

12. C. D. C. Allen, T. Okada, H. L. Tang, J. G. Cyster, Imaging of germinal center selection events during affinity maturation. *Science*. **315**, 528–531 (2007).

13. K. Suzuki, I. Grigorova, T. G. Phan, L. M. Kelly, J. G. Cyster, Visualizing B cell capture of cognate antigen from follicular dendritic cells. *J. Exp. Med.* **206**, 1485–1493 (2009).

14. S. Han, K. Hathcock, B. Zheng, T. B. Kepler, R. Hodes, G. Kelsoe, Cellular interaction in germinal centers. Roles of CD40 ligand and B7-2 in established germinal centers. *J. Immunol.* **155**, 556–567 (1995).

15. J. B. Beltman, C. D. C. Allen, J. G. Cyster, R. J. de Boer, B cells within germinal centers migrate preferentially from dark to light zone. *Proc. Natl. Acad. Sci. U.S.A.* **108**, 8755–8760 (2011).

16. T. B. Kepler, A. S. Perelson, Cyclic re-entry of germinal center B cells and the efficiency of affinity maturation. *Immunol. Today*. **14**, 412–415 (1993).

17. J. M. J. Tas, L. Mesin, G. Pasqual, S. Targ, J. T. Jacobsen, Y. M. Mano, C. S. Chen, J.-C. Weill, C.-A. Reynaud, E. P. Browne, M. Meyer-Hermann, G. D. Victora, Visualizing antibody affinity maturation in germinal centers. *Science*. **351**, 1048–1054 (2016).

18. T. G. Phan, D. Paus, T. D. Chan, M. L. Turner, S. L. Nutt, A. Basten, R. Brink, High affinity germinal center B cells are actively selected into the plasma cell compartment. *J. Exp. Med.* **203**, 2419–2424 (2006).

19. D. Suan, N. J. Krautler, J. L. V. Maag, D. Butt, K. Bourne, J. R. Hermes, D. T. Avery, C. Young, A. Statham, M. Elliott, M. E. Dinger, A. Basten, S. G. Tangye, R. Brink, CCR6 Defines Memory B Cell Precursors in Mouse and Human Germinal Centers, Revealing Light-Zone Location and Predominant Low Antigen Affinity. *Immunity*. **47**, 1142-1153.e4 (2017).

20. K. Ochiai, M. Maienschein-Cline, G. Simonetti, J. Chen, R. Rosenthal, R. Brink, A. S. Chong, U. Klein, A. R. Dinner, H. Singh, R. Sciammas, Transcriptional regulation of germinal center B and plasma cell fates by dynamical control of IRF4. *Immunity*. **38**, 918–929 (2013).

21. K. Basso, M. Saito, P. Sumazin, A. A. Margolin, K. Wang, W.-K. Lim, Y. Kitagawa, C. Schneider, M. J. Alvarez, A. Califano, R. Dalla-Favera, Integrated biochemical and computational approach identifies BCL6 direct target genes controlling multiple pathways in normal germinal center B cells. *Blood*. **115**, 975–984 (2010).

22. C. Huang, H. Geng, I. Boss, L. Wang, A. Melnick, Cooperative transcriptional repression by BCL6 and BACH2 in germinal center. *Blood*. **123**, 1012–1020 (2014).

23. L. M. Corcoran, D. Emslie, T. Kratina, W. Shi, S. Hirsch, N. Taubenheim, S. Chevrier, Oct2 and Obf1 as Facilitators of B:T Cell Collaboration during a Humoral Immune Response. *Front. Immunol.* **5** (2014), doi:10.3389/fimmu.2014.00108.

24. D. Dominguez-Sola, J. Kung, A. B. Holmes, V. A. Wells, T. Mo, K. Basso, R. Dalla-Favera, The FOXO1 Transcription Factor Instructs the Germinal Center Dark Zone Program. *Immunity*. **43**, 1064–1074 (2015).

25. C. E. Sayegh, M. W. Quong, Y. Agata, C. Murre, E-proteins directly regulate expression of activation-induced deaminase in mature B cells. *Nat. Immunol.* **4**, 586–593 (2003).

26. H. Gonda, M. Sugai, Y. Nambu, T. Katakai, Y. Agata, K. J. Mori, Y. Yokota, A. Shimizu, The balance between Pax5 and Id2 activities is the key to AID gene expression. *J. Exp. Med.* **198**, 1427–1437 (2003).

27. C. H. Lee, M. Melchers, H. Wang, T. A. Torrey, R. Slota, C.-F. Qi, J. Y. Kim, P. Lugar, H. J. Kong, L. Farrington, B. van der Zouwen, J. X. Zhou, V. Lougaris, P. E. Lipsky, A. C. Grammer, H. C. Morse, Regulation of the germinal center gene program by interferon (IFN) regulatory factor 8/IFN consensus sequence-binding protein. *J. Exp. Med.* **203**, 63–72 (2006).

28. T. Inoue, R. Shinnakasu, W. Ise, C. Kawai, T. Egawa, T. Kurosaki, The transcription factor Foxo1 controls germinal center B cell proliferation in response to T cell help. *J. Exp. Med.* **214**, 1181–1198 (2017).

29. R. Sciammas, A. L. Shaffer, J. H. Schatz, H. Zhao, L. M. Staudt, H. Singh, Graded expression of interferon regulatory factor-4 coordinates isotype switching with plasma cell differentiation. *Immunity*. **25**, 225–236 (2006).

30. K. A. Pape, V. Kouskoff, D. Nemazee, H. L. Tang, J. G. Cyster, L. E. Tze, K. L. Hippen, T. W. Behrens, M. K. Jenkins, Visualization of the genesis and fate of isotype-switched B cells during a primary immune response. *J. Exp. Med.* **197**, 1677–1687 (2003).

31. J. A. Roco, L. Mesin, S. C. Binder, C. Nefzger, P. Gonzalez-Figueroa, P. F. Canete, J. Ellyard, Q. Shen, P. A. Robert, J. Cappello, H. Vohra, Y. Zhang, C. R. Nowosad, A. Schiepers, L. M. Corcoran, K.-M. Toellner, J. M. Polo, M. Meyer-Hermann, G. D. Victora, C. G. Vinuesa, Class-Switch Recombination Occurs Infrequently in Germinal Centers. *Immunity*. **51**, 337-350.e7 (2019).

32. W. Luo, F. Weisel, M. J. Shlomchik, B Cell Receptor and CD40 Signaling Are Rewired for Synergistic Induction of the c-Myc Transcription Factor in Germinal Center B Cells. *Immunity*. **48**, 313-326.e5 (2018).

33. D. Dominguez-Sola, G. D. Victora, C. Y. Ying, R. T. Phan, M. Saito, M. C. Nussenzweig, R. Dalla-Favera, The proto-oncogene MYC is required for selection in the germinal center and cyclic reentry. *Nat. Immunol.* **13**, 1083–1091 (2012).

34. A. Kallies, S. L. Nutt, Terminal differentiation of lymphocytes depends on Blimp-1. *Curr. Opin. Immunol.* **19**, 156–162 (2007).

35. A. M. Reimold, N. N. Iwakoshi, J. Manis, P. Vallabhajosyula, E. Szomolanyi-Tsuda, E. M. Gravallese, D. Friend, M. J. Grusby, F. Alt, L. H. Glimcher, Plasma cell differentiation requires the transcription factor XBP-1. *Nature*. **412**, 300–307 (2001).

36. C. Tunyaplin, A. L. Shaffer, C. D. Angelin-Duclos, X. Yu, L. M. Staudt, K. L. Calame, Direct repression of prdm1 by Bcl-6 inhibits plasmacytic differentiation. *J. Immunol.* **173**, 1158–1165 (2004).

37. K.-P. Nera, P. Kohonen, E. Narvi, A. Peippo, L. Mustonen, P. Terho, K. Koskela, J.-M. Buerstedde, O. Lassila, Loss of Pax5 promotes plasma cell differentiation. *Immunity*. **24**, 283–293 (2006).

38. M. Saito, J. Gao, K. Basso, Y. Kitagawa, P. M. Smith, G. Bhagat, A. Pernis, L. Pasqualucci, R. Dalla-Favera, A signaling pathway mediating downregulation of BCL6 in germinal center B cells is blocked by BCL6 gene alterations in B cell lymphoma. *Cancer Cell*. **12**, 280–292 (2007).

39. U. Klein, S. Casola, G. Cattoretti, Q. Shen, M. Lia, T. Mo, T. Ludwig, K. Rajewsky, R. Dalla-Favera, Transcription factor IRF4 controls plasma cell differentiation and class-switch recombination. *Nat. Immunol.* **7**, 773–782 (2006).

40. R. Shinnakasu, T. Inoue, K. Kometani, S. Moriyama, Y. Adachi, M. Nakayama, Y. Takahashi, H. Fukuyama, T. Okada, T. Kurosaki, Regulated selection of germinal-center cells into the memory B cell compartment. *Nat. Immunol.* **17**, 861–869 (2016).

41. G. B. Lesinski, M. A. Westerink, Novel vaccine strategies to T-independent antigens. *J. Microbiol. Methods*. **47**, 135–149 (2001).

42. N. E. Holodick, N. Rodríguez-Zhurbenko, A. M. Hernández, Defining Natural Antibodies. *Front Immunol*. **8** (2017), doi:10.3389/fimmu.2017.00872.

43. K. Hayakawa, R. R. Hardy, D. R. Parks, L. A. Herzenberg, The Ly-1 B cell subpopulation in normal immunodefective, and autoimmune mice. *J Exp Med*. **157**, 202–218 (1983).

44. S. M. Wells, A. B. Kantor, A. M. Stall, CD43 (S7) expression identifies peripheral B cell subsets. *J. Immunol.* **153**, 5503–5515 (1994).

45. R. Francés, J. R. Tumang, T. L. Rothstein, Extreme skewing of annexin II and S100A6 expression identified by proteomic analysis of peritoneal B-1 cells. *Int. Immunol.* **19**, 59–65 (2007).

46. E. E. Waffarn, C. J. Hastey, N. Dixit, Y. S. Choi, S. Cherry, U. Kalinke, S. I. Simon, N. Baumgarth, Infection-induced type I interferons activate CD11b on B-1 cells for subsequent lymph node accumulation. *Nat Commun*. **6**, 8991 (2015).

47. C.-Y. Wang, C.-F. Lin, Annexin A2: Its Molecular Regulation and Cellular Expression in Cancer Development. *Dis Markers*. **2014** (2014), doi:10.1155/2014/308976.

48. A. B. Kantor, A. M. Stall, S. Adams, L. A. Herzenberg, L. A. Herzenberg, Differential development of progenitor activity for three B-cell lineages. *PNAS*. **89**, 3320–3324 (1992).

49. P. A. Lalor, An evolutionarily-conserved role for murine Ly-1 B cells in protection against bacterial infections. *Autoimmunity*. **10**, 71–76 (1991).

50. Y. S. Choi, J. A. Dieter, K. Rothaeusler, Z. Luo, N. Baumgarth, B-1 cells in the bone marrow are a significant source of natural IgM. *Eur. J. Immunol.* **42**, 120–129 (2012).

51. J. J. Bunker, T. M. Flynn, J. C. Koval, D. G. Shaw, M. Meisel, B. D. McDonald, I. E. Ishizuka, A. L. Dent, P. C. Wilson, B. Jabri, D. A. Antonopoulos, A. Bendelac, Innate and Adaptive Humoral Responses Coat Distinct Commensal Bacteria with Immunoglobulin A. *Immunity*. **43**, 541–553 (2015).

52. P. X. Shaw, S. Hörkkö, M. K. Chang, L. K. Curtiss, W. Palinski, G. J. Silverman, J. L. Witztum, Natural antibodies with the T15 idiotype may act in atherosclerosis, apoptotic clearance, and protective immunity. *J. Clin. Invest.* **105**, 1731–1740 (2000).

53. T. T. T. Nguyen, R. A. Elsner, N. Baumgarth, Natural IgM Prevents Autoimmunity by Enforcing B Cell Central Tolerance Induction. *The Journal of Immunology*. **194**, 1489–1502 (2015).

54. N. Baumgarth, A Hard(y) Look at B-1 Cell Development and Function. *The Journal of Immunology*. **199**, 3387–3394 (2017).

55. R. R. Hardy, C. E. Carmack, S. A. Shinton, R. J. Riblet, K. Hayakawa, A single VH gene is utilized predominantly in anti-BrMRBC hybridomas derived from purified Ly-1 B cells. Definition of the VH11 family. *The Journal of Immunology*. **142**, 3643–3651 (1989).

56. L. A. Herzenberg, B-1 cells: the lineage question revisited. *Immunological Reviews*. **175**, 9–22 (2000).

57. H. Gu, I. Förster, K. Rajewsky, Sequence homologies, N sequence insertion and JH gene utilization in VHDJH joining: implications for the joining mechanism and the ontogenetic timing of Ly1 B cell and B-CLL progenitor generation. *EMBO J.* **9**, 2133–2140 (1990).

58. A. J. Feeney, Lack of N regions in fetal and neonatal mouse immunoglobulin V-D-J junctional sequences. *J. Exp. Med.* **172**, 1377–1390 (1990).

59. U. C. Tornberg, D. Holmberg, B-1a, B-1b and B-2 B cells display unique VHDJH repertoires formed at different stages of ontogeny and under different selection pressures. *EMBO J.* **14**, 1680–1689 (1995).

60. N. E. Holodick, T. Vizconde, T. J. Hopkins, T. L. Rothstein, Age-related Decline in Natural IgM Function: Diversification and Selection of the B-1a Cell Pool with Age. *J Immunol*. **196**, 4348–4357 (2016).

61. L. W. Arnold, C. A. Pennell, S. K. McCray, S. H. Clarke, Development of B-1 cells: segregation of phosphatidyl choline-specific B cells to the B-1 population occurs after immunoglobulin gene expression. *J. Exp. Med.* **179**, 1585–1595 (1994).

62. K. P. Lam, K. Rajewsky, B cell antigen receptor specificity and surface density together determine B-1 versus B-2 cell development. *J. Exp. Med.* **190**, 471–477 (1999).

63. K. Hayakawa, M. Asano, S. A. Shinton, M. Gui, D. Allman, C. L. Stewart, J. Silver, R. R. Hardy, Positive selection of natural autoreactive B cells. *Science*. **285**, 113–116 (1999).

64. J. B. Wong, S. L. Hewitt, L. M. Heltemes-Harris, M. Mandal, K. Johnson, K. Rajewsky, S. B. Koralov, M. R. Clark, M. A. Farrar, J. A. Skok, B-1a cells acquire their unique characteristics by bypassing the pre-BCR selection stage. *Nature Communications*. **10**, 1–15 (2019).

65. R. Graf, J. Seagal, K. L. Otipoby, K.-P. Lam, S. Ayoub, B. Zhang, S. Sander, V. T. Chu, K. Rajewsky, BCR-dependent lineage plasticity in mature B cells. *Science*. **363**, 748–753 (2019).

66. A. E. Bussard, G. J. V. Nossal, J. C. Mazie, H. Lewis, IN VITRO STIMULATION OF ANTIBODY FORMATION BY PERITONEAL CELLS. *J Exp Med*. **131**, 917–935 (1970).

67. Y. Yang, J. W. Tung, E. E. B. Ghosn, L. A. Herzenberg, L. A. Herzenberg, Division and differentiation of natural antibody-producing cells in mouse spleen. *Proc Natl Acad Sci U S A*. **104**, 4542–4546 (2007).

68. S. Ha, M. Tsuji, K. Suzuki, B. Meek, N. Yasuda, T. Kaisho, S. Fagarasan, Regulation of B1 cell migration by signals through Toll-like receptors. *J Exp Med*. **203**, 2541–2550 (2006).

69. M. Gururajan, J. Jacob, B. Pulendran, Toll-Like Receptor Expression and Responsiveness of Distinct Murine Splenic and Mucosal B-Cell Subsets. *PLOS ONE*. **2**, e863 (2007).

70. A. Meyer-Bahlburg, D. J. Rawlings, Differential impact of Toll-like receptor signaling on distinct B cell subpopulations. *Front Biosci*. **17**, 1499–1516 (2012).

71. A. Gagro, N. Mccloskey, A. Challa, M. Holder, G. Grafton, J. D. Pound, J. Gordon, CD5-positive and CD5-negative human B cells converge to an indistinguishable population on signalling through B-cell receptors and CD40. *Immunology*. **101**, 201–209 (2000).

72. T. L. Rothstein, T. D. Quach, The human counterpart of mouse B-1 cells. *Ann N Y Acad Sci*. **1362**, 143–152 (2015).

73. D. O. Griffin, N. E. Holodick, T. L. Rothstein, Human B1 cells in umbilical cord and adult peripheral blood express the novel phenotype CD20+ CD27+ CD43+ CD70-. *J. Exp. Med.* **208**, 67–80 (2011).

74. M. Descatoire, J.-C. Weill, C.-A. Reynaud, S. Weller, A human equivalent of mouse B-1 cells? *J. Exp. Med.* **208**, 2563–2564 (2011).

75. M. Perez-Andres, C. Grosserichter-Wagener, C. Teodosio, J. J. M. van Dongen, A. Orfao, M. C. van Zelm, The nature of circulating CD27+CD43+ B cells. *J. Exp. Med.* **208**, 2565–2566 (2011).

76. K. Covens, B. Verbinnen, N. Geukens, I. Meyts, F. Schuit, L. Van Lommel, M. Jacquemin, X. Bossuyt, Characterization of proposed human B-1 cells reveals pre-plasmablast phenotype. *Blood*. **121**, 5176–5183 (2013).

77. B. Roy, S. Shukla, M. Łyszkiewicz, M. Krey, N. Viegas, S. Düber, S. Weiss, Somatic hypermutation in peritoneal B1b cells. *Molecular Immunology*. **46**, 1613–1619 (2009).

78. J. J. Bunker, S. A. Erickson, T. M. Flynn, C. Henry, J. C. Koval, M. Meisel, B. Jabri, D. A. Antonopoulos, P. C. Wilson, A. Bendelac, Natural polyreactive IgA antibodies coat the intestinal microbiota. *Science*. **358** (2017), doi:10.1126/science.aan6619.

79. C. N. Arnold, E. Pirie, P. Dosenovic, G. M. McInerney, Y. Xia, N. Wang, X. Li, O. M. Siggs, G. B. Karlsson Hedestam, B. Beutler, A forward genetic screen reveals roles for Nfkbid, Zeb1, and Ruvbl2 in humoral immunity. *Proc. Natl. Acad. Sci. U.S.A.* **109**, 12286–12293 (2012).

80. G. K. Pedersen, M. Àdori, S. Khoenkhoen, P. Dosenovic, B. Beutler, G. B. Karlsson Hedestam, B-1a transitional cells are phenotypically distinct and are lacking in mice deficient in IκBNS. *Proc. Natl. Acad. Sci. U.S.A.* **111**, E4119-4126 (2014).

81. M. Kitabatake, M. Soma, T. Zhang, K. Kuwahara, Y. Fukushima, T. Nojima, D. Kitamura, N. Sakaguchi, JNK Regulatory Molecule G5PR Induces IgG Autoantibody–Producing Plasmablasts from Peritoneal B1a Cells. *The Journal of Immunology* (2015), doi:10.4049/jimmunol.1401127.

82. B. Duan, L. Morel, Role of B-1a cells in autoimmunity. *Autoimmunity Reviews*. **5**, 403–408 (2006).

83. P. L. Kendall, E. J. Woodward, C. Hulbert, J. W. Thomas, Peritoneal B cells govern the outcome of diabetes in non-obese diabetic mice. *European Journal of Immunology*. **34**, 2387–2395 (2004).

84. A. Narang, F. Qiao, C. Atkinson, H. Zhu, X. Yang, L. Kulik, V. M. Holers, S. Tomlinson, Natural IgM antibodies that bind neoepitopes exposed as a result of spinal cord injury , drive secondary injury by activating complement. *Journal of Neuroinflammation*. **14**, 120 (2017).

85. J. Diana, Y. Simoni, L. Furio, L. Beaudoin, B. Agerberth, F. Barrat, A. Lehuen, Crosstalk between neutrophils, B-1a cells and plasmacytoid dendritic cells initiates autoimmune diabetes. *Nature Medicine*. **19**, 65–73 (2013).

86. H. Wardemann, S. Yurasov, A. Schaefer, J. W. Young, E. Meffre, M. C. Nussenzweig, Predominant autoantibody production by early human B cell precursors. *Science*. **301**, 1374–1377 (2003).

87. D. A. Nemazee, K. Bürki, Clonal deletion of B lymphocytes in a transgenic mouse bearing anti-MHC class I antibody genes. *Nature*. **337**, 562–566 (1989).

88. C. C. Goodnow, J. Crosbie, S. Adelstein, T. B. Lavoie, S. J. Smith-Gill, R. A. Brink, H. Pritchard-Briscoe, J. S. Wotherspoon, R. H. Loblay, K. Raphael, Altered immunoglobulin expression and functional silencing of self-reactive B lymphocytes in transgenic mice. *Nature*. **334**, 676–682 (1988).

89. D. Gay, T. Saunders, S. Camper, M. Weigert, Receptor editing: an approach by autoreactive B cells to escape tolerance. *J Exp Med*. **177**, 999–1008 (1993).

90. T. D. Quách, N. Manjarrez-Orduño, D. G. Adlowitz, L. Silver, H. Yang, C. Wei, E. C. B. Milner, I. Sanz, Anergic responses characterize a large fraction of human autoreactive naive B cells expressing low levels of surface IgM. *J. Immunol.* **186**, 4640–4648 (2011).

91. D. A. Fulcher, A. Basten, Reduced life span of anergic self-reactive B cells in a double-transgenic model. *J. Exp. Med.* **179**, 125–134 (1994).

92. J. G. Cyster, S. B. Hartley, C. C. Goodnow, Competition for follicular niches excludes self-reactive cells from the recirculating B-cell repertoire. *Nature*. **371**, 389–395 (1994).

93. J. G. Cyster, C. C. Goodnow, Antigen-induced exclusion from follicles and anergy are separate and complementary processes that influence peripheral B cell fate. *Immunity*. **3**, 691–701 (1995).

94. A. Cappione, J. H. Anolik, A. Pugh-Bernard, J. Barnard, P. Dutcher, G. Silverman, I. Sanz, Germinal center exclusion of autoreactive B cells is defective in human systemic lupus erythematosus. *J Clin Invest*. **115**, 3205–3216 (2005).

95. T. D. Chan, K. Wood, J. R. Hermes, D. Butt, C. J. Jolly, A. Basten, R. Brink, Elimination of germinal-center-derived self-reactive B cells is governed by the location and concentration of self-antigen. *Immunity*. **37**, 893–904 (2012).

96. A. N. Suthers, S. Sarantopoulos, TLR7/TLR9- and B Cell Receptor-Signaling Crosstalk: Promotion of Potentially Dangerous B Cells. *Front. Immunol.* **8** (2017), doi:10.3389/fimmu.2017.00775.

97. S. W. Jackson, N. E. Scharping, N. S. Kolhatkar, S. Khim, M. A. Schwartz, Q.-Z. Li, K. L. Hudkins, C. E. Alpers, D. Liggitt, D. J. Rawlings, Opposing impact of B cell-intrinsic TLR7 and TLR9 signals on autoantibody repertoire and systemic inflammation. *J. Immunol.* **192**, 4525–4532 (2014).

98. R. J. DeHoratius, R. Pillarisetty, R. P. Messner, N. Talal, Anti-nucleic acid antibodies in systemic lupus erythematosus patients and their families. Incidence and correlation with lymphocytotoxic antibodies. *J Clin Invest*. **56**, 1149–1154 (1975).

99. Y. H. Lee, S. J. Choi, J. D. Ji, G. G. Song, Association between toll-like receptor polymorphisms and systemic lupus erythematosus: a meta-analysis update. *Lupus*. **25**, 593–601 (2016).

100. Y. Shoenfeld, O. Segol, Anti-histone antibodies in SLE and other autoimmune diseases. *Clin. Exp. Rheumatol.* **7**, 265–271 (1989).

101. G. R. Harvey, S. Butts, A. L. Rands, Y. Patel, N. J. McHugh, Clinical and serological associations with anti-RNA polymerase antibodies in systemic sclerosis. *Clin Exp Immunol*. **117**, 395–402 (1999).

102. S. Janwityanuchit, M. Vanichapuntu, O. Verasertniyom, K. Totemchokchyakarn, M. Vatanasuk, Antinucleolar antibodies and their disease association. *Asian Pac. J. Allergy Immunol.* **12**, 43–49 (1994).

103. S. Bolland, Y.-S. Yim, K. Tus, E. K. Wakeland, J. V. Ravetch, Genetic Modifiers of Systemic Lupus Erythematosus in FcγRIIB−/− Mice. *J Exp Med*. **195**, 1167–1174 (2002).

104. P. Pisitkun, J. A. Deane, M. J. Difilippantonio, T. Tarasenko, A. B. Satterthwaite, S. Bolland, Autoreactive B Cell Responses to RNA-Related Antigens Due to TLR7 Gene Duplication. *Science*. **312**, 1669–1672 (2006).

105. D. Braun, I. Caramalho, J. Demengeot, IFN - α / β enhances BCR - dependent B cell responses. *Int Immunol*. **14**, 411–419 (2002).

106. I. B. Bekeredjian-Ding, I. B. Berkeredjian-Ding, M. Wagner, V. Hornung, T. Giese, M. Schnurr, S. Endres, G. Hartmann, Plasmacytoid dendritic cells control TLR7 sensitivity of naive B cells via type I IFN. *J. Immunol.* **174**, 4043–4050 (2005).

107. S. B. Chodisetti, A. J. Fike, P. P. Domeier, H. Singh, N. M. Choi, C. Corradetti, Y. I. Kawasawa, T. K. Cooper, R. Caricchio, Z. S. M. Rahman, Type II but Not Type I IFN Signaling Is Indispensable for TLR7-Promoted Development of Autoreactive B Cells and Systemic Autoimmunity. *J. Immunol.* **204**, 796–809 (2020).

108. V. Oke, I. Gunnarsson, J. Dorschner, S. Eketjäll, A. Zickert, T. B. Niewold, E. Svenungsson, High levels of circulating interferons type I, type II and type III associate with distinct clinical features of active systemic lupus erythematosus. *Arthritis Research & Therapy*. **21**, 107 (2019).

109. F. Mackay, P. Schneider, Cracking the BAFF code. *Nat Rev Immunol*. **9**, 491–502 (2009).

110. R. Goenka, A. H. Matthews, B. Zhang, P. J. O'Neill, J. L. Scholz, T.-S. Migone, W. J. Leonard, W. Stohl, U. Hershberg, M. P. Cancro, Local BLyS production by T follicular cells mediates retention of high affinity B cells during affinity maturation. *J Exp Med*. **211**, 45–56 (2014).

111. A. K. Dubey, S. S. Handu, S. Dubey, P. Sharma, K. K. Sharma, Q. M. Ahmed, Belimumab: First targeted biological treatment for systemic lupus erythematosus. *J Pharmacol Pharmacother*. **2**, 317–319 (2011).

112. M. Leslie, Immunity goes local. *Science*. **352**, 21–23 (2016).

113. A. Chang, S. G. Henderson, D. Brandt, N. Liu, R. Guttikonda, C. Hsieh, N. Kaverina, T. O. Utset, S. M. Meehan, R. J. Quigg, E. Meffre, M. R. Clark, In situ B cell-mediated immune

responses and tubulointerstitial inflammation in human lupus nephritis. *J. Immunol.* **186**, 1849–1860 (2011).

114. A. Cipponi, M. Mercier, T. Seremet, J.-F. Baurain, I. Théate, J. van den Oord, M. Stas, T. Boon, P. G. Coulie, N. van Baren, Neogenesis of lymphoid structures and antibody responses occur in human melanoma metastases. *Cancer Res.* **72**, 3997–4007 (2012).

115. V. M. Liarski, N. Kaverina, A. Chang, D. Brandt, D. Yanez, L. Talasnik, G. Carlesso, R. Herbst, T. O. Utset, C. Labno, Y. Peng, Y. Jiang, M. L. Giger, M. R. Clark, Cell distance mapping identifies functional T follicular helper cells in inflamed human renal tissue. *Sci Transl Med*. **6**, 230ra46 (2014).

116. F. Humby, M. Bombardieri, A. Manzo, S. Kelly, M. C. Blades, B. Kirkham, J. Spencer, C. Pitzalis, Ectopic lymphoid structures support ongoing production of class-switched autoantibodies in rheumatoid synovium. *PLoS Med.* **6**, e1 (2009).

117. A. J. Kinloch, A. Chang, K. Ko, C. J. Henry Dunand, S. Henderson, M. Maienschein-Cline, N. Kaverina, B. H. Rovin, M. Salgado Ferrer, D. Wolfgeher, V. Liarski, D. J. Haddon, P. J. Utz, P. C. Wilson, M. R. Clark, Vimentin is a dominant target of in situ humoral immunity in human lupus tubulointerstitial nephritis. *Arthritis & Rheumatology (Hoboken, N.J.)*. **66**, 3359–3370 (2014).

118. A. J. Kinloch, A. MOhsin, Y. Asano, C. Henry, R. Abraham, A. Chang, C. Labno, N. Mor-Vaknin, M. Legendre, D. Markovitsz, P. C. Wilson, M. R. Clark, In situ humoral affinity maturation in human lupus tubulointerstitial inflammation. *in preparation*.

119. E. Corsiero, M. Bombardieri, E. Carlotti, F. Pratesi, W. Robinson, P. Migliorini, C. Pitzalis, Single cell cloning and recombinant monoclonal antibodies generation from RA synovial B cells reveal frequent targeting of citrullinated histones of NETs. *Annals of the Rheumatic Diseases*. **75**, 1866–1875 (2016).

120. E. Corsiero, L. Jagemann, M. Perretti, C. Pitzalis, M. Bombardieri, Characterization of a Synovial B Cell-Derived Recombinant Monoclonal Antibody Targeting Stromal Calreticulin in the Rheumatoid Joints. *J. Immunol.* **201**, 1373–1381 (2018).

121. J. Weinberger, R. Jimenez-Heredia, S. Schaller, S. Suessner, J. Sunzenauer, R. Reindl-Schwaighofer, R. Weiss, S. Winkler, C. Gabriel, M. Danzer, R. Oberbauer, Immune Repertoire Profiling Reveals that Clonally Expanded B and T Cells Infiltrating Diseased Human Kidneys Can Also Be Tracked in Blood. *PLOS ONE*. **10**, e0143125 (2015).

122. H. R. Seay, E. Yusko, S. J. Rothweiler, L. Zhang, A. L. Posgai, M. Campbell-Thompson, M. Vignali, R. O. Emerson, J. S. Kaddis, D. Ko, M. Nakayama, M. J. Smith, J. C. Cambier, A. Pugliese, M. A. Atkinson, H. S. Robins, T. M. Brusko, Tissue distribution and clonal diversity of the T and B cell repertoire in type 1 diabetes. *JCI Insight*. **1**, doi:10.1172/jci.insight.88242.

123. K. Ko, J. Wang, S. Perper, Y. Jiang, D. Yanez, N. Kaverina, J. Ai, V. M. Liarski, A. Chang, Y. Peng, L. Lan, S. Westmoreland, L. Olson, M. L. Giger, L. Chun Wang, M. R. Clark, Bcl-2

as a Therapeutic Target in Human Tubulointerstitial Inflammation. *Arthritis Rheumatol*. **68**, 2740–2751 (2016).

124. K. Rubtsova, A. V. Rubtsov, M. P. Cancro, P. Marrack, Age-Associated B Cells: A T-bet-Dependent Effector with Roles in Protective and Pathogenic Immunity. *J. Immunol.* **195**, 1933–1937 (2015).

125. A. V. Rubtsov, K. Rubtsova, A. Fischer, R. T. Meehan, J. Z. Gillis, J. W. Kappler, P. Marrack, Toll-like receptor 7 (TLR7)–driven accumulation of a novel CD11c+ B-cell population is important for the development of autoimmunity. *Blood*. **118**, 1305–1315 (2011).

126. Y. Hao, P. O'Neill, M. S. Naradikian, J. L. Scholz, M. P. Cancro, A B-cell subset uniquely responsive to innate stimuli accumulates in aged mice. *Blood*. **118**, 1294–1304 (2011).

127. K. Rubtsova, A. V. Rubtsov, L. F. van Dyk, J. W. Kappler, P. Marrack, T-box transcription factor T-bet, a key player in a unique type of B-cell activation essential for effective viral clearance. *Proc. Natl. Acad. Sci. U.S.A.* **110**, E3216-3224 (2013).

128. L. Yeo, H. Lom, M. Juarez, M. Snow, C. D. Buckley, A. Filer, K. Raza, D. Scheel-Toellner, Expression of FcRL4 defines a pro-inflammatory, RANKL-producing B cell subset in rheumatoid arthritis. *Ann Rheum Dis*. **74**, 928–935 (2015).

129. S. Wang, J. Wang, V. Kumar, J. L. Karnell, B. Naiman, P. S. Gross, S. Rahman, K. Zerrouki, R. Hanna, C. Morehouse, N. Holoweckyj, H. Liu, Z. Manna, R. Goldbach-Mansky, S. Hasni, R. Siegel, M. Sanjuan, K. Streicher, M. P. Cancro, R. Kolbeck, R. Ettinger, IL-21 drives expansion and plasma cell differentiation of autoreactive CD11chiT-bet+ B cells in SLE. *Nat Commun*. **9** (2018), doi:10.1038/s41467-018-03750-7.

130. A. Arazi, D. A. Rao, C. C. Berthier, A. Davidson, Y. Liu, P. J. Hoover, A. Chicoine, T. M. Eisenhaure, A. H. Jonsson, S. Li, D. J. Lieb, F. Zhang, K. Slowikowski, E. P. Browne, A. Noma, D. Sutherby, S. Steelman, D. E. Smilek, P. Tosta, W. Apruzzese, E. Massarotti, M. Dall'Era, M. Park, D. L. Kamen, R. A. Furie, F. Payan-Schober, W. F. 3rd Pendergraft, E. A. McInnis, J. P. Buyon, M. A. Petri, C. Putterman, K. C. Kalunian, E. S. Woodle, J. A. Lederer, D. A. Hildeman, C. Nusbaum, S. Raychaudhuri, M. Kretzler, J. H. Anolik, M. B. Brenner, D. Wofsy, N. Hacohen, B. Diamond, The immune cell landscape in kidneys of patients with lupus nephritis. *Nat Immunol*. **20**, 902–914 (2019).

131. B. Schiemann, J. L. Gommerman, K. Vora, T. G. Cachero, S. Shulga-Morskaya, M. Dobles, E. Frew, M. L. Scott, An Essential Role for BAFF in the Normal Development of B Cells Through a BCMA-Independent Pathway. *Science*. **293**, 2111–2114 (2001).

132. M. Manni, S. Gupta, E. Ricker, Y. Chinenov, S. H. Park, M. Shi, T. Pannellini, R. Jessberger, L. Ivashkiv, A. B. Pernis, Regulation of Age-associated B cells by IRF5 in systemic autoimmunity. *Nat Immunol*. **19**, 407–419 (2018).

133. L. M. Russell Knode, M. S. Naradikian, A. Myles, J. L. Scholz, Y. Hao, D. Liu, M. L. Ford, J. W. Tobias, M. P. Cancro, P. J. Gearhart, Age-Associated B Cells Express a Diverse

Repertoire of VH and Vκ Genes with Somatic Hypermutation. *J. Immunol.* **198**, 1921–1927 (2017).

134. C. T. Taylor, G. Doherty, P. G. Fallon, E. P. Cummins, Hypoxia-dependent regulation of inflammatory pathways in immune cells. *J. Clin. Invest.* **126**, 3716–3724 (2016).

135. P.-M. Chen, P. C. Wilson, J. A. Shyer, M. Veselits, H. R. Steach, C. Cui, G. Moeckel, M. R. Clark, J. Craft, Kidney tissue hypoxia dictates T cell–mediated injury in murine lupus nephritis. *Science Translational Medicine*. **12** (2020), doi:10.1126/scitranslmed.aay1620.

136. B. E. Barnett, R. P. Staupe, P. M. Odorizzi, O. Palko, V. T. Tomov, A. E. Mahan, B. Gunn, D. Chen, M. A. Paley, G. Alter, S. L. Reiner, G. M. Lauer, J. R. Teijaro, E. J. Wherry, Cutting Edge: B Cell-Intrinsic T-bet Expression Is Required To Control Chronic Viral Infection. *J. Immunol.* **197**, 1017–1022 (2016).

137. D. Lau, L. Y.-L. Lan, S. F. Andrews, C. Henry, K. T. Rojas, K. E. Neu, M. Huang, Y. Huang, B. DeKosky, A.-K. E. Palm, G. C. Ippolito, G. Georgiou, P. C. Wilson, Low CD21 expression defines a population of recent germinal center graduates primed for plasma cell differentiation. *Sci Immunol*. **2** (2017), doi:10.1126/sciimmunol.aai8153.

138. S. H. Cho, A. L. Raybuck, K. Stengel, M. Wei, T. C. Beck, E. Volanakis, J. W. Thomas, S. Hiebert, V. H. Haase, M. R. Boothby, Germinal centre hypoxia and regulation of antibody qualities by a hypoxia response system. *Nature*. **537**, 234–238 (2016).

139. M. Hassanein, J. J. Augustine, in *StatPearls* (StatPearls Publishing, Treasure Island (FL), 2020; http://www.ncbi.nlm.nih.gov/books/NBK549762/).

140. J. Robinson, J. A. Halliwell, J. D. Hayhurst, P. Flicek, P. Parham, S. G. E. Marsh, The IPD and IMGT/HLA database: allele variant databases. *Nucleic Acids Res*. **43**, D423–D431 (2015).

141. R. Zhang, Donor-Specific Antibodies in Kidney Transplant Recipients. *Clin J Am Soc Nephrol*. **13**, 182–192 (2018).

142. A. Djamali, D. B. Kaufman, T. M. Ellis, W. Zhong, A. Matas, M. Samaniego, Diagnosis and management of antibody-mediated rejection: current status and novel approaches. *Am J Transplant*. **14**, 255–271 (2014).

143. C. Lawrence, M. Willicombe, P. A. Brookes, E. Santos-Nunez, R. Bajaj, T. Cook, C. Roufosse, D. Taube, A. N. Warrens, Preformed complement-activating low-level donor-specific antibody predicts early antibody-mediated rejection in renal allografts. *Transplantation*. **95**, 341–346 (2013).

144. A. Picascia, T. Infante, C. Napoli, Luminex and antibody detection in kidney transplantation. *Clin Exp Nephrol*. **16**, 373–381 (2012).

145. P. C. Grenzi, R. de Marco, R. Z. R. Silva, E. F. Campos, M. Gerbase-DeLima, Antibodies against denatured HLA class II molecules detected in luminex-single antigen assay. *Hum. Immunol.* **74**, 1300–1303 (2013).

146. M. J. Gandhi, D. M. Carrick, S. Jenkins, S. De Goey, N. A. Ploeger, G. A. Wilson, J. H. Lee, J. L. Winters, J. R. Stubbs, P. Toy, P. J. Norris, Lot-to-Lot Variability in HLA Antibody Screening Using a Multiplexed Bead Based Assay. *Transfusion*. **53**, 1940–1947 (2013).

147. D. Bertrand, F. Farce, C. Laurent, F. Hamelin, A. François, D. Guerrot, I. Etienne, F. Hau, Comparison of Two Luminex Single-antigen Bead Flow Cytometry Assays for Detection of Donor-specific Antibodies After Renal Transplantation. *Transplantation*. **103**, 597–603 (2019).

148. R. J. Duquesnoy, M. Marrari, Usefulness of the ElliPro epitope predictor program in defining the repertoire of. *Hum Immunol*. **78**, 481–488 (2017).

149. Q. Zhang, E. F. Reed, The importance of non-HLA antibodies in transplantation. *Nat Rev Nephrol*. **12**, 484–495 (2016).

150. A. M. Jackson, M. B. Kuperman, R. A. Montgomery, Multiple hyperacute rejections in the absence of detectable complement activation in a patient with endothelial cell reactive antibody. *Am. J. Transplant.* **12**, 1643–1649 (2012).

151. D. Dragun, D. N. Müller, J. H. Bräsen, L. Fritsche, M. Nieminen-Kelhä, R. Dechend, U. Kintscher, B. Rudolph, J. Hoebeke, D. Eckert, I. Mazak, R. Plehm, C. Schönemann, T. Unger, K. Budde, H.-H. Neumayer, F. C. Luft, G. Wallukat, Angiotensin II type 1-receptor activating antibodies in renal-allograft rejection. *N. Engl. J. Med.* **352**, 558–569 (2005).

152. H. Cardinal, M. Dieudé, N. Brassard, S. Qi, N. Patey, M. Soulez, D. Beillevaire, F. Echeverry, C. Daniel, Y. Durocher, F. Madore, M. J. Hébert, Antiperlecan antibodies are novel accelerators of immune-mediated vascular injury. *Am. J. Transplant.* **13**, 861–874 (2013).

153. R. Reindl-Schwaighofer, A. Heinzel, A. Kainz, J. van Setten, K. Jelencsics, K. Hu, B.-L. Loza, M. Kammer, G. Heinze, P. Hruba, A. Koňaříková, O. Viklicky, G. A. Boehmig, F. Eskandary, G. Fischer, F. Claas, J. C. Tan, T. J. Albert, J. Patel, B. Keating, R. Oberbauer, iGeneTRAiN consortium, Contribution of non-HLA incompatibility between donor and recipient to kidney allograft survival: genome-wide analysis in a prospective cohort. *Lancet*. **393**, 910–917 (2019).

154. E. Goulmy, B. A. Bradley, Q. Lansbergen, J. J. van Rood, The importance of H-Y incompatibility in human organ transplantation. *Transplantation*. **25**, 315–319 (1978).

155. A. Gratwohl, B. Döhler, M. Stern, G. Opelz, H-Y as a minor histocompatibility antigen in kidney transplantation: a retrospective cohort study. *Lancet*. **372**, 49–53 (2008).

156. D. B. Miklos, H. T. Kim, K. H. Miller, L. Guo, E. Zorn, S. J. Lee, E. P. Hochberg, C. J. Wu, E. P. Alyea, C. Cutler, V. Ho, R. J. Soiffer, J. H. Antin, J. Ritz, Antibody responses to H-

Y minor histocompatibility antigens correlate with chronic graft-versus-host disease and disease remission. *Blood*. **105**, 2973–2978 (2005).

157. E. Spierings, Minor histocompatibility antigens: past, present, and future. *Tissue Antigens*. **84**, 374–360 (2014).

158. Y. Zou, P. Stastny, C. Süsal, B. Döhler, G. Opelz, Antibodies against MICA antigens and kidney-transplant rejection. *N. Engl. J. Med.* **357**, 1293–1300 (2007).

159. A. M. Miltenburg, M. E. Meijer-Paape, J. J. Weening, M. R. Daha, L. A. van Es, F. J. van der Woude, Induction of antibody-dependent cellular cytotoxicity against endothelial cells by renal transplantation. *Transplantation*. **48**, 681–688 (1989).

160. K. Murata, W. M. Baldwin, Mechanisms of complement activation, C4d deposition, and their contribution to the pathogenesis of antibody mediated rejection. *Transplant Rev (Orlando)*. **23**, 139–150 (2009).

161. A. M. Herzenberg, J. S. Gill, O. Djurdjev, A. B. Magil, C4d deposition in acute rejection: an independent long-term prognostic factor. *J. Am. Soc. Nephrol.* **13**, 234–241 (2002).

162. M. Sarwal, M.-S. Chua, N. Kambham, S.-C. Hsieh, T. Satterwhite, M. Masek, O. J. Salvatierra, Molecular heterogeneity in acute renal allograft rejection identified by DNA microarray profiling. *N Engl J Med*. **349**, 125–138 (2003).

163. B. E. Hippen, A. DeMattos, W. J. Cook, C. E. 2nd Kew, R. S. Gaston, Association of CD20+ infiltrates with poorer clinical outcomes in acute cellular rejection of renal allografts. *Am J Transplant*. **5**, 2248–2252 (2005).

164. E. W. Tsai, P. Rianthavorn, D. W. Gjertson, W. D. Wallace, E. F. Reed, R. B. Ettenger, CD20+ lymphocytes in renal allografts are associated with poor graft survival in pediatric patients. *Transplantation*. **82**, 1769–1773 (2006).

165. L. K. Kayler, F. G. Lakkis, C. Morgan, A. Basu, D. Blisard, H. P. Tan, J. McCauley, C. Wu, R. Shapiro, P. S. Randhawa, Acute cellular rejection with CD20-positive lymphoid clusters in kidney transplant patients following lymphocyte depletion. *Am. J. Transplant.* **7**, 949–954 (2007).

166. C. Doria, F. di Francesco, C. B. Ramirez, A. Frank, M. Iaria, G. Francos, I. R. Marino, J. L. Farber, The presence of B-cell nodules does not necessarily portend a less favorable outcome to therapy in patients with acute cellular rejection of a renal allograft. *Transplant. Proc.* **38**, 3441–3444 (2006).

167. S. M. Bagnasco, W. Tsai, M. H. Rahman, E. S. Kraus, L. Barisoni, R. Vega, L. C. Racusen, M. Haas, B. S. Mohammed, A. A. Zachary, R. A. Montgomery, CD20-positive infiltrates in renal allograft biopsies with acute cellular rejection are not associated with worse graft survival. *Am. J. Transplant.* **7**, 1968–1973 (2007).

168. J. Cheng, A. Torkamani, R. K. Grover, T. M. Jones, D. I. Ruiz, N. J. Schork, M. M. Quigley, F. W. Hall, D. R. Salomon, R. A. Lerner, Ectopic B-cell clusters that infiltrate transplanted human kidneys are clonal. *Proc Natl Acad Sci U S A*. **108**, 5560–5565 (2011).

169. J. Ferdman, F. Porcheray, B. Gao, C. Moore, J. DeVito, S. Dougherty, M. V. Thomas, E. A. Farkash, N. Elias, T. Kawai, S. K. Malek, S. G. Tullius, W. Wong, E. Zorn, Expansion and somatic hypermutation of B cell clones in rejected human kidney grafts. *Transplantation*. **98**, 766–772 (2014).

170. V. N. Carpio, I. de L. Noronha, H. L. Martins, L. F. Jobim, B. C. Gil, A. S. Kulzer, M. da S. Loreto, L. F. S. Goncalves, R. C. Manfro, F. V. Veronese, Expression patterns of B cells in acute kidney transplant rejection. *Exp Clin Transplant*. **12**, 405–414 (2014).

171. V. Zarkhin, N. Kambham, L. Li, S. Kwok, S.-C. Hsieh, O. Salvatierra, M. M. Sarwal, Characterization of intra-graft B cells during renal allograft rejection. *Kidney Int*. **74**, 664–673 (2008).

172. O. Thaunat, N. Patey, G. Caligiuri, C. Gautreau, M. Mamani-Matsuda, Y. Mekki, M.-C. Dieu-Nosjean, G. Eberl, R. Ecochard, J.-B. Michel, S. Graff-Dubois, A. Nicoletti, Chronic Rejection Triggers the Development of an Aggressive Intragraft Immune Response through Recapitulation of Lymphoid Organogenesis. *The Journal of Immunology*. **185**, 717–728 (2010).

173. L. Kühne, B. Jung, H. Poth, A. Schuster, S. Wurm, P. Ruemmele, B. Banas, T. Bergler, Renal allograft rejection, lymphocyte infiltration, and de novo donor-specific antibodies in a novel model of non-adherence to immunosuppressive therapy. *BMC Immunology*. **18**, 52 (2017).

174. T. Liao, Y. Xue, D. Zhao, S. Li, M. Liu, J. Chen, D. D. Brand, H. Zheng, Y. Zhang, S. G. Zheng, Q. Sun, In Vivo Attenuation of Antibody-Mediated Acute Renal Allograft Rejection by Ex Vivo TGF-β-Induced CD4+Foxp3+ Regulatory T Cells. *Front Immunol*. **8**, 1334 (2017).

175. N. F. Smirnova, T. M. Conlon, C. Morrone, P. Dorfmuller, M. Humbert, G. T. Stathopoulos, S. Umkehrer, F. Pfeiffer, A. Ö. Yildirim, O. Eickelberg, Inhibition of B cell–dependent lymphoid follicle formation prevents lymphocytic bronchiolitis after lung transplantation. *JCI Insight*. **4** (2019), doi:10.1172/jci.insight.123971.

176. D. Jain, D. Yin, A. S. Chong, *The Journal of Immunology*, in press.

177. Z. Zhang, L. Zhu, D. Quan, B. Garcia, N. Ozcay, J. Duff, C. Stiller, A. Lazarovits, D. Grant, R. Zhong, Pattern of liver, kidney, heart, and intestine allograft rejection in different mouse strain combinations. *Transplantation*. **62**, 1267–1272 (1996).

178. R. S. Gaston, J. M. Cecka, B. L. Kasiske, A. M. Fieberg, R. Leduc, F. C. Cosio, S. Gourishankar, J. Grande, P. Halloran, L. Hunsicker, R. Mannon, D. Rush, A. J. Matas, Evidence for antibody-mediated injury as a major determinant of late kidney allograft failure. *Transplantation*. **90**, 68–74 (2010).

179. N. M. Bath, X. Ding, B. M. Verhoven, N. A. Wilson, L. Coons, A. Sukhwal, W. Zhong, R. R. R. Iii, Autoantibody production significantly decreased with APRIL/BLyS blockade in murine chronic rejection kidney transplant model. *PLOS ONE*. **14**, e0223889 (2019).

180. Win Thet Su, Rehakova Sylvia, Negus Margaret C., Saeb-Parsy Kourosh, Goddard Martin, Conlon Thomas M., Bolton Eleanor M., Bradley J. Andrew, Pettigrew Gavin J., Donor CD4 T Cells Contribute to Cardiac Allograft Vasculopathy by Providing Help for Autoantibody Production. *Circulation: Heart Failure*. **2**, 361–369 (2009).

181. D. Metes, A. Logar, W. A. Rudert, A. Zeevi, J. Woodward, A. J. Demetris, K. Abu-Elmagd, B. Eghtesad, R. Shapiro, J. J. Fung, M. Trucco, T. E. Starzl, N. Murase, Four-color flow cytometric analysis of peripheral blood donor cell chimerism. *Human Immunology*. **64**, 787–795 (2003).

182. C. C. Anderson, P. Matzinger, Immunity or tolerance: Opposite outcomes of microchimerism from skin grafts. *Nature Medicine*. **7**, 80–87 (2001).

183. F. Porcheray, J. DeVito, Y. Helou, I. Dargon, J. W. Fraser, P. Nobecourt, J. Ferdman, S. Germana, T. C. Girouard, T. Kawai, S. L. Saidman, W. Wong, R. B. Colvin, C. Leguern, E. Zorn, Expansion of polyreactive B cells cross-reactive to HLA and self in the blood of a patient with kidney graft rejection. *Am J Transplant*. **12**, 2088–2097 (2012).

184. J. M. Walch, Q. Zeng, Q. Li, M. H. Oberbarnscheidt, R. A. Hoffman, A. L. Williams, D. M. Rothstein, W. D. Shlomchik, J. V. Kim, G. Camirand, F. G. Lakkis, Cognate antigen directs CD8+ T cell migration to vascularized transplants. *J. Clin. Invest.* **123**, 2663–2671 (2013).

185. S. R. Allie, J. E. Bradley, U. Mudunuru, M. D. Schultz, B. A. Graf, F. E. Lund, T. D. Randall, The establishment of resident memory B cells in the lung requires local antigen encounter. *Nature Immunology*. **20**, 97–108 (2019).

186. V. Pistoia, Production of cytokines by human B cells in health and disease. *Immunol. Today*. **18**, 343–350 (1997).

187. D. P. Harris, L. Haynes, P. C. Sayles, D. K. Duso, S. M. Eaton, N. M. Lepak, L. L. Johnson, S. L. Swain, F. E. Lund, Reciprocal regulation of polarized cytokine production by effector B and T cells. *Nat. Immunol.* **1**, 475–482 (2000).

188. V. Abadie, B. Jabri, IL-15: a central regulator of celiac disease immunopathology. *Immunol Rev*. **260**, 221–234 (2014).

189. R. Schneider, A. N. Mohebiany, I. Ifergan, D. Beauseigle, P. Duquette, A. Prat, N. Arbour, B cell-derived IL-15 enhances CD8 T cell cytotoxicity and is increased in multiple sclerosis patients. *J Immunol*. **187**, 4119–4128 (2011).

190. M. Pavlakis, J. Strehlau, M. Lipman, M. Shapiro, W. Maslinski, T. B. Strom, Intragraft IL-15 transcripts are increased in human renal allograft rejection. *Transplantation*. **62**, 543–545 (1996).

191. B. Peng, Y. Ming, C. Yang, Regulatory B cells: the cutting edge of immune tolerance in kidney transplantation. *Cell Death Dis*. **9**, 109 (2018).

192. L. C. Lighaam, P.-P. A. Unger, D. W. Vredevoogd, D. Verhoeven, E. Vermeulen, A. W. Turksma, A. ten Brinke, T. Rispens, S. M. van Ham, In vitro-Induced Human IL-10+ B Cells Do Not Show a Subset-Defining Marker Signature and Plastically Co-express IL-10 With Pro-Inflammatory Cytokines. *Front. Immunol.* **9** (2018), doi:10.3389/fimmu.2018.01913.

193. J. Durand, E. Chiffoleau, B cells with regulatory properties in transplantation tolerance. *World J Transplant*. **5**, 196–208 (2015).

194. J.-D. Bouaziz, S. Calbo, M. Maho-Vaillant, A. Saussine, M. Bagot, A. Bensussan, P. Musette, IL-10 produced by activated human B cells regulates CD4(+) T-cell activation in vitro. *Eur. J. Immunol.* **40**, 2686–2691 (2010).

195. Y. Iwata, T. Matsushita, M. Horikawa, D. J. Dilillo, K. Yanaba, G. M. Venturi, P. M. Szabolcs, S. H. Bernstein, C. M. Magro, A. D. Williams, R. P. Hall, E. W. St Clair, T. F. Tedder, Characterization of a rare IL-10-competent B-cell subset in humans that parallels mouse regulatory B10 cells. *Blood*. **117**, 530–541 (2011).

196. K. A. Newell, A. Asare, A. D. Kirk, T. D. Gisler, K. Bourcier, M. Suthanthiran, W. J. Burlingham, W. H. Marks, I. Sanz, R. I. Lechler, M. P. Hernandez-Fuentes, L. A. Turka, V. L. Seyfert-Margolis, Identification of a B cell signature associated with renal transplant tolerance in humans. *J Clin Invest*. **120**, 1836–1847 (2010).

197. A. Pallier, S. Hillion, R. Danger, M. Giral, M. Racapé, N. Degauque, E. Dugast, J. Ashton-Chess, S. Pettré, J. J. Lozano, R. Bataille, A. Devys, A. Cesbron-Gautier, C. Braudeau, C. Larrose, J.-P. Soulillou, S. Brouard, Patients with drug-free long-term graft function display increased numbers of peripheral B cells with a memory and inhibitory phenotype. *Kidney Int.* **78**, 503–513 (2010).

198. M. R. Clatworthy, C. J. E. Watson, G. Plotnek, V. Bardsley, A. N. Chaudhry, J. A. Bradley, K. G. C. Smith, B-cell-depleting induction therapy and acute cellular rejection. *N. Engl. J. Med.* **360**, 2683–2685 (2009).

199. F. Vincenti, R. Kirkman, S. Light, G. Bumgardner, M. Pescovitz, P. Halloran, J. Neylan, A. Wilkinson, H. Ekberg, R. Gaston, L. Backman, J. Burdick, Interleukin-2–Receptor Blockade with Daclizumab to Prevent Acute Rejection in Renal Transplantation. *New England Journal of Medicine*. **338**, 161–165 (1998).

200. K. E. Neu, J. J. Guthmiller, M. Huang, J. La, M. C. Vieira, K. Kim, N.-Y. Zheng, M. Cortese, M. E. Tepora, N. J. Hamel, K. T. Rojas, C. Henry, D. Shaw, C. L. Dulberger, B. Pulendran, S. Cobey, A. A. Khan, P. C. Wilson, Spec-seq unveils transcriptional subpopulations of antibody-secreting cells following influenza vaccination. *J Clin Invest*. **129**, 93–105 (2019).

201. T. Gomes, S. A. Teichmann, C. Talavera-Lopez, Immunology Driven by Large-Scale Single-Cell Sequencing. *Trends Immunol*. **40**, 1011–1021 (2019).

202. S. Picelli, O. R. Faridani, A. K. Bjorklund, G. Winberg, S. Sagasser, R. Sandberg, Full-length RNA-seq from single cells using Smart-seq2. *Nat Protoc*. **9**, 171–181 (2014).

203. D. Risso, J. Ngai, T. P. Speed, S. Dudoit, Normalization of RNA-seq data using factor analysis of control genes or samples. *Nat Biotechnol*. **32**, 896–902 (2014).

204. K. S. Kobayashi, P. J. van den Elsen, NLRC5: a key regulator of MHC class I-dependent immune responses. *Nat Rev Immunol*. **12**, 813–820 (2012).

205. O. Thaunat, N. Patey, C. Gautreau, S. Lechaton, V. Fremeaux-Bacchi, M.-C. Dieu-Nosjean, E. Cassuto-Viguier, C. Legendre, M. Delahousse, P. Lang, J.-B. Michel, A. Nicoletti, B cell survival in intragraft tertiary lymphoid organs after rituximab therapy. *Transplantation*. **85**, 1648–1653 (2008).

206. Y. Kochi, K. Myouzen, R. Yamada, A. Suzuki, T. Kurosaki, Y. Nakamura, K. Yamamoto, FCRL3, an autoimmune susceptibility gene, has inhibitory potential on B-cell receptor-mediated signaling. *J Immunol*. **183**, 5502–5510 (2009).

207. D. Matza, A. Badou, K. S. Kobayashi, K. Goldsmith-Pestana, Y. Masuda, A. Komuro, D. McMahon-Pratt, V. T. Marchesi, R. A. Flavell, A scaffold protein, AHNAK1, is required for calcium signaling during T cell activation. *Immunity*. **28**, 64–74 (2008).

208. T. S. P. Heng, M. W. Painter, The Immunological Genome Project: networks of gene expression in immune cells. *Nat Immunol*. **9**, 1091–1094 (2008).

209. C. Wu, Q. Fu, Q. Guo, S. Chen, S. Goswami, S. Sun, T. Li, X. Cao, F. Chu, Z. Chen, M. Liu, Y. Liu, T. Fu, P. Hao, Y. Hao, N. Shen, C. Bao, X. Zhang, Lupus-associated atypical memory B cells are mTORC1-hyperactivated and functionally dysregulated. *Annals of the Rheumatic Diseases*. **78**, 1090–1100 (2019).

210. J. A. Ramilowski, T. Goldberg, J. Harshbarger, E. Kloppmann, M. Lizio, V. P. Satagopam, M. Itoh, H. Kawaji, P. Carninci, B. Rost, A. R. R. Forrest, A draft network of ligand-receptor-mediated multicellular signalling in human. *Nat Commun*. **6**, 7866 (2015).

211. S. Dubois, J. Mariner, T. A. Waldmann, Y. Tagaya, IL-15Ralpha recycles and presents IL-15 In trans to neighboring cells. *Immunity*. **17**, 537–547 (2002).

212. A. C. Vendel, J. Calemine-Fenaux, A. Izrael-Tomasevic, V. Chauhan, D. Arnott, D. L. Eaton, B and T Lymphocyte Attenuator Regulates B Cell Receptor Signaling by Targeting Syk and BLNK. *The Journal of Immunology*. **182**, 1509–1517 (2009).

213. K. Huse, M. Bakkebø, M. P. Oksvold, L. Forfang, V. I. Hilden, T. Stokke, E. B. Smeland, J. H. Myklebust, Bone morphogenetic proteins inhibit CD40L/IL-21-induced Ig production in

human B cells: differential effects of BMP-6 and BMP-7. *Eur. J. Immunol.* **41**, 3135–3145 (2011).

214. S. Goodison, V. Urquidi, D. Tarin, CD44 cell adhesion molecules. *Mol Pathol*. **52**, 189–196 (1999).

215. J. Xie, R. Li, P. Kotovuori, C. Vermot-Desroches, J. Wijdenes, M. A. Arnaout, P. Nortamo, C. G. Gahmberg, Intercellular adhesion molecule-2 (CD102) binds to the leukocyte integrin CD11b/CD18 through the A domain. *J. Immunol.* **155**, 3619–3628 (1995).

216. R. Bacher, L.-F. Chu, N. Leng, A. P. Gasch, J. A. Thomson, R. M. Stewart, M. Newton, C. Kendziorski, SCnorm: robust normalization of single-cell RNA-seq data. *Nat Methods*. **14**, 584–586 (2017).

217. C. Hafemeister, R. Satija, Normalization and variance stabilization of single-cell RNA-seq data using regularized negative binomial regression. *Genome Biol.* **20**, 296 (2019).

218. T. Stuart, A. Butler, P. Hoffman, C. Hafemeister, E. Papalexi, W. M. Mauck, Y. Hao, M. Stoeckius, P. Smibert, R. Satija, Comprehensive Integration of Single-Cell Data. *Cell*. **177**, 1888-1902.e21 (2019).

219. J. T. Leek, W. E. Johnson, H. S. Parker, A. E. Jaffe, J. D. Storey, The sva package for removing batch effects and other unwanted variation in high-throughput experiments. *Bioinformatics*. **28**, 882–883 (2012).

220. M. Magnone, J. L. Holley, R. Shapiro, V. Scantlebury, J. McCauley, M. Jordan, C. Vivas, T. Starzl, J. P. Johnson, Interferon-alpha-induced acute renal allograft rejection. *Transplantation*. **59**, 1068–1070 (1995).

221. P. Saint-Mezard, C. C. Berthier, H. Zhang, A. Hertig, S. Kaiser, M. Schumacher, G. Wieczorek, M. Bigaud, J. Kehren, E. Rondeau, F. Raulf, H.-P. Marti, Analysis of independent microarray datasets of renal biopsies identifies a robust transcript signature of acute allograft rejection. *Transpl. Int.* **22**, 293–302 (2009).

222. H. Ciferska, P. Horak, Y. Konttinen, K. Krejci, T. Tichy, Z. Hermanova, J. Zadrazil, Expression of nucleic acid binding Toll-like receptors in control, lupus and transplanted kidneys – a preliminary pilot study. *Lupus*. **17**, 580–585 (2008).

223. A. Lanzavecchia, F. Sallusto, Toll-like receptors and innate immunity in B-cell activation and antibody responses. *Curr Opin Immunol*. **19**, 268–274 (2007).

224. J. Chavarría-Smith, P. S. Mitchell, A. M. Ho, M. D. Daugherty, R. E. Vance, Functional and Evolutionary Analyses Identify Proteolysis as a General Mechanism for NLRP1 Inflammasome Activation. *PLoS Pathog*. **12** (2016), doi:10.1371/journal.ppat.1006052.

225. P. S. Mitchell, A. Sandstrom, R. E. Vance, The NLRP1 inflammasome: new mechanistic insights and unresolved mysteries. *Current Opinion in Immunology*. **60**, 37–45 (2019).

226. A. L. Burkhardt, T. Costa, Z. Misulovin, B. Stealy, J. B. Bolen, M. C. Nussenzweig, Ig alpha and Ig beta are functionally homologous to the signaling proteins of the T-cell receptor. *Mol. Cell. Biol.* **14**, 1095–1103 (1994).

227. X. Zheng-Bradley, J. Rung, H. Parkinson, A. Brazma, Large scale comparison of global gene expression patterns in human and mouse. *Genome Biology*. **11**, R124 (2010).

228. A. Dal Canton, Adhesion molecules in renal disease. *Kidney International*. **48**, 1687–1696 (1995).

229. D. Wolf, N. Anto-Michel, H. Blankenbach, A. Wiedemann, K. Buscher, J. D. Hohmann, B. Lim, M. Bäuml, A. Marki, M. Mauler, D. Duerschmied, Z. Fan, H. Winkels, D. Sidler, P. Diehl, D. M. Zajonc, I. Hilgendorf, P. Stachon, T. Marchini, F. Willecke, M. Schell, B. Sommer, C. von zur Muhlen, J. Reinöhl, T. Gerhardt, E. F. Plow, V. Yakubenko, P. Libby, C. Bode, K. Ley, K. Peter, A. Zirlik, A ligand-specific blockade of the integrin Mac-1 selectively targets pathologic inflammation while maintaining protective host-defense. *Nat Commun*. **9** (2018), doi:10.1038/s41467-018-02896-8.

230. X. X. Zheng, W. Gao, E. Donskoy, M. Neuberg, M. Ruediger, T. B. Strom, T. Moll, An antagonist mutant IL-15/Fc promotes transplant tolerance. *Transplantation*. **81**, 109–116 (2006).

231. S. Haustein, J. Kwun, J. Fechner, A. Kayaoglu, J.-P. Faure, D. Roenneburg, J. Torrealba, S. J. Knechtle, Interleukin-15 receptor blockade in non-human primate kidney transplantation. *Transplantation*. **89**, 937–944 (2010).

232. K. Smith, L. Garman, J. Wrammert, N.-Y. Zheng, J. D. Capra, R. Ahmed, P. C. Wilson, Rapid generation of fully human monoclonal antibodies specific to a vaccinating antigen. *Nat Protoc*. **4**, 372–384 (2009).

233. X. Brochet, M.-P. Lefranc, V. Giudicelli, IMGT/V-QUEST: the highly customized and integrated system for IG and TR standardized V-J and V-D-J sequence analysis. *Nucleic Acids Res.* **36**, W503-508 (2008).

234. E. Alamyar, V. Giudicelli, P. Duroux, M.-P. Lefranc, IMGT/HighV-QUEST: A High-Throughput System and Web Portal for the Analysis of Rearranged Nucleotide Sequences of Antigen Receptors - High-Throughput Version of IMGT/V-QUEST -, 1.

235. Q. Xu, T. Pearce, E. Johnson, D. Rich-Sperling, K. Gorkoff, T. Akister, J. Li, 32-OR: ARE ALL ANTI-HLA-Cw ANTIBODIES DETECTED WITH LUMINEX SINGLE ANTIGEN BEAD REAL ANTIBODIES? *Human Immunology*. **73**, 27 (2012).

236. G. Tumer, T. K. Roberts-Wilson, R. A. Bray, H. M. Gebel, 44-P: ANTIBODIES AGAINST DENATURED C-LOCUS ANTIGENS IN TWO PATIENTS WITH VENTRICULAR ASSIST DEVICES (VAD). *Human Immunology*. **74**, 80 (2013).

237. J. Visentin, T. Bachelet, O. Aubert, A. Del Bello, C. Martinez, F. Jambon, G. Guidicelli, M. Ralazamahaleo, C. Bouthemy, M. Cargou, N. Congy-Jolivet, T. Nong, J.-H. Lee, R. Sberro-Soussan, L. Couzi, N. Kamar, C. Legendre, P. Merville, J.-L. Taupin, Reassessment of the clinical impact of preformed donor-specific anti-HLA-Cw antibodies in kidney transplantation. *Am. J. Transplant.* (2019), doi:10.1111/ajt.15766.

238. S. F. Andrews, Y. Huang, K. Kaur, L. I. Popova, I. Y. Ho, N. T. Pauli, C. J. Henry Dunand, W. M. Taylor, S. Lim, M. Huang, X. Qu, J.-H. Lee, M. Salgado-Ferrer, F. Krammer, P. Palese, J. Wrammert, R. Ahmed, P. C. Wilson, Immune history profoundly affects broadly protective B cell responses to influenza. *Sci Transl Med*. **7**, 316ra192 (2015).

239. Y. Liu, J. R. McDaniel, S. Khan, P. Campisi, E. J. Propst, T. Holler, E. Grunebaum, G. Georgiou, G. C. Ippolito, G. R. A. Ehrhardt, Antibodies Encoded by FCRL4-Bearing Memory B Cells Preferentially Recognize Commensal Microbial Antigens. *J Immunol*. **200**, 3962–3969 (2018).

240. H. Qin, K. Suzuki, M. Nakata, S. Chikuma, N. Izumi, L. T. Huong, M. Maruya, S. Fagarasan, M. Busslinger, T. Honjo, H. Nagaoka, Activation-Induced Cytidine Deaminase Expression in CD4+ T Cells is Associated with a Unique IL-10-Producing Subset that Increases with Age. *PLOS ONE*. **6**, e29141 (2011).

241. D. B. Bloch, D. Rabkina, K. D. Bloch, The cell proliferation-associated protein Ki-67 is a target of autoantibodies in the serum of MRL mice. *Lab Invest*. **73**, 366–371 (1995).

242. Y. Muro, T. Kano, K. Sugiura, M. Hagiwara, Low frequency of autoantibodies against Ki-67 antigen in Japanese patients with systemic autoimmune diseases. *J Autoimmun*. **10**, 499–503 (1997).

243. M. Bleakley, B. E. Otterud, J. L. Richardt, A. D. Mollerup, M. Hudecek, T. Nishida, C. N. Chaney, E. H. Warren, M. F. Leppert, S. R. Riddell, Leukemia-associated minor histocompatibility antigen discovery using T-cell clones isolated by in vitro stimulation of naive CD8+ T cells. *Blood*. **115**, 4923–4933 (2010).

244. A. Choudhury, M. A. Maldonado, P. L. Cohen, R. A. Eisenberg, The Role of Host CD4 T Cells in the Pathogenesis of the Chronic Graft-versus-Host Model of Systemic Lupus Erythematosus. *The Journal of Immunology*. **174**, 7600–7609 (2005).

245. M. Koyama, P. Mukhopadhyay, I. S. Schuster, A. S. Henden, J. Hülsdünker, A. Varelias, M. Vetizou, R. D. Kuns, R. J. Robb, P. Zhang, B. R. Blazar, R. Thomas, J. Begun, N. Waddell, G. Trinchieri, R. Zeiser, A. D. Clouston, M. A. Degli-Esposti, G. R. Hill, MHC Class II Antigen Presentation by the Intestinal Epithelium Initiates Graft-versus-Host Disease and Is Influenced by the Microbiota. *Immunity*. **51**, 885-898.e7 (2019).

246. S. Li, C. Kurts, F. Köntgen, S. R. Holdsworth, P. G. Tipping, Major Histocompatibility Complex Class II Expression by Intrinsic Renal Cells Is Required for Crescentic Glomerulonephritis. *J Exp Med*. **188**, 597–602 (1998).

247. R. Berland, H. H. Wortis, Origins and functions of B-1 cells with notes on the role of CD5. *Annu Rev Immunol*. **20**, 253–300 (2002).

248. W.-A. Pan, H.-Y. Tsai, S.-C. Wang, M. Hsiao, P.-Y. Wu, M.-D. Tsai, The RNA recognition motif of NIFK is required for rRNA maturation during cell cycle progression. *RNA Biol*. **12**, 255–267 (2015).

249. S. Bursać, D. Jurada, S. Volarević, New insights into HEATR1 functions. *Cell Cycle*. **17**, 143–144 (2018).

250. F. Rascio, P. Pontrelli, M. Accetturo, A. Oranger, M. Gigante, G. Castellano, M. Gigante, A. Zito, G. Zaza, A. Lupo, E. Ranieri, G. Stallone, L. Gesualdo, G. Grandaliano, A type I interferon signature characterizes chronic antibody-mediated rejection in kidney transplantation. *J. Pathol.* **237**, 72–84 (2015).

251. W. Pongpirul, W. Chancharoenthana, K. Pongpirul, A. Leelahavanichkul, W. Kittikowit, K. Jutivorakool, B. Nonthasoot, Y. Avihingsanon, S. Eiam-Ong, K. Praditpornsilpa, N. Townamchai, B-cell activating factor, a predictor of antibody mediated rejection in kidney transplantation recipients. *Nephrology (Carlton)*. **23**, 169–174 (2018).

252. X.-Z. Wang, Z. Wan, W.-J. Xue, J. Zheng, Y. Li, C. G. Ding, B-Cell Activating Factor Predicts Acute Rejection Risk in Kidney Transplant Recipients: A 6-Month Follow-Up Study. *Front Immunol*. **10**, 1046 (2019).

253. B. Jabri, V. Abadie, IL-15 functions as a danger signal to regulate tissue-resident T cells and tissue destruction. *Nat Rev Immunol*. **15**, 771–783 (2015).

254. Y. K. Chae, W. M. Choi, W. H. Bae, J. Anker, A. A. Davis, S. Agte, W. T. Iams, M. Cruz, M. Matsangou, F. J. Giles, Overexpression of adhesion molecules and barrier molecules is associated with differential infiltration of immune cells in non-small cell lung cancer. *Scientific Reports*. **8**, 1–10 (2018).

255. Q. Zhang, Y. He, N. Luo, S. J. Patel, Y. Han, R. Gao, M. Modak, S. Carotta, C. Haslinger, D. Kind, G. W. Peet, G. Zhong, S. Lu, W. Zhu, Y. Mao, M. Xiao, M. Bergmann, X. Hu, S. P. Kerkar, A. B. Vogt, S. Pflanz, K. Liu, J. Peng, X. Ren, Z. Zhang, Landscape and Dynamics of Single Immune Cells in Hepatocellular Carcinoma. *Cell*. **179**, 829-845.e20 (2019).

256. J. L. Johnson, R. L. Rosenthal, J. J. Knox, A. Myles, M. S. Naradikian, J. Madej, M. Kostiv, A. M. Rosenfeld, W. Meng, S. R. Christensen, S. E. Hensley, J. Yewdell, D. H. Canaday, J. Zhu, A. B. McDermott, Y. Dori, M. Itkin, E. J. Wherry, N. Pardi, D. Weissman, A. Naji, E. T. L. Prak, M. R. Betts, M. P. Cancro, The Transcription Factor T-bet Resolves Memory B Cell Subsets with Distinct Tissue Distributions and Antibody Specificities in Mice and Humans. *Immunity* (2020), doi:10.1016/j.immuni.2020.03.020.

257. M. Mathieu, N. Cotta-Grand, J.-F. Daudelin, S. Boulet, R. Lapointe, N. Labrecque, CD40-Activated B Cells Can Efficiently Prime Antigen-Specific Naïve CD8+ T Cells to Generate Effector but Not Memory T cells. *PLOS ONE*. **7**, e30139 (2012).

258. M. Frentsch, R. Stark, N. Matzmohr, S. Meier, S. Durlanik, A. R. Schulz, U. Stervbo, K. Jürchott, F. Gebhardt, G. Heine, M. A. Reuter, M. R. Betts, D. Busch, A. Thiel, CD40L expression permits CD8+ T cells to execute immunologic helper functions. *Blood*. **122**, 405–412 (2013).

259. K. M. Valentine, D. Davini, T. J. Lawrence, G. N. Mullins, M. Manansala, M. Al-Kuhlani, J. M. Pinney, J. K. Davis, A. E. Beaudin, S. S. Sindi, D. M. Gravano, K. K. Hoyer, CD8 Follicular T Cells Promote B Cell Antibody Class Switch in Autoimmune Disease. *The Journal of Immunology*. **201**, 31–40 (2018).

260. V. M. Liarski, A. Sibley, N. van Panhuys, J. Ai, A. Chang, D. Kennedy, M. Merolle, R. N. Germain, M. L. Giger, M. R. Clark, Quantifying in situ adaptive immune cell cognate interactions in humans. *Nat. Immunol.* **20**, 503–513 (2019).

261. J. Wagner, M. A. Rapsomaniki, S. Chevrier, T. Anzeneder, C. Langwieder, A. Dykgers, M. Rees, A. Ramaswamy, S. Muenst, S. D. Soysal, A. Jacobs, J. Windhager, K. Silina, M. van den Broek, K. J. Dedes, M. Rodríguez Martínez, W. P. Weber, B. Bodenmiller, A Single-Cell Atlas of the Tumor and Immune Ecosystem of Human Breast Cancer. *Cell*. **177**, 1330-1345.e18 (2019).

262. S. R. Greig, Current perspectives on the role of tonsillectomy. *J Paediatr Child Health*. **53**, 1065–1070 (2017).

263. A. Smit, R. Hubley, P. Green, RepeatMasker Open-4.0. 2013-2015, (available at <http://www.repeatmasker.org>).

264. N. L. Bray, H. Pimentel, P. Melsted, L. Pachter, Near-optimal probabilistic RNA-seq quantification. *Nat. Biotechnol.* **34**, 525–527 (2016).

265. M. D. Robinson, D. J. McCarthy, G. K. Smyth, edgeR: a Bioconductor package for differential expression analysis of digital gene expression data. *Bioinformatics*. **26**, 139–140 (2010).

266. G. Yu, L.-G. Wang, Y. Han, Q.-Y. He, clusterProfiler: an R package for comparing biological themes among gene clusters. *OMICS*. **16**, 284–287 (2012).

267. P. Shannon, A. Markiel, O. Ozier, N. S. Baliga, J. T. Wang, D. Ramage, N. Amin, B. Schwikowski, T. Ideker, Cytoscape: a software environment for integrated models of biomolecular interaction networks. *Genome Res.* **13**, 2498–2504 (2003).

268. F. Sievers, D. G. Higgins, Clustal Omega, accurate alignment of very large numbers of sequences. *Methods Mol. Biol.* **1079**, 105–116 (2014).

269. A. Rambaut, A. J. Drummond, *FigTree version 1.4. 0* (2012).

270. R. J. Duquesnoy, M. Marrari, L. C. D. da M. Sousa, J. R. P. de M. Barroso, K. M. de S. U. Aita, A. S. da Silva, S. J. H. do Monte, 16th IHIW: A Website for Antibody-Defined HLA Epitope Registry. *International Journal of Immunogenetics*. **40**, 54–59 (2013).